

DIPOLE ANTENNA LOADED WITH PASSIVE ELEMENTS

A Thesis

Presented to

The Faculty of Graduate Studies

The University of Manitoba

In Partial Fulfillment

of the Requirements for the Degree of

Master of Science

in

Electrical Engineering

by

APISAK ITTIPIBOON

August, 1976

"DIPOLE ANTENNA LOADED WITH PASSIVE ELEMENTS"

by

APISAD ITTIPIBOON

**A dissertation submitted to the Faculty of Graduate Studies of
the University of Manitoba in partial fulfillment of the requirements
of the degree of**

MASTER OF SCIENCE

© 1976

**Permission has been granted to the LIBRARY OF THE UNIVER-
SITY OF MANITOBA to lend or sell copies of this dissertation, to
the NATIONAL LIBRARY OF CANADA to microfilm this
dissertation and to lend or sell copies of the film, and UNIVERSITY
MICROFILMS to publish an abstract of this dissertation.**

**The author reserves other publication rights, and neither the
dissertation nor extensive extracts from it may be printed or other-
wise reproduced without the author's written permission.**

ABSTRACT

A study of a dipole antenna symmetrically loaded on each arm with a lumped impedance is investigated with a view to improving the gain and other radiation characteristics. The current distribution is determined for the unloaded case by the method of moments, using Pocklington's integral equation. The solution is then modified to include the effect of lumped load impedance which makes it possible to express the current distribution in terms of the resistive and reactive components of the load. This leads to expressions for the directive gain in the vertical plane, radiated power and antenna input impedance as function of resistive and reactive components of the load. Using Rosenbrock's method of hill-climbing, the load impedance is optimized for any fixed location along the dipole for either maximum directive gain in the vertical plane or total radiated power. From these results, it is found that the optimum load for maximum directive gain in the vertical plane is purely reactive. It is also found that the gain of the dipole loaded with the optimum load impedance is increased by about 2.72 dB over the unloaded case but its radiated power is drastically reduced. For a short dipole the optimum load for maximum radiated power is also reactive and is equal in magnitude and location to that which would be needed to resonate the dipole. Numerical results for the current distribution and radiation pattern for the dipole antenna loaded with the optimum load impedance are also presented to illustrate the advantages of this type of passive loading.

ACKNOWLEDGEMENTS

The author wishes to express his appreciation to Dr. M.A.K. Hamid for his guidance and encouragement throughout this research.

The financial assistance by Canadian International Development Agency (C.I.D.A.) and the Centre for Transportation Studies of the University of Manitoba are gratefully acknowledged.

TABLE OF CONTENTS

	PAGE
ABSTRACT	i
ACKNOWLEDGEMENTS	ii
TABLE OF CONTENTS	iii
LIST OF FIGURES	v
LIST OF TABLES	viii
CHAPTER 1 INTRODUCTION	1
CHAPTER 2 ANALYSIS OF DIPOLE LOADED WITH PASSIVE ELEMENTS	6
2.1 Derivation of the Integral Equation	6
2.1.1 Integral Representation	6
2.1.2 Integral Equation for a Cylindrical Antenna	8
2.1.3 Thin-Wire Approximation	11
2.2 Solution by the Method of Moments	12
2.2.1 Solution of the Integral Equation	12
2.2.2 Extension to Loaded Dipole	17
2.3 Numerical Results	18
2.3.1 Unloaded Dipole	18
2.3.2 Loaded Dipole	19
CHAPTER 3 OPTIMIZATION OF DIRECTIVE GAIN	40
3.1 Derivation of Directive Gain vs Load Impedance	40
3.2 Optimization of Directive Gain as a Function of Connected Load Impedance	44
3.3 Numerical Results	47

	PAGE
CHAPTER 4 OPTIMIZATION OF RADIATED POWER	58
4.1 Optimization Procedure	58
4.2 Numerical Results	61
CHAPTER 5 INPUT IMPEDANCE OF LOADED DIPOLE	77
5.1 Antenna Impedance	77
5.2 Optimization of $ \text{Im}(Z_{in}) $	81
5.3 Numerical Results	83
CHAPTER 6 EXTENSION TO DIPOLE LOADED WITH FINITE SIZE LOAD IMPEDANCES	96
6.1 Dipole Loaded with Finite Size Load Impedance	96
6.2 Optimization for Directive Gain in the Vertical Plane	102
6.3 Numerical Results	107
CHAPTER 7 DISCUSSION AND CONCLUSION	112
7.1 Discussion	112
7.2 Conclusion	118
7.3 Suggestion for Future Research	119
APPENDIX A	121
APPENDIX B	123
APPENDIX C	126
BIBLIOGRAPHY	151

LIST OF FIGURES

	PAGE	
Fig. 2.1	Cylindrical antenna	9
Fig. 2.2	Current distribution as the sum of triangular sinusoidal pulses	14
Fig. 2.3	Geometry of fields near the antenna	14
Fig. 2.4	Current in upper half of half-wave dipole	21
Fig. 2.5	Current in upper half of full-wave dipole	22
Fig. 2.6	Current in upper half of antenna loaded with resistive load	23
Fig. 2.7	Current in upper half of short dipole loaded with inductive load	24
Fig. 2.8	Current in upper half of half-wave dipole loaded with inductive load	25
Fig. 2.9	Current in upper half of full-wave dipole loaded with inductive load	26
Fig. 2.10	Current in upper half of short dipole loaded with capacitive load	27
Fig. 2.11	Current in upper half of half-wave dipole loaded with capacitive load	28
Fig. 2.12	Current in upper half of full-wave dipole loaded with capacitive load	29
Fig. 2.13	Current in upper half of short dipole loaded with resistive load	30
Fig. 2.14	Current in upper half of half-wave dipole loaded with resistive load	31
Fig. 2.15	Current in upper half of full-wave dipole loaded with resistive load	32
Fig. 2.16	Normalized radiation pattern for short dipole loaded with inductive load	33
Fig. 2.17	Normalized radiation pattern for half-wave dipole loaded with inductive load	34
Fig. 2.18	Normalized radiation pattern for full-wave dipole loaded with inductive load	35

	PAGE	
Fig. 2.19	Current in upper half of short dipole loaded with inductive load at various locations	36
Fig. 2.20	Normalized radiation pattern for short dipole loaded with inductive load at $d/h = 0.867$	37
Fig. 2.21	Normalized radiation pattern for short dipole loaded with inductive load at $d/h = 0.133$	38
Fig. 2.22	Theoretical and experimental input impedance of antenna as a function of loading reactance X_L for load impedances	39
Fig. 3.1	Geometry for far-field of the antenna	45
Fig. 3.2	Antenna configuration	45
Fig. 3.3	Optimum loading impedances as function of d/h for various h/λ	48
Fig. 3.4	Current distribution for $L/\lambda = 0.1$ dipole loaded with optimum load for maximum directivity	49
Fig. 3.5	Current distribution for $L/\lambda = 0.2$ dipole loaded with optimum load for maximum directivity	50
Fig. 3.6	Current distribution for half-wave dipole loaded with optimum load for maximum directivity	51
Fig. 3.7	Normalized radiation pattern for $L/\lambda = 0.1$ dipole loaded with optimum load for maximum directivity	52
Fig. 3.8	Normalized radiation pattern for $L/\lambda = 0.2$ dipole loaded with optimum load for maximum directivity	53
Fig. 3.9	Normalized radiation pattern for half-wave dipole loaded with optimum load for maximum directivity	54
Fig. 4.1	Optimum loading impedances for enhanced radiation as functions of d/h for various h/λ	63
Fig. 4.2	Current distribution for $L/\lambda = 0.1$ dipole loaded at $d/h = 0.2$ with optimum load for enhanced radiation	64
Fig. 4.3	Current distribution for $L/\lambda = 0.1$ dipole loaded at $d/h = 0.6$ with optimum load for enhanced radiation	65
Fig. 4.14	Current distribution for $L/\lambda = 0.1$ dipole loaded at $d/h = 0.9$ with optimum load for enhanced radiation	66
Fig. 4.5	Current distribution for $L/\lambda = 0.2$ dipole loaded at $d/h = 0.133$ with optimum load for enhanced radiation	67

	PAGE	
Fig. 4.6	Current distribution for $L/\lambda = 0.2$ dipole loaded at $d/h = 0.533$ with optimum load for enhanced radiation	68
Fig. 4.7	Current distribution for $L/\lambda = 0.2$ dipole loaded at $d/h = 0.933$ with optimum load for enhanced radiation	69
Fig. 4.8	Current distribution for half-wave dipole loaded at $d/h = 0.45$ with optimum load for enhanced radiation	70
Fig. 4.9	Normalized radiation pattern for $L/\lambda = 0.1$ dipole loaded with optimum load for enhanced radiation	71
Fig. 4.10	Normalized radiation pattern for $L/\lambda = 0.2$ dipole loaded with optimum load for enhanced radiation	72
Fig. 4.11	Normalized radiation pattern for half-wave dipole loaded with optimum load for enhanced radiation	73
Fig. 5.1	Current distribution for $L/\lambda = 0.1$ dipole loaded with resonating load	84
Fig. 5.2	Current distribution for $L/\lambda = 0.2$ dipole loaded with resonating load	85
Fig. 5.3	Current distribution for half-wave dipole loaded with resonating load	86
Fig. 5.4	Normalized radiation pattern for $L/\lambda = 0.1$ dipole loaded with resonating load	87
Fig. 5.5	Normalized radiation pattern for $L/\lambda = 0.2$ dipole loaded with resonating load	88
Fig. 5.6	Normalized radiation pattern for half-wave dipole with resonating load	89
Fig. 6.1	Current distribution for short dipole loaded with finite size inductive load	108
Fig. 6.2	Current distribution for short dipole loaded with finite size optimum load, impedance for maximum directivity	109
Fig. 6.3	Normalized radiation pattern for short dipole loaded with finite size inductive load	110
Fig. 6.4	Normalized radiation pattern for short dipole loaded with finite size optimum load impedance for maximum directivity	111

LIST OF TABLES

	PAGE	
Table 3.1	Relationships of load impedance, antenna input impedance and directivity at various loading points for $L/\lambda = 0.1$ dipole	55
Table 3.2	Relationships of load impedance, antenna input impedance and directivity at various loading points for $L/\lambda = 0.2$ dipole	56
Table 3.3	Relationships of load impedance, antenna input impedance and directivity at various loading points for half-wave dipole	57
Table 4.1	Antenna input impedance and directivity at various loading points for $L/\lambda = 0.1$ dipole loaded with optimum load for enhanced radiation	74
Table 4.2	Antenna input impedance and directivity at various loading points for $L/\lambda = 0.2$ dipole loaded with optimum load for enhanced radiation	75
Table 4.3	Antenna input impedance and directivity at various loading points for half-wave dipole loaded with optimum load for enhanced radiation	76
Table 5.1	Relationships of load impedance, antenna input impedance and directivity at various loading points for $L/\lambda = 0.1$ dipole loaded with complex resonating load	90
Table 5.2	Relationships of load impedance, antenna input impedance and directivity at various loading points for $L/\lambda = 0.2$ dipole loaded with complex resonating load	91
Table 5.3	Relationships of load impedance, antenna input impedance and directivity at various loading points for half-wave dipole loaded with complex resonating load	92
Table 5.4	Relationships of load impedance, antenna input impedance and directivity at various loading points for $L/\lambda = 0.1$ dipole loaded with reactive resonating load	93
Table 5.5	Relationships of load impedance, antenna input impedance and directivity at various loading points for $L/\lambda = 0.2$ dipole loaded with reactive resonating load	94

Table 5.6

Relationships of load impedance, antenna input impedance and directivity at various loading points for half-wave dipole loaded with reactive resonating load

95

CHAPTER 1

INTRODUCTION

A dipole antenna is considered to be the simplest antenna type and most economical to construct. Because of these characteristics it has been employed in many applications, such as in broadcast antennas, VHF and UHF communication antennas. Though it has the advantage of simplicity and economy, it has the disadvantages of relatively poor gain and wide beamwidth, small power capacity and narrow bandwidth. Because of these disadvantages many researches have been done to improve these performances.

The performance of a dipole antenna can be determined if the current distribution along its length is known. For engineering purposes it has been assumed to be a sinusoidal distribution from which the characteristics of the dipole are determined. It has been found that this assumption gives reasonable accuracy. A more accurate solution for current distribution of a dipole antenna has been studied by King⁽¹⁾ and Hallen⁽²⁾ using the integral equation method. The current distribution obtained is very complicated and requires lengthy calculations. Harrington,⁽³⁾ did not attempt to solve the integral equation but was instead able to obtain the current distribution by the moment method. To improve the performance of the dipole, the technique is to upset the current distribution and at the same time attempt to optimize and realize the resulting current distribution.

2

One method for modifying the behaviour of a dipole is to change the geometrical shape of the radiating wire. Thus by bending the antenna's arm, Hamid et al⁽⁴⁾ showed that the radiation characteristics of a dipole are modified. It was shown that the circularly and parabolically bent antennas operating at the first resonance have a radiation pattern approaching omnidirection as the bending curvature is optimized.

Another technique for modifying the behaviour of dipole is by changing the position of excitation. Harrington and Mautz⁽⁵⁾ analyzed thin-wire antennas with arbitrary excitation by the moment method and found that the current distribution, input admittance and radiation pattern can be modified. Strait and Hirasawa⁽⁶⁾ demonstrated that with multiple excitations on the wire antenna gain in specified direction can be maximized.

Another procedure for improving the current distribution is to load the dipole with active or passive elements along the wire. This leads to active and passive dipoles, respectively. The study of active dipoles occupies a prominent position in antenna theory, particularly since many new types of high frequency semiconductors have been developed. An active antenna can be classified into two major types. One contains active devices and radiating sections, such that its performance cannot be described by an amplifier in series with a passive antenna formed by the removal of the active elements. The other type is the combination of amplifier and the passive antenna.

The advantage of an active antenna is that it leads to higher gain or signal to noise ratio or, alternatively a reduction in the overall length of the antenna for the same gain. Some types of active antennas which have

been developed and reported are the parametric amplifier antenna,^{(7), (8)} the Esaki diode antenna⁽⁹⁾ and the antennafier^{(10), (11)}.

Apart from active antenna, studies to improve the characteristics of a dipole antenna have also been centred on the passively-loaded structure which does not contain any active elements. There are two types of loading, one is continuous loading and the other is lumped impedance loading.

In this thesis the study is centred on lumped impedance loading, primarily because of the availability of experimental data carried on elsewhere which permits comparison of analytical predictions. The properties of a cylindrical antenna with a continuous ohmic resistance along its length were studied by King and Wu⁽¹²⁾ who found that this type of antenna is directive and broadband but its efficiency is highly deteriorated. It was also shown by Wu and King⁽¹³⁾ that a travelling wave antenna characteristic can be obtained by continuously loading the antenna with a proper resistive load per unit length.

A dipole loaded with lumped impedance is obviously an easier method for improving the antenna performance by passive loading. Altshuler⁽¹⁴⁾ showed that by loading the dipole with resistors of suitable value at a quarter-wavelength distance from each open end of the antenna, the current distribution can be made of the travelling-wave distribution type which results in a better bandwidth compared to the conventional dipole antennas. Nyquist and Chen⁽¹⁵⁾ were also able to obtain the travelling-wave behaviour by double impedance loading. But instead of loading with a resistor as done by Altshuler, a purely reactive load is placed at a proper position along each arm. This results in a higher efficiency as compared to Altshuler's

travelling-wave antenna. Later it was demonstrated by Rao et al,⁽¹⁶⁾ and Popovic and Dragovic⁽¹⁷⁾ that a broadband antenna can also be obtained by capacitive loading. Lin et al,⁽¹⁸⁾ also analyzed a short dipole antenna doubly loaded with a pair of identical impedances and showed that the radiated power of a short dipole antenna can be increased. It was also shown that with a proper choice of load, the directivity of a short antenna can be increased at the expense of the radiated power and efficiency.

The main purpose of this thesis is to investigate the possibility of improving characteristics of dipole antennas through the use of the lumped impedance loading technique. The antenna under consideration is assumed to consist of a thin cylindrical dipole, doubly loaded with a pair of identical impedances placed at symmetrical locations along the two halves of the antenna. The resulting current distribution is determined in terms of the real and imaginary parts of the load impedance. This results in the equations for directive gain, radiated power and input impedance in terms of real and imaginary parts of the load impedance. Using an optimization technique which is used throughout this thesis, Rosenbrock's method of hill climbing, the optimum values of load impedance for maximum directive gain and maximum radiated power can be determined. Also by a proper choice of load impedance, the antenna input impedance can be transformed to almost any value.

The derivation of the integral equation for the current distribution on a dipole antenna is given in Chapter 2. The thin-wire approximation is used and the integral equation is solved by the moment method. The solution is then applied to the loaded dipole antenna leading to numerical results for the loaded dipole.

The relation for the directive gain is derived in Chapter 3. The optimum load for a maximum gain is determined and numerical results are given to illustrate the improvement in gain at the expense of efficiency.

The relation for the radiated power is derived in Chapter 4. The optimum load for maximum radiated power is determined. The numerical results are given to demonstrate the improvement for radiated power.

The antenna input impedance as a function of the connected load is derived in Chapter 5. The equation is then applied to find the load impedance which resonates the antenna. Numerical results are also presented for illustration.

The dipole antenna loaded with finite size load impedance is treated in Chapter 6. The relation for the directive gain is also derived. The optimum load for a maximum gain is then determined and numerical results are also given to compare with the results obtained for delta load impedance case. A general discussion is given in Chapter 7 followed by the conclusion of the study.

CHAPTER 2

ANALYSIS OF DIPOLE LOADED WITH PASSIVE ELEMENTS

The solution of antenna problems is based on the fact that a differential equation together with the boundary conditions may often be converted into an integral equation, that is, an equation containing the unknown function under the integral sign. In the case of antenna problems the unknown function usually represents the antenna current or more generally the current density. The current distribution is then determined by solving this integral equation.

2.1 Derivation of the Integral Equation

2.1.1 Integral Representation

Before the integral equation of a dipole antenna is derived, the general form of integral representation of fields will be reviewed. Starting from Maxwell's equation for time-harmonic fields with $e^{j\omega t}$ time dependence, we have

$$\nabla \times \bar{E} = -j\omega \bar{B} \quad (2.1.1)$$

$$\nabla \times \bar{H} = \bar{J} + j\omega \epsilon \bar{E} \quad (2.1.2)$$

$$\nabla \cdot \bar{B} = 0 \quad (2.1.3)$$

$$\nabla \cdot \bar{D} = \rho \quad (2.1.4)$$

Where \bar{J} and ρ are, respectively, the current and volumetric charge densities. According to equation (2.1.3) the field of the vector \bar{B} is always solenoidal. Consequently \bar{B} can be represented as the curl

of another vector \bar{A} which is usually called the magnetic vector potential, i.e.,

$$\bar{B} = \nabla \times \bar{A} \quad (2.1.5)$$

If now \bar{B} is replaced in equation (2.1.1), we obtain

$$\nabla \times (\bar{E} + j\omega\bar{A}) = 0 \quad (2.1.6)$$

Thus the field of the vector $\bar{E} + j\omega\bar{A}$ is irrotational and equal to the gradient of a scalar function ϕ which is usually called the electric scalar potential, i.e.,

$$\bar{E} = -\nabla\phi - j\omega\bar{A} \quad (2.1.7)$$

\bar{A} and ϕ under consideration satisfy the Lorentz condition

$$\nabla \cdot \bar{A} = -j\omega\epsilon\mu\phi \quad (2.1.8)$$

while Maxwell's equations and the Lorentz condition allow \bar{A} to be written as the solution of

$$\nabla^2 \bar{A} + k^2 \bar{A} = -\mu \bar{J} \quad (2.1.9)$$

leading to the result⁽¹⁹⁾

$$\bar{A} = \frac{\mu}{4\pi} \int_{V'} \bar{J}(\bar{r}') \frac{e^{-jk|\bar{r} - \bar{r}'|}}{|\bar{r} - \bar{r}'|} dv' \quad (2.1.10)$$

where the prime superscript represents source coordinates, k is $2\pi/\lambda$, λ is the wavelength and $|\bar{r} - \bar{r}'|$ is the distance from source to the observation point.

From equation (2.1.7) and the Lorentz condition one obtains

$$\begin{aligned} \bar{E} &= \frac{-j}{\omega\epsilon\mu} \nabla(\nabla \cdot \bar{A}) - j\omega\bar{A} \\ &= \frac{-j}{\omega\epsilon\mu} (\nabla\nabla \cdot + k^2) \bar{A} \end{aligned} \quad (2.1.11)$$

Substituting for \bar{A} from equation (2.1.10), the integral representation for the electric field as a function of source current density is obtained as

$$\bar{E} = -\frac{j}{4\pi\omega\epsilon} (\nabla\nabla \cdot + k^2) \int_{V'} \bar{J}(\bar{r}') \frac{e^{-jk|\bar{r} - \bar{r}'|}}{|\bar{r} - \bar{r}'|} dv' \quad (2.1.12)$$

2.1.2 Integral Equation for a Cylindrical Antenna

Equation (2.1.12) is the integral representation of the electric field as a function of source current density. This integral representation, when applied to a cylindrical antenna with the current flowing only on the surface, will reduce to surface integration.

For field and source points on the surface of the cylindrical antenna shown in figure 2.1, the integral representation is reduced to

$$\bar{E} = -\frac{j}{4\pi\omega\epsilon} (\nabla\nabla \cdot + k^2) \int_{S'} \bar{J}(\bar{r}') \frac{e^{-jkR}}{R} dS' \quad (2.1.13)$$

where

$$R = |\bar{r}' - \bar{r}| = \sqrt{(z - z')^2 + (2a \sin\phi'/2)^2}$$

Assuming that the cylindrical antenna under consideration has only a \hat{z} component of current and is independent of ϕ' , then equation (2.1.13) reduces to

$$E_z = -\frac{j}{\omega\epsilon} \left(\frac{d^2}{dz^2} + k^2 \right) \int_0^L I(z') \frac{K_s}{4\pi} dz' \quad (2.1.14)$$

where $I(z')$ is the total surface current flow and equals $2\pi a J(z')$, while the kernel K_s is given by

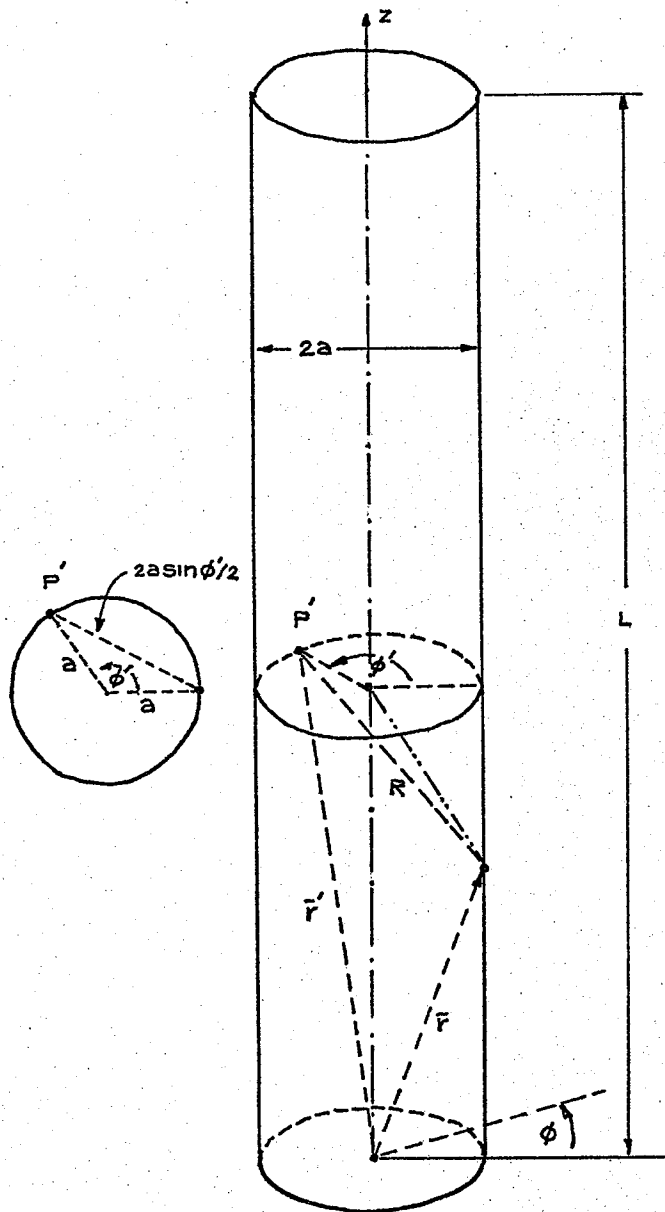


Fig. 2.1 Cylindrical Antenna

$$K_s = \frac{1}{2\pi} \int_0^{2\pi} \frac{e^{-jkR}}{R} d\phi' \quad (2.1.15)$$

As is stated by Harrington⁽²⁰⁾ that "the distinction between antennas and scatterers is primarily the location of the source. If the source is on the object it is considered as antenna; if the source is distant from the object it is viewed as a scatterer. Hence, by analyzing the object in an arbitrary impressed field, we are effectively considering both cases at once". These statements can be confirmed as follows: Equation (2.1.14), obtained from equation (2.1.12), shows the relation between the field and source current density. Thus when it is applied to scatterer, E_z is the scattered field and $I(z)$ is the induced current. On a perfectly conducting wire, the boundary condition is

$$\hat{n} \times \bar{E}_t = 0 \quad (2.1.16)$$

where \bar{E}_t is the total field. Thus,

$$E_z^S = - E_z^i \quad (2.1.17)$$

where E_z^S and E_z^i are the scattered and incident fields, respectively. Substituting for E_z^S in equation (2.1.14), the integral equation for the current distribution as a function of incident field is obtained

$$E_z^i = \frac{j}{\omega\epsilon} \left(\frac{d^2}{dz^2} + k^2 \right) \int_0^L I(z') \frac{K_s}{4\pi} dz' \quad (2.1.18)$$

When equation (2.1.14) is applied to an antenna, E_z is the field produced by the source current $I(z)$. Applying the boundary condition

which requires that the tangential component of the electric field vanishes at the surface of a perfect conductor, we have

$$E_z = \begin{cases} 0 & z \neq z_0 \\ -E_0 \delta(z - z_0) & \text{in the feed gap region} \end{cases} \quad (2.1.19)$$

where z_0 is the point of excitation. Substituting for E_z in equation (2.1.14) we obtain

$$E_0 \delta(z - z_0) = \frac{j}{\omega \epsilon} \left(\frac{d^2}{dz^2} + k^2 \right) \int_0^L I(z') \frac{K_S}{4\pi} dz' \quad (2.1.20)$$

which is the integral equation for the current distribution.

Equation (2.1.18) can be made equivalent to equation (2.1.20) if a constraint is put on E_z^i such that

$$E_z^i = E_0 \delta(z - z_0) \quad (2.1.21)$$

That is equation (2.1.18) can be used to solve for the current distribution of both antennas and scatterers if the proper value of E_z^i corresponding to each case is used.

2.1.3 Thin-Wire Approximation

The dipole antenna under practical conditions is usually made very thin compared with the wavelength at the operating frequency, so that the thin-wire approximation can be applied. The thin-wire approximation involves the following assumptions⁽²¹⁾:

- (a) The only significant component of current on the wire is the axial component, which can be expressed in terms of the net $I(z)$ at any point z along the wire axis.

(b) The kernel K_s is replaced by the thin-wire kernel, i.e.

$$K_s \approx \frac{e^{-jkr''}}{r''}$$

where

$$r'' = \sqrt{a^2 + (z-z')^2}$$

By using this thin-wire approximation, the integral equation (2.1.18) is reduced to

$$E_z^i = \frac{j}{4\pi\omega\epsilon} \left(\frac{d^2}{dz^2} + k^2 \right) \int_0^L I(z') \frac{e^{-jkr''}}{r''} dz' \quad (2.1.22)$$

which is the integral equation for a thin dipole antenna.

2.2 Solution by the Method of Moments

2.2.1 Solution of the Integral Equation

The integral equation (2.1.22) will be solved numerically by the subsectional base technique of the moment method of Harrington⁽²²⁾. The procedure is basically one for which the wire is divided into subsections, and a generalized impedance matrix $[Z]$ obtained to describe the electromagnetic interaction between subsections. The problem is thus reduced to a matrix equation of the form

$$[Z][I] = [V] \quad (2.2.1)$$

From which $[I]$ can be solved, i.e.

$$\begin{aligned} [I] &= [Z]^{-1}[V] \\ &= [Y][V] \end{aligned} \quad (2.2.2)$$

In order to obtain the matrix equation shown above, the current distribution along the antenna will be assumed as the sum of triangular sinusoidal pulses of the form (see figure 2.2)

$$I_i = \begin{cases} \frac{J_i \sin k\{\Delta z - (z' - i\Delta z)\}}{\sin k\Delta z}; & i\Delta z \leq z' \leq (i+1)\Delta z \\ \frac{J_i \sin k\{\Delta z + (z' - i\Delta z)\}}{\sin k\Delta z}; & (i-1)\Delta z \leq z' \leq i\Delta z \\ 0 & \text{otherwise} \end{cases}$$

Thus the current distribution along the antenna is

$$I = \sum_{i=1}^{N-1} I_i \quad (2.2.4)$$

where N is the number of subsections of the wire. This current distribution as shown satisfies the boundary condition for the current which is

$$I(z) = 0 \quad \text{for } z = 0, L \quad (2.2.5)$$

An advantage of the triangular sinusoidal pulse form is that the electric field can be calculated exactly in terms of distances from discontinuities in the slope of the current as shown by Klein and Mittra⁽²³⁾.

The electric field due to a triangular sinusoidal pulse was shown by Jordan and Balmain to be⁽²⁴⁾

$$E_{zi} = -j \left(\frac{30}{\sin k\Delta z} \right) J_i \left(\frac{e^{-jkR_1}}{R_1} + \frac{e^{-jkR_2}}{R_2} - 2 \cos k\Delta z \frac{e^{-jkr}}{r} \right) \quad (2.2.6)$$

where

E_{zi} = electric field due to I_i

$$R_1 = \sqrt{a^2 + \{z - (i+1)\Delta z\}^2}$$

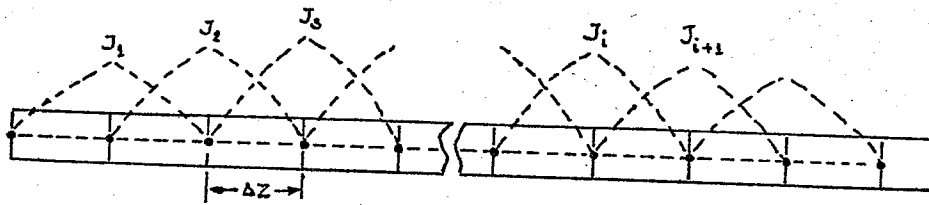


Fig. 2.2 Current distribution as the sum of triangular sinusoidal pulses.

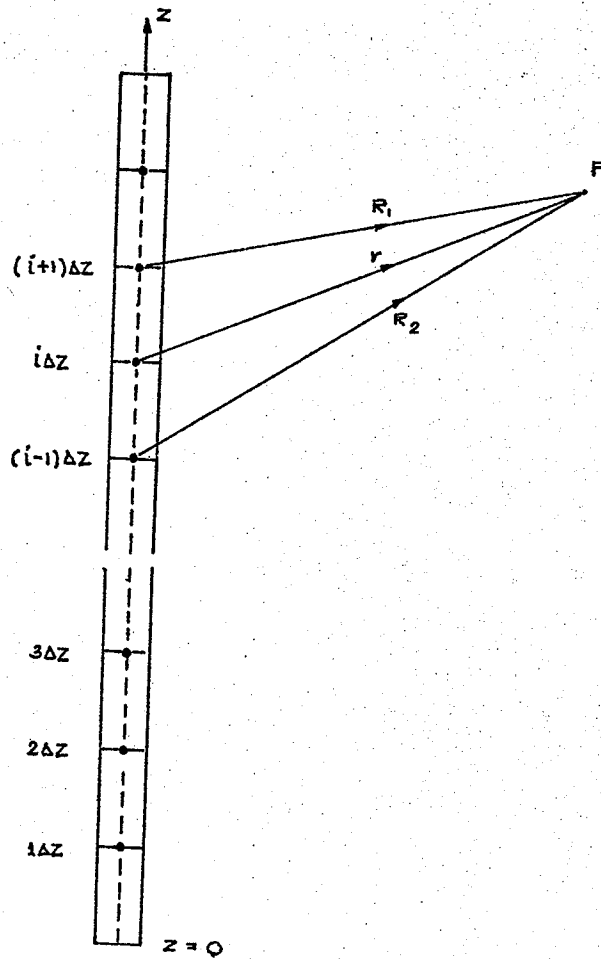


Fig. 2.3 Geometry for fields near the antenna.

$$R_2 = \sqrt{a^2 + \{z - (i - 1)\Delta z\}^2}$$

$$r = \sqrt{a^2 + (z - i\Delta z)^2}$$

Thus the total electric field at observation point P, as shown in fig. 2.3, is

$$\begin{aligned} E_z &= \sum_{i=1}^{N-1} E_{zi} \\ &= \sum_{i=1}^{N-1} \left(\frac{-j 30}{\sin k\Delta z} \right) J_i \left(\frac{e^{-jkR_1}}{R_1} + \frac{e^{-jkR_2}}{R_2} - 2 \cos k\Delta z \frac{e^{-jkr}}{r} \right) \quad (2.2.7) \end{aligned}$$

For a perfectly conducting wire antenna we have

$$E_z = -E_z^i$$

Hence

$$E_z^i = \sum_{i=1}^{N-1} \left(\frac{j 30}{\sin k\Delta z} \right) J_i \left(\frac{e^{-jkR_1}}{R_1} + \frac{e^{-jkR_2}}{R_2} - 2 \cos k\Delta z \frac{e^{-jkr}}{r} \right) \quad (2.2.8)$$

From which the following expression is obtained.

$$v(z_m) = \sum_{i=1}^{N-1} Z(m, i) J_i \quad ; \quad m = 1, 2, \dots, N-1 \quad (2.2.9)$$

where

$$\begin{aligned} Z(m, i) &= \left(\frac{j 30}{\sin k\Delta z} \right) \int_{(m-\frac{1}{2})\Delta z}^{(m+\frac{1}{2})\Delta z} \left(\frac{e^{-jkR_1}}{R_1} + \frac{e^{-jkR_2}}{R_2} - 2 \cos k\Delta z \frac{e^{-jkr}}{r} \right) dz \\ &\quad (2.2.10a) \end{aligned}$$

or

$$\begin{aligned}
Z(m,i) = & \left(\frac{j30\Delta z}{\sin k\Delta z} \right) \left(\frac{e^{-jk\sqrt{a^2 + \{(m-i-1)\Delta z\}^2}}}{\sqrt{a^2 + \{(m-i-1)\Delta z\}^2}} \right. \\
& + \frac{e^{-jk\sqrt{a^2 + \{(m-i+1)\Delta z\}^2}}}{\sqrt{a^2 + \{(m-i+1)\Delta z\}^2}} \\
& \left. - 2 \cos k\Delta z \frac{e^{-jk\sqrt{a^2 + \{(m-i)\Delta z\}^2}}}{\sqrt{a^2 + \{(m-i)\Delta z\}^2}} \right) \quad (2.2.10b)
\end{aligned}$$

When the testing functions are pulses of width Δz or delta functions, respectively.

Equation (2.2.9) can be written in matrix form as

$$[V] = [Z][J] \quad (2.2.11)$$

where $[Z]$ is a matrix with elements given by equation (2.2.10).

Hence

$$[V] = [Z][J] \quad (2.2.12)$$

where

$[Z]$ = generalized impedance matrix

$[V]$ = excitation matrix

$$= \begin{bmatrix} V_1 \\ \cdot \\ \cdot \\ \cdot \\ V_{N-1} \end{bmatrix}$$

$$[J] = \begin{bmatrix} J_1 \\ \cdot \\ \cdot \\ \cdot \\ J_{N-1} \end{bmatrix}$$

From equation (2.2.12) we obtain

$$\begin{aligned} [J] &= [Z]^{-1}[V] \\ &= [Y][V] \end{aligned} \quad (2.2.13)$$

From equation (2.2.12) it is possible, when the current distribution at $N-1$ different points along the antenna is specified, to find the values of excitations at $N-1$ points in order to obtain the specified current distribution. From equation (2.2.13) the current distribution can be determined when the excitation voltages along the antenna are given.

2.2.2 Extension to Loaded Dipole

For a loaded dipole antenna equation (2.2.12) can be modified as

$$[Z][J] = [V_0] + [V_L] \quad (2.2.14)$$

Where $[V_0]$ is the excitation matrix which for a center-driven antenna is given by

$$[V_0] = \begin{bmatrix} 0 \\ \cdot \\ V_0 \\ \cdot \\ 0 \end{bmatrix}$$

$$[V_L] = -[Z_L][J]$$

$[Z_L]$ = diagonal load matrix

It should be noted that the above modification neglects the effect of radiation from the impedance loads.

From equation (2.2.14) we may write

$$[Z + Z_L][J] = [V_0] \quad (2.2.15)$$

which permits determination of:

- (a) input impedance of antenna due to multiple loading
- (b) current distribution due to multiple loading and
- (c) current distribution due to multiple loading and excitation.

Also equations (2.2.14) and (2.2.15) will be used in the analysis to be presented in later chapters.

2.3 Numerical Results

2.3.1 Unloaded Dipole

The computer program for calculation of the current distribution of an unloaded dipole antenna is written based on the method of moment just described. The computations have been made for typical antennas for which extensive measurements and calculations are available. For these antennas $a/\lambda = 7.022 \times 10^{-3}$, the parameters for the two critical lengths $\beta_0 h = \pi/2$ (with $\Omega = 2\ln(2h/a) = 8.54$) and $\beta_0 h = \pi$ (with $\Omega = 9.92$) are chosen. The numerical results are shown in figures 2.4 and 2.5. From the comparison with other results shown, it is found that, in general, our results based on the method of moments agree very well with

those obtained by experiment. However, these results are a little different from the results based on the three-term theory. These differences can be attributed to the discarding of higher order terms in the three-term theory. The differences, due to the assumed geometry of the input terminal of the antenna, can indeed give a different value for the input impedance.

2.3.2 Loaded Dipole

For the case of a loaded dipole antenna, the numerical results obtained for the current distribution are compared with those of Altshuler⁽¹⁴⁾. The antenna under consideration has a radius $a = 0.3175$ cm, length $L = 62$ cm and is operated at a frequency of 600 MHz. The antenna is loaded with a resistive load at $\lambda/4$ from the ends. The agreement between the theoretical current by the method of moment and the experimental current by Altshuler is quite good as shown in figure 2.6. The small disagreement can be attributed largely to the assumed geometry of the feed gap, i.e. whether the excitation is that of a delta function generator or a capacitor feed in the other extreme of a wide gap.

The numerical results for the current distribution of a loaded dipole are shown in figures 2.7 to 2.9 for an inductive load, in figures 2.10 to 2.12 for a capacitive load and in figures 2.13 to 2.15 for a resistive load. In all cases the magnitude of loads are arbitrarily chosen to be 2500 ohms. The antennas under consideration are of the same radius $a = 0.150$ cm and for each type of load three different lengths are chosen for comparison. From the results shown it is found that the current distributions are largely modified by the loading when

compared with the corresponding unloaded antennas. The current distributions of dipole are also different for different types of load. With the effect of load on the current distribution, the modification of input impedance and radiation pattern is implied. The radiation patterns for dipole antenna loaded with an inductive load of 2500 ohms are shown in figures 2.16 to 2.18. They are different from the corresponding unloaded dipoles. When the dipoles are loaded with the same load, but at the different positions, the effect of loading on the current distribution is different as shown in figure 2.19 which shows the current distribution for different positions of load. Thus the input impedances and the radiation patterns must be different. The radiation patterns for different positions of load are shown in figure 2.20 and 2.21.

In figure 2.22 the theoretical and experimental input impedance of antenna as a function of loading reactance X_L are shown. The theoretical results as obtained by using delta and pulse as testing functions are almost the same. The difference between theoretical and experimental results can be attributed to the errors in simulation of the load reactance and in making the measurement.

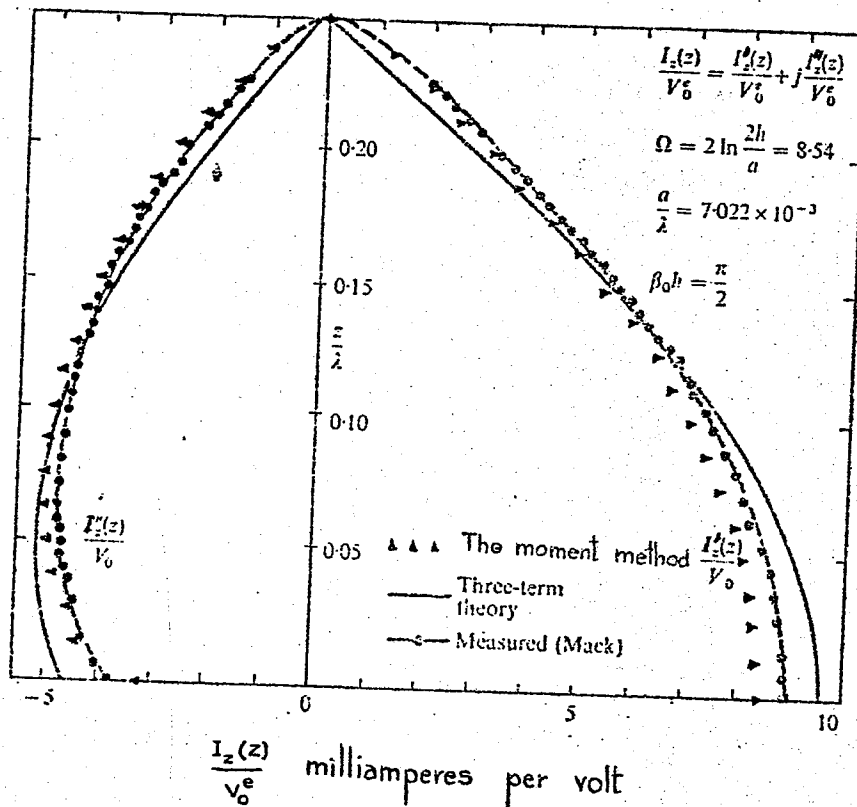


Fig. 2.4 Current in upper half of half-wave dipole. After King et al(30).

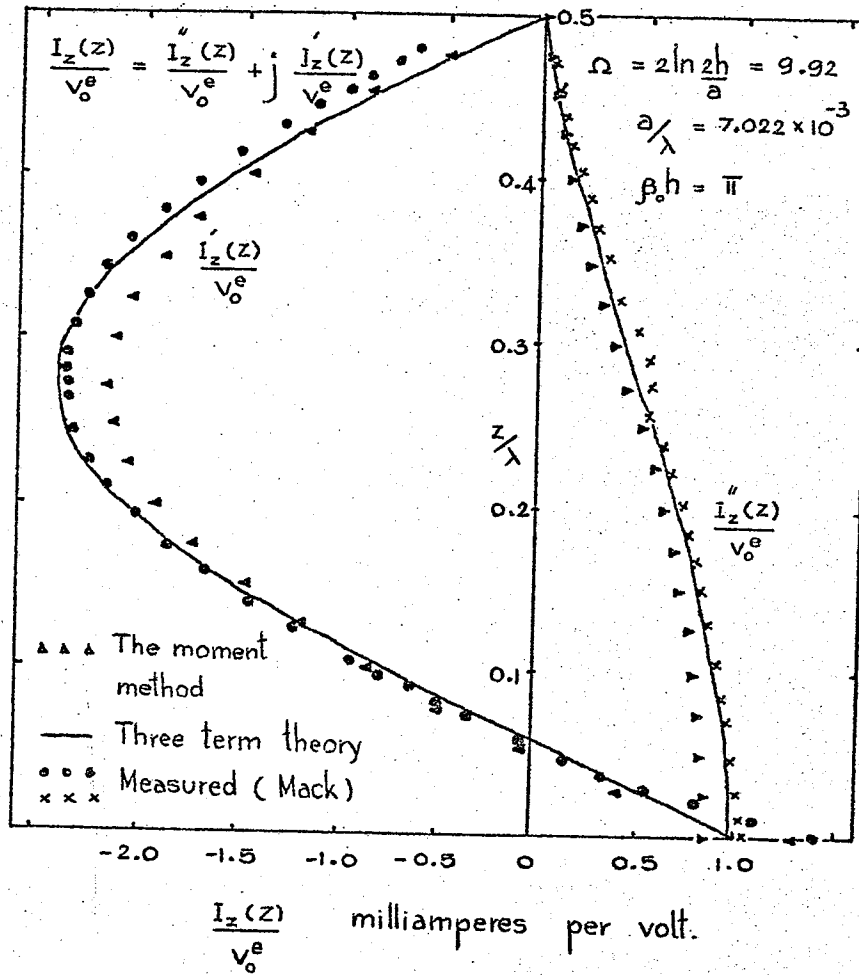


Fig. 2.5 Current in upper half of full-wave dipole. After King et al⁽³⁰⁾.

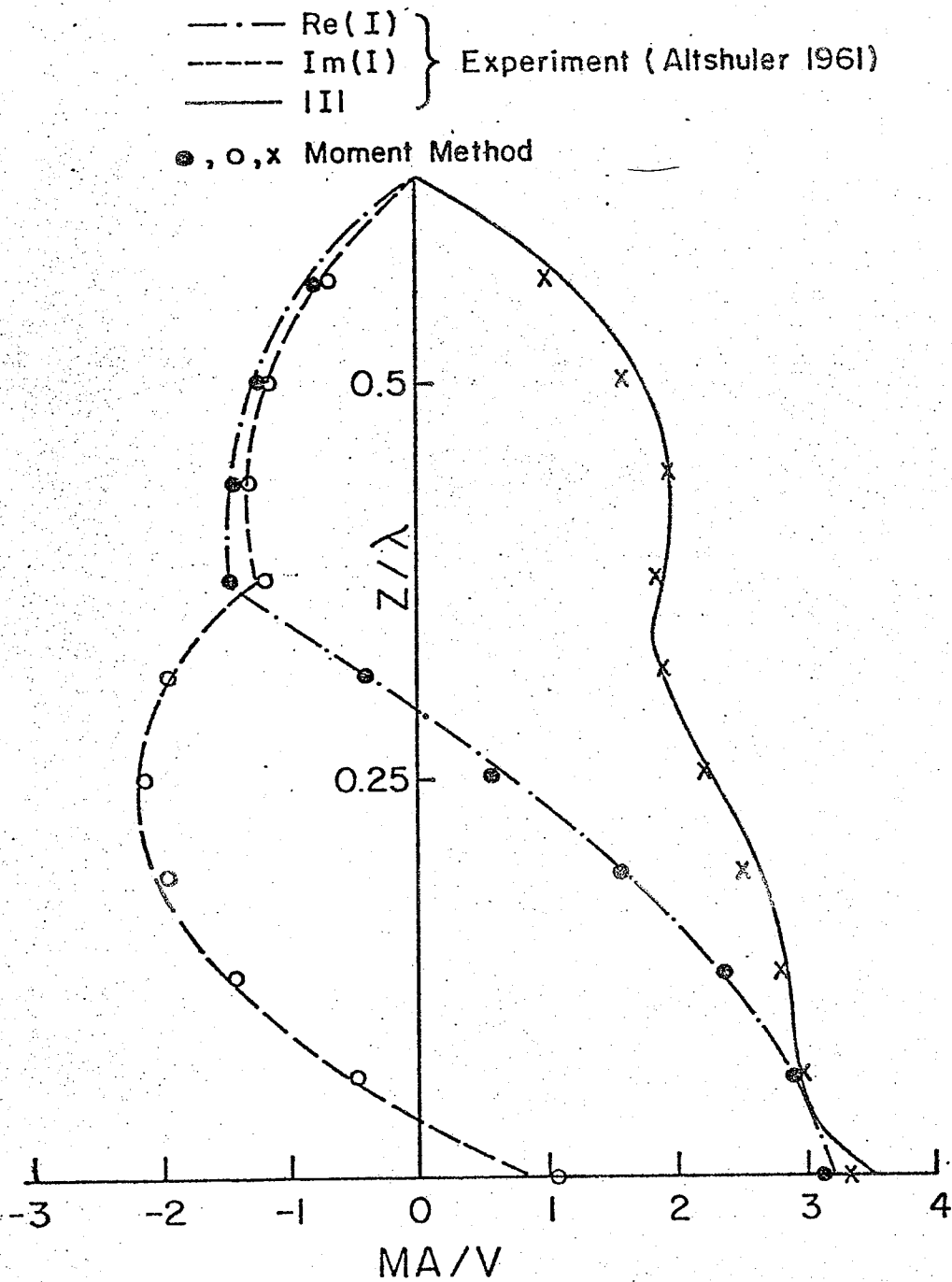


Fig. 2.6 Current in upper half of antenna loaded with resistive load.

(a = 0.3175 cm, h = 31.25 cm, λ = 50.0 cm, d = 18.75 cm,
 Z_L = 240 Ω)

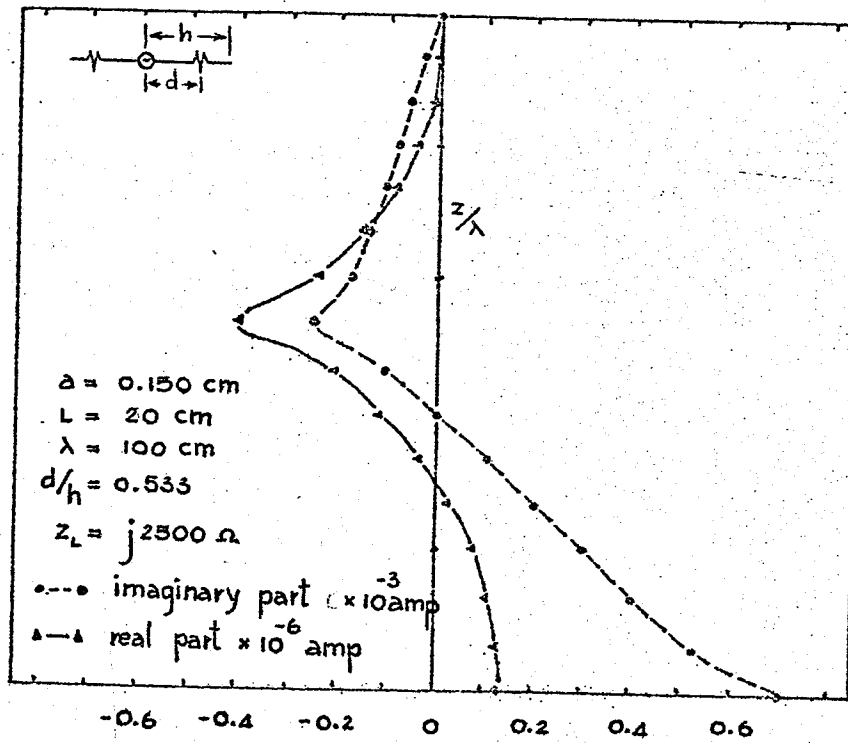


Fig. 2.7 Current in upper half of short dipole loaded with inductive load.

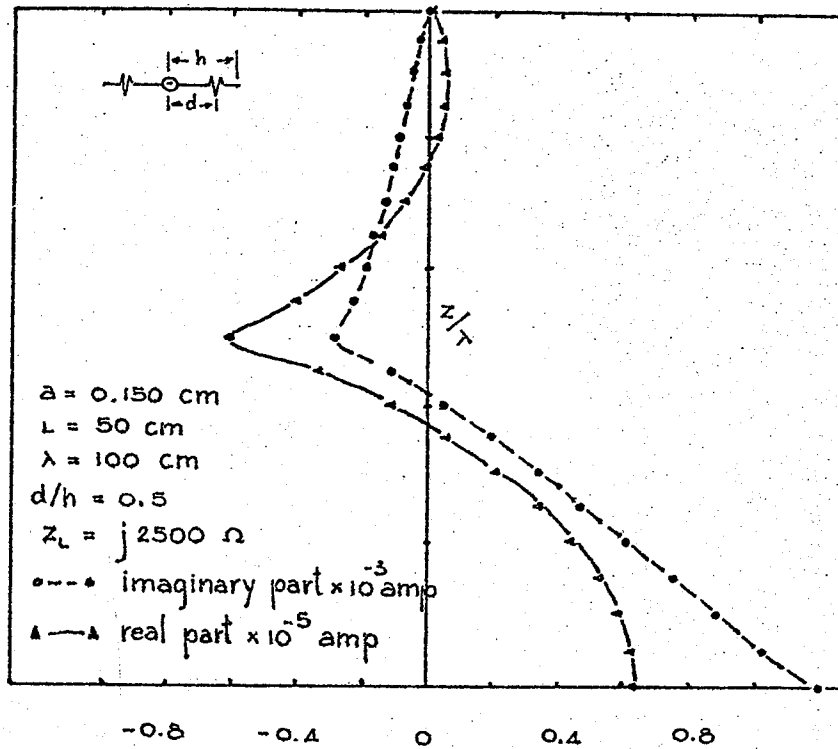


Fig. 2.8 Current in upper half of half-wave dipole loaded with inductive load.

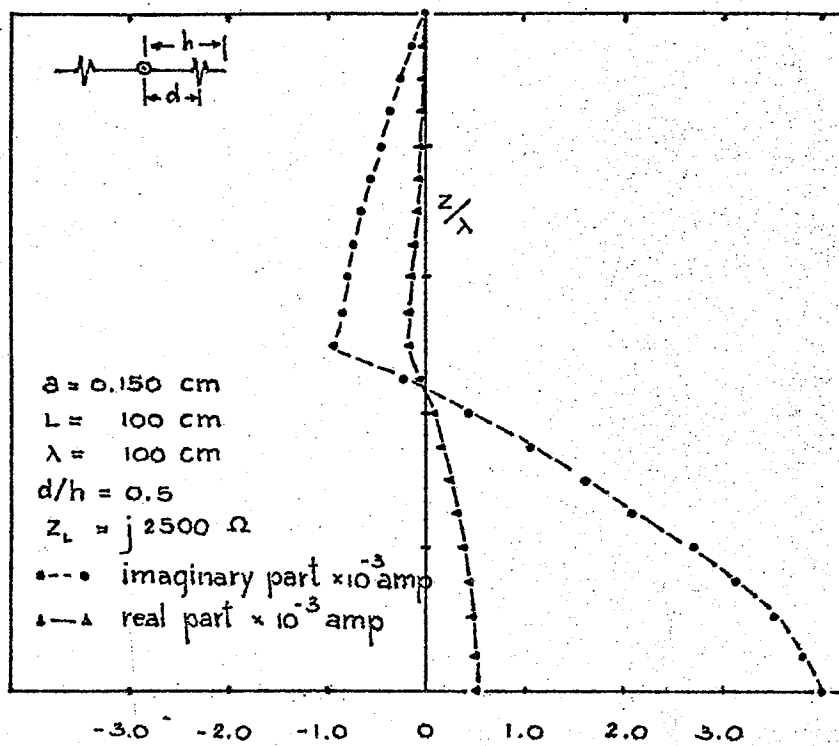


Fig. 2.9 Current in upper half of full-wave dipole loaded with inductive load.

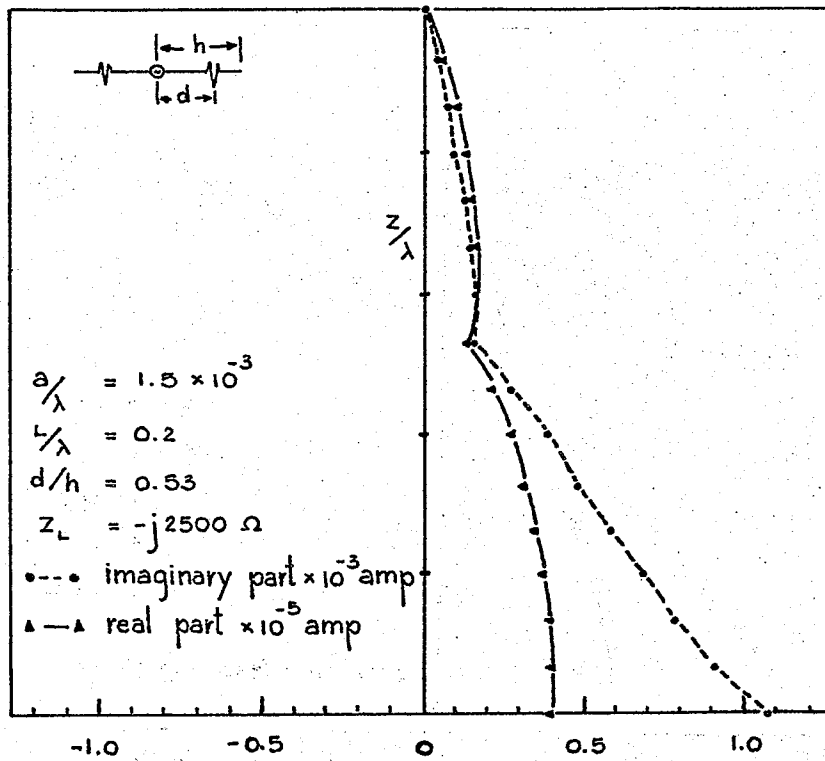


Fig. 2.10 Current in upper half of short dipole loaded with capacitive load.

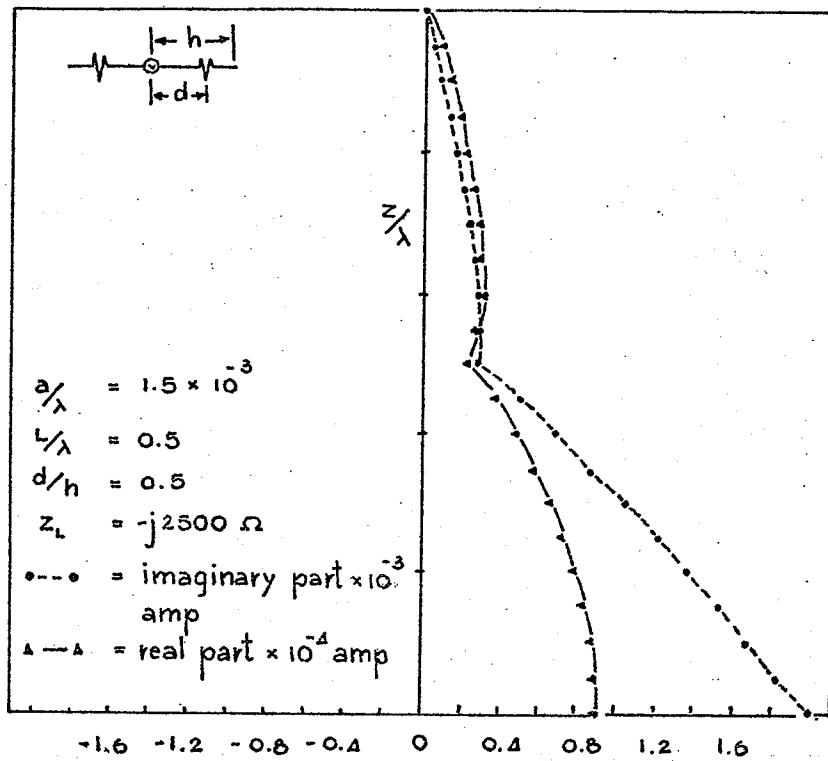


Fig. 2.11 Current in upper half of half-wave dipole loaded with capacitive load.

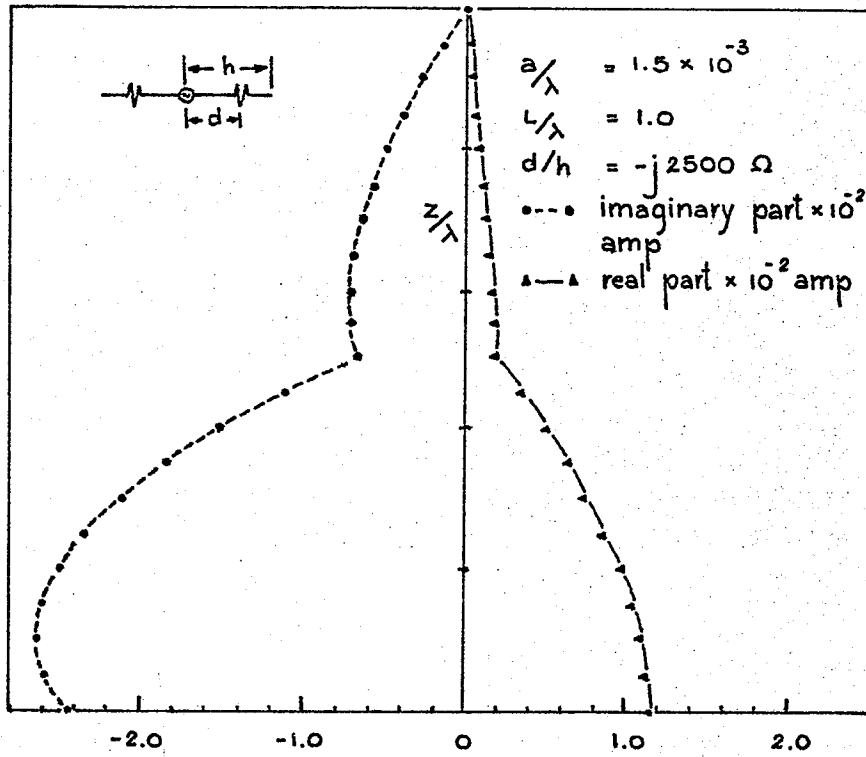


Fig. 2.12 Current in upper half of full-wave dipole loaded with capacitive load.

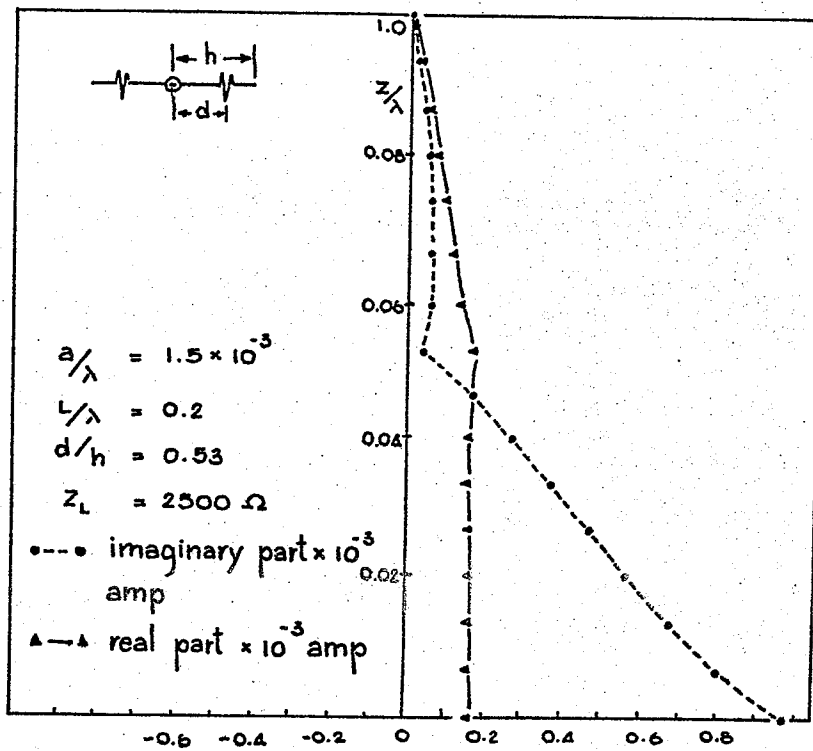


Fig. 2.13 Current in upper half of short dipole loaded with resistive load.

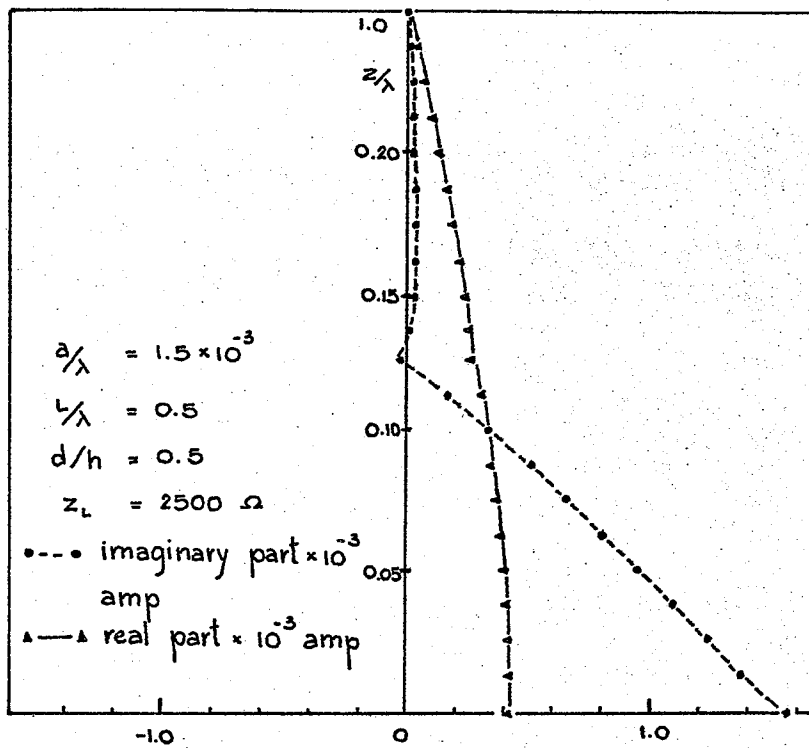


Fig. 2.14 Current in upper half of half-wave dipole loaded with resistive load.

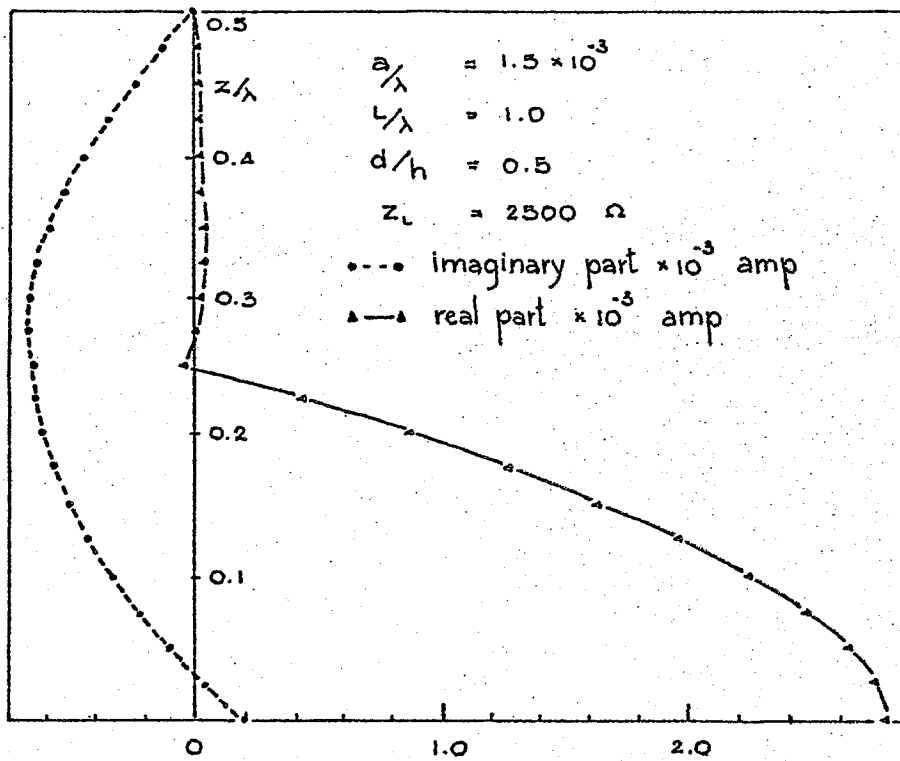


Fig. 2.15 Current in upper half of full-wave dipole loaded with resistive load.

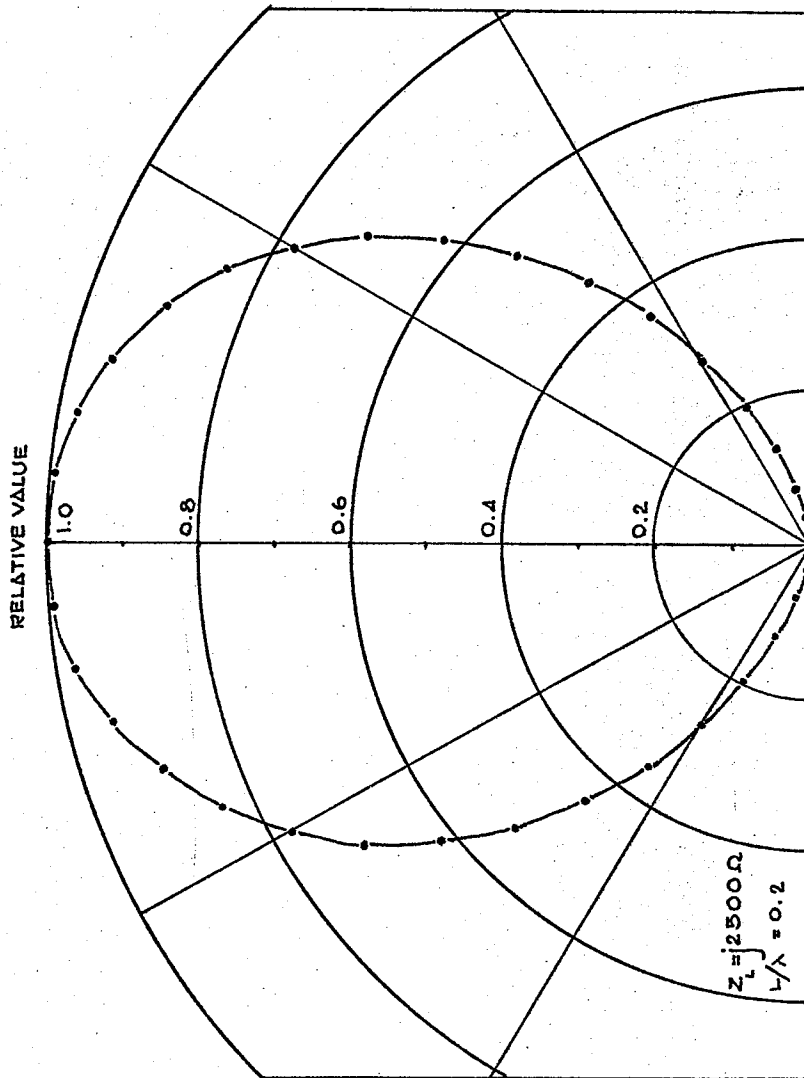


Fig. 2.16 Normalized radiation pattern for short dipole loaded with inductive load.

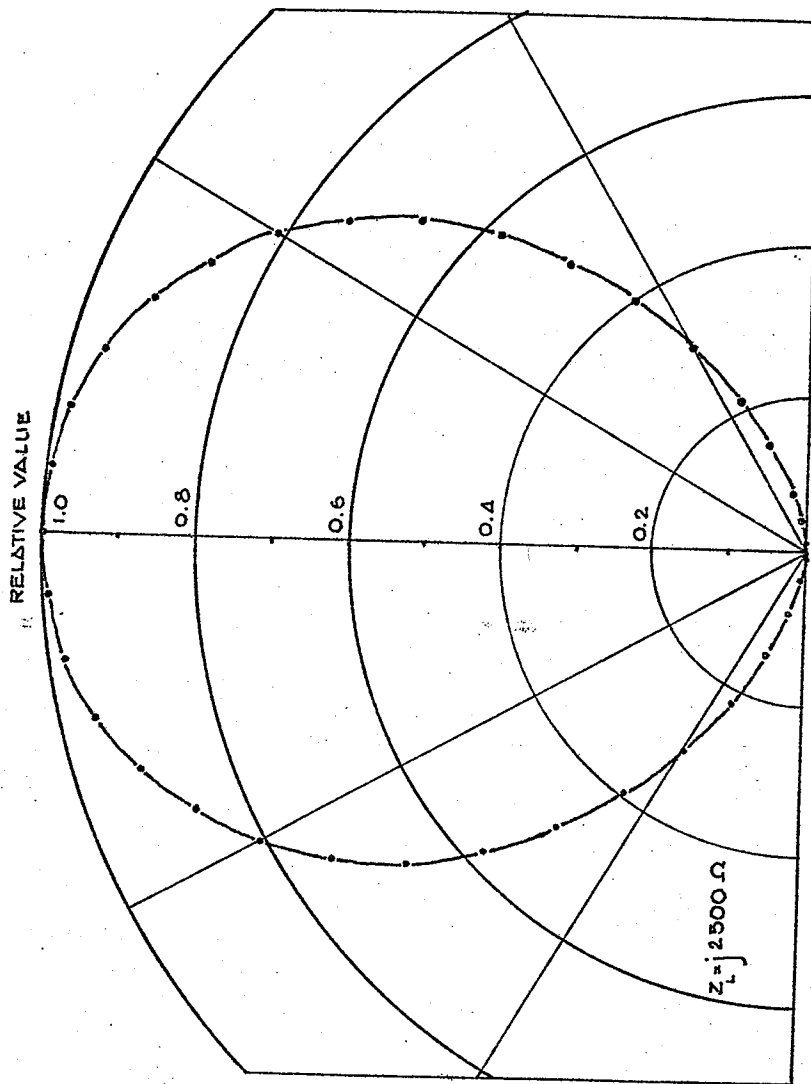


Fig. 2.17 Normalized radiation pattern for half-wave dipole loaded with inductive load.

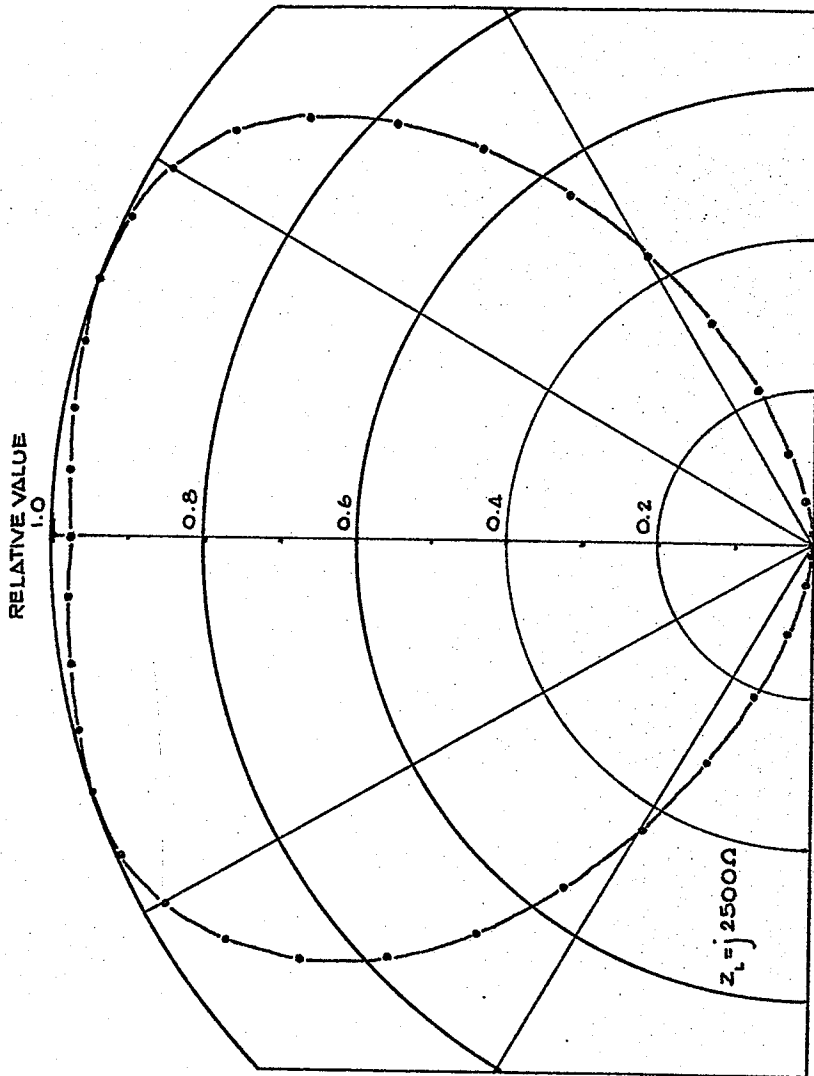


Fig. 2.18 Normalized radiation pattern for full-wave dipole loaded with inductive load.

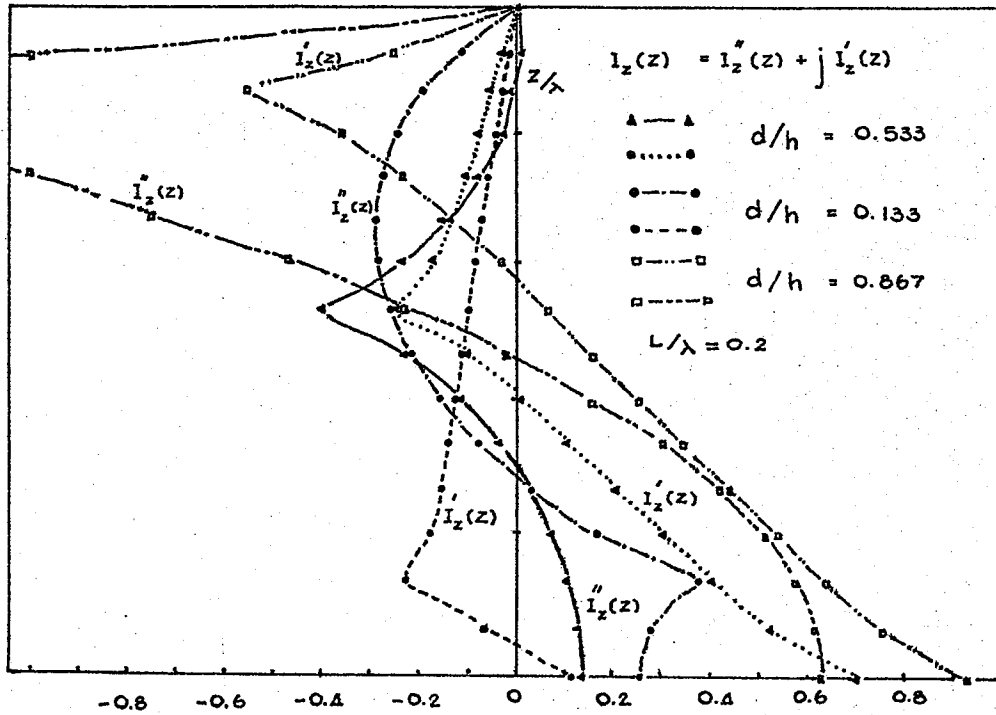


Fig. 2.19 Current in upper half of short dipole loaded with inductive load at various locations.

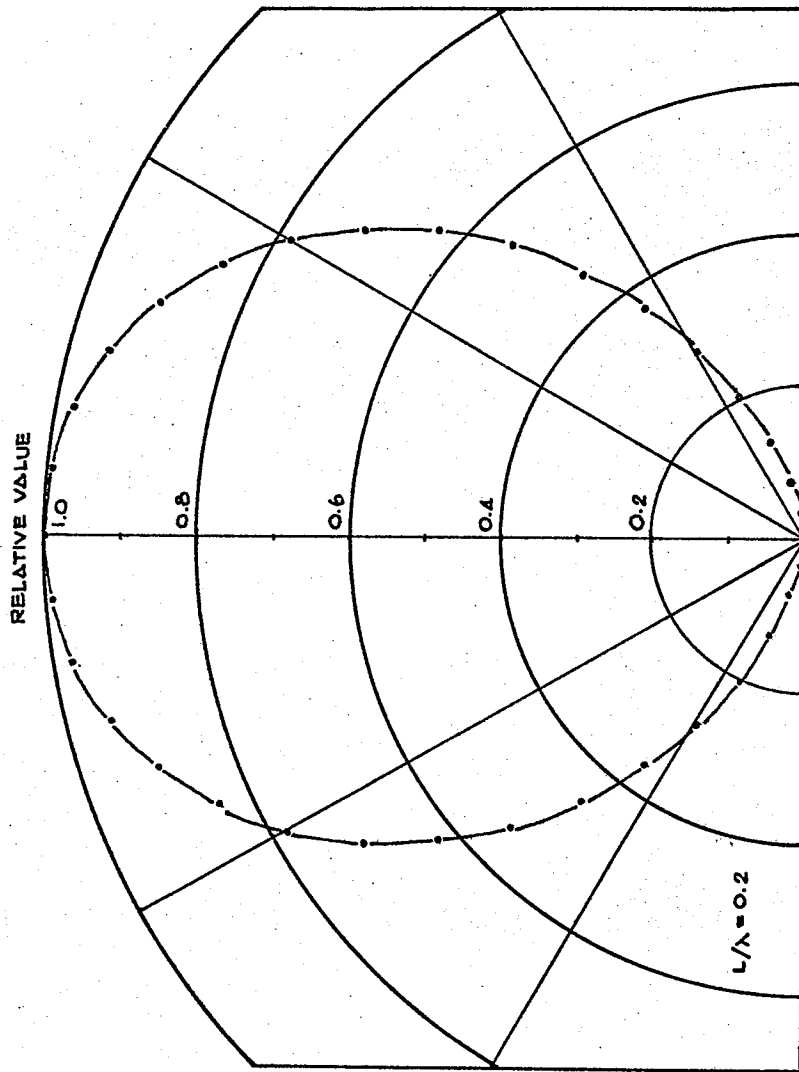


Fig. 2.20 Normalized radiation pattern for short dipole loaded with inductive load at $d/h = 0.867$.

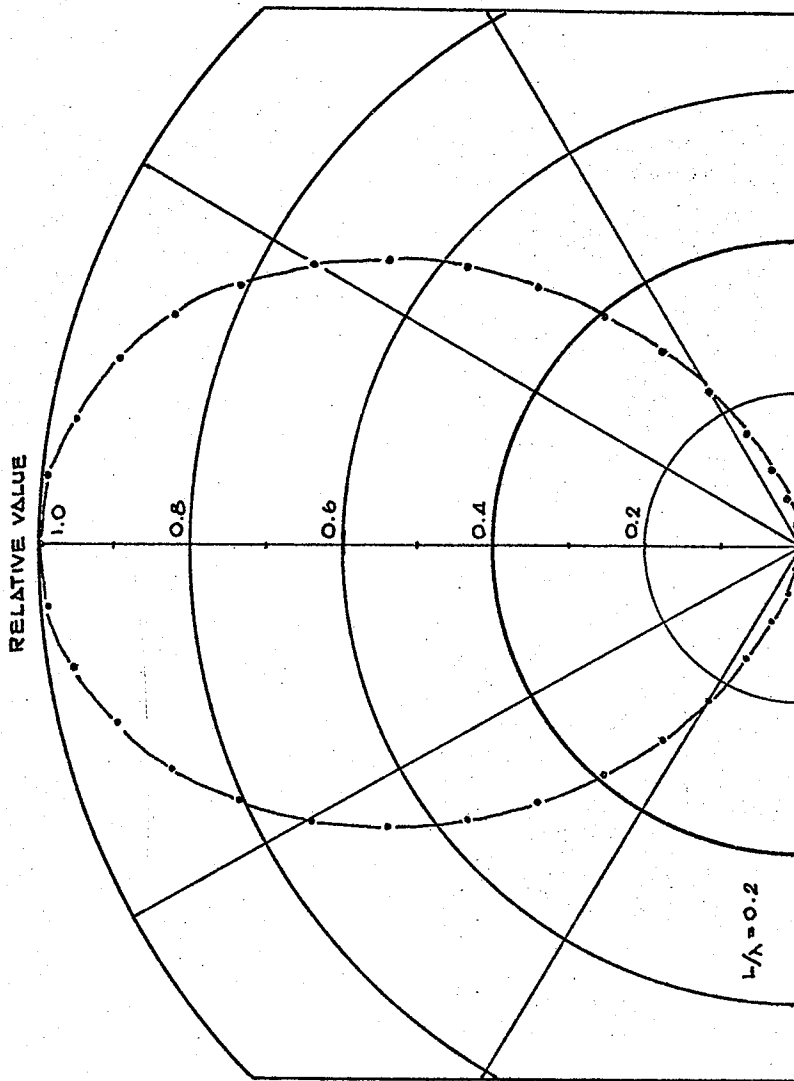


Fig. 2.21 Normalized radiation pattern for short dipole loaded with inductive load at $d/h = 0.133$.

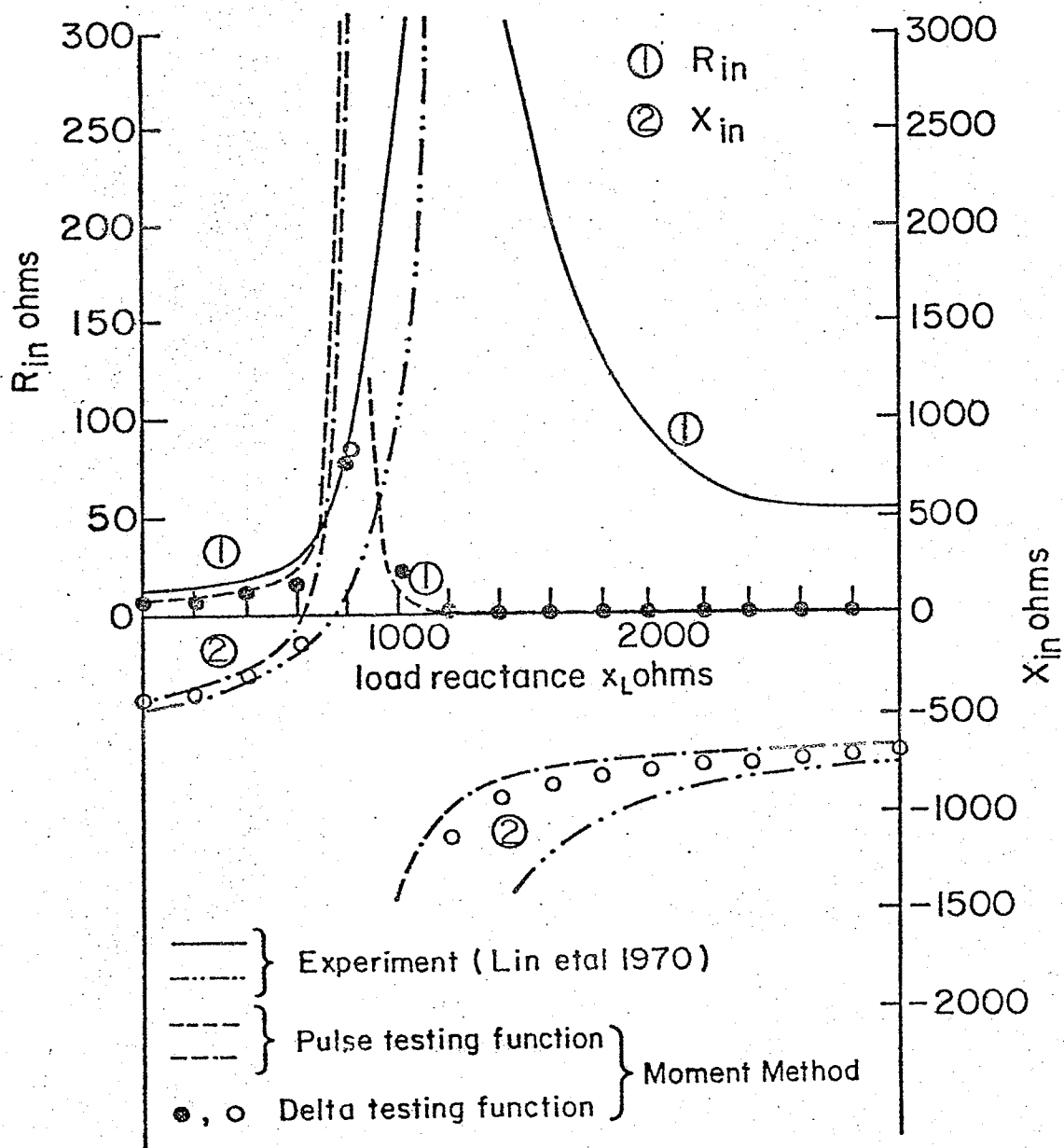


Fig. 2.22 Theoretical and experimental input impedance of antenna as a function of loading reactance X_L for load impedances.

CHAPTER 3

OPTIMIZATION OF DIRECTIVE GAIN

It is well known that the current distribution has a significant effect on the characteristic parameters of a dipole antenna, that is a small change in the current distribution can significantly change the values of some of these parameters. It was shown in Chapter 2 that the current distribution can be changed by lumped impedance loading. Thus with the proper value of load impedance, an improvement in the dipole performance can be achieved. To study the improvement of the directive gain of a dipole by impedance loading, the expression for directive gain as function of connected load impedance based on the method of moment is developed. The directive gain in the desire direction is then maximized with respect to the load impedance. Keep in mind that our model is based on infinitesimally small and symmetrically located loads and, where applicable, lossless reactive load component.

3.1 Derivation of Directive Gain vs Load Impedance

The directive gain is defined as follows⁽²⁵⁾

$$D(\theta, \phi) = 4\pi \frac{\Phi(\theta, \phi)}{P_r} \quad (3.1.1)$$

For a dipole antenna, there is no variation along ϕ because of symmetric property, thus equation (3.1.1) reduces to

$$D(\theta) = 4\pi \frac{\Phi(\theta)}{P_r} \quad (3.1.2)$$

Where $\Phi(\theta)$ is the radiation intensity in the θ direction and P_r is the total radiated power or the power delivered by the generator minus the power dissipated along the dipole wire or lumped impedance loads. The far field of a dipole is given in spherical coordinates by⁽²⁶⁾

$$E_\theta = j \frac{\omega\mu}{4\pi} \sin\theta \int_0^L I(z') \frac{e^{-jkR}}{R} dz' \quad (3.1.3)$$

which after integration, using $I(z')$ given in equation (2.2.4), can be written as

$$E_\theta = j \frac{\omega\mu}{4\pi} \frac{e^{-jkr}}{r} \frac{2}{k \sin k\Delta z} \left[\frac{\cos(k\Delta z \cos\theta) - \cos k\Delta z}{\sin\theta} \right] \sum_{i=1}^{N-1} e^{jki\Delta z \cos\theta} J_i \quad (3.1.4)$$

This equation can be written in the matrix form

$$E_\theta = j \frac{\omega\mu}{4\pi} \frac{e^{-jkr}}{r} \frac{2}{k \sin k\Delta z} \left[\frac{\cos(k\Delta z \cos\theta) - \cos k\Delta z}{\sin\theta} \right] [A] [J] \quad (3.1.5)$$

Where

$$[A] = [e^{jk\Delta z \cos\theta} \ e^{2jk\Delta z \cos\theta} \ \dots \ e^{(N-1)jk\Delta z \cos\theta}] \quad (3.1.6)$$

The radiation intensity of the dipole can be found from the expression⁽²⁷⁾

$$\Phi(\theta) = \frac{r^2}{120\pi} |E_\theta|^2 \quad (3.1.7)$$

Hence

$$\Phi(\theta) = \frac{1}{4\pi} \frac{120}{(\sin k\Delta z)^2} \left[\frac{\cos(k\Delta z \cos\theta) - \cos k\Delta z}{\sin\theta} \right]^2$$

$$[\tilde{J}]^* [A] [A] [\tilde{J}] \quad (3.1.8)$$

Where $[\tilde{\cdot}]^*$ represents the conjugate transpose of the matrix. From equation (2.2.14) we have

$$[Z] [\tilde{J}] = [V_0] + [V_L] = [V]$$

$$[\tilde{J}] = [Z]^{-1} [V]$$

$$= [Y] [V] \quad (3.1.9)$$

Substituting equation (3.1.9) into equation (3.1.8) we obtain

$$4\pi \Phi(\theta) = \frac{120}{(\sin k\Delta z)^2} \left[\frac{\cos(k\Delta z \cos\theta) - \cos k\Delta z}{\sin\theta} \right]^2$$

$$[\tilde{V}]^* [Y]^* [A]^* [A] [Y] [V] \quad (3.1.10)$$

The total radiated power can be determined from the integral expression

$$P_r = \int_0^{2\pi} \int_0^\pi \Phi(\theta, \phi) \sin\theta \, d\theta \, d\phi \quad (3.1.11)$$

Using $\Phi(\theta, \phi)$, as given in equation (3.1.10), integrate and write the result in matrix form

$$P_r = \frac{60}{(\sin k\Delta z)^2} \begin{matrix} \sim^* & \sim^* \\ [V] & [Y] [U] [Y] [V] \end{matrix} \quad (3.1.12)$$

The elements of matrix [U] are given in Appendix A. Hence

$$D(\theta) = 2 \left[\frac{\cos(k\Delta z \cos\theta) - \cos k\Delta z}{\sin\theta} \right]^2$$

$$\frac{\begin{matrix} \sim^* & \sim^* & \sim^* \\ [V] & [Y] [A] [A] [Y] [V] \end{matrix}}{\begin{matrix} \sim^* & \sim^* \\ [V] & [Y] [U] [Y] [V] \end{matrix}} \quad (3.1.13)$$

In this thesis only $\theta = \frac{\pi}{2}$ is considered, thus

$$D = 2 (1 - \cos k\Delta z)^2 \frac{\begin{matrix} \sim^* & \sim^* & \sim^* \\ [V] [Y] [A] [A] [Y] [V] \end{matrix}}{\begin{matrix} \sim^* & \sim^* \\ [V] [Y] [U] [Y] [V] \end{matrix}} \quad (3.1.14)$$

From equation (3.1.14), the optimum value of excitations for maximum 'D' can be determined by maximizing this equation with respect to excitation [V]. But our main emphasis is only devoted to the optimization of 'D' with respect to the connected loads. Though it is possible to obtain loads from a knowledge of optimum [V], by optimizing equation (3.1.14), such load can have negative resistance. To eliminate the possibility of negative resistance, optimization with respect to connected load is performed with the constraint that the real part of the connected load must be positive.

3.2 Optimization of Directive Gain as a Function of Connected Load Impedance

Equation (3.1.14) is rewritten in order to express 'D' as function of the real and imaginary parts of connected load. Let the antenna be loaded at z_j and z_k and fed at z_i as shown in figure 3.2. It can be shown that

$$([I_u] + [Z_L][Y])[V_L] = -[Z_L][Y][V_0] \quad (3.2.1)$$

Where

$[I_u]$ = unit matrix

$$[V_L] = \begin{bmatrix} V_L \\ \vdots \\ \vdots \\ \vdots \\ \vdots \\ V_{LN-1} \end{bmatrix} = -[Z_L][J]$$

$$[V_0] = \begin{bmatrix} 0 \\ \vdots \\ \vdots \\ V_i \\ \vdots \\ \vdots \\ 0 \end{bmatrix}$$

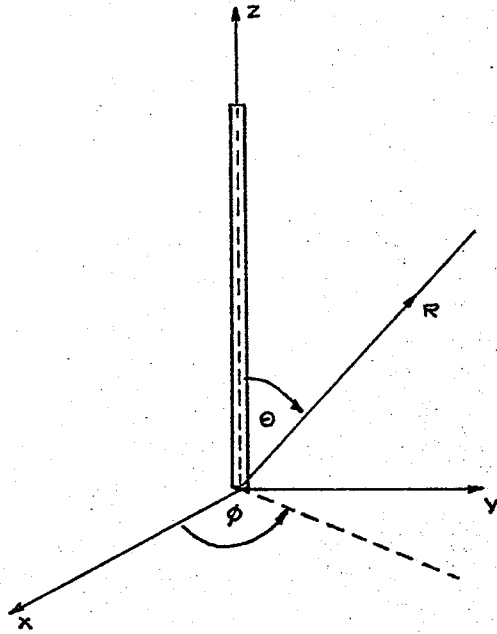


Fig. 3.1 Geometry for far-field of the antenna.

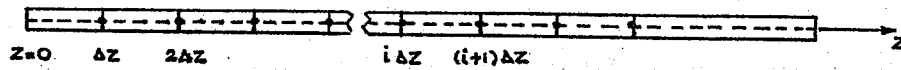


Fig. 3.2 Antenna configuration.

Then V_{Lj} and V_{Lk} can be expressed as

$$V_{Lj} = V_{Lk} = \frac{-y_{ji}}{y_{Lj} + y_{jj} + y_{jk}} V_i \quad (3.2.2)$$

where V_{Lj} and V_{Lk} are the voltage drops due to load impedance at z_j and z_k , respectively.

$$y_{Lj} = \frac{1}{Z_{Lj}} = x'(1) + jx'(2) \quad (3.2.3)$$

$$Z_{Lj} = Z_{Lk}$$

Where Z_{Lj} and Z_{Lk} are connected loads at $z = z_j$ and z_k , respectively.

By using equations (3.2.2) and (3.2.3), 'D' can be written as follows

$$D = 2(1 - \cos k\Delta z)^2 \left(\frac{\gamma_1 + \gamma_2 x^2(1) + \gamma_2 x^2(2) + \gamma_3 x(1) + \gamma_4 x(2)}{\alpha_1 + \alpha_2 x^2(1) + \alpha_2 x^2(2) + \alpha_3 x(1) + \alpha_4 x(2)} \right) \quad (3.2.4)$$

Where the constants $\gamma_1, \gamma_2, \gamma_3, \gamma_4, \alpha_1, \alpha_2, \alpha_3$ and α_4 are determined in Appendix B

$$x(1) = x'(1) + \text{Re}(y_{jj}) + \text{Re}(y_{jk}) \quad (3.2.5)$$

$$x(2) = x'(2) + \text{Im}(y_{jj}) + \text{Im}(y_{jk}) \quad (3.2.6)$$

Equation (3.2.4) is maximized with respect to $x(1)$ and $x(2)$ under the conditions;

- (I) $x(1)$ and $x(2)$ are real.
 (II) $x(1) \geq \operatorname{Re}(y_{jj}) + \operatorname{Re}(y_{jk})$, $x(2)$ arbitrary.

3.3 Numerical Results

Three different lengths L/λ of the dipoles were chosen to equal 0.1, 0.2 and 0.5, respectively. These values of L/λ are arbitrarily selected for the study of the effects of the optimum loads to the dipoles.

Figure 3.3 shows the variation of optimum load value with its position. The results obtained by Lin et al.⁽¹⁸⁾, their method can only be applied to a short dipole, are given here for comparison purposes. It is found that the optimum loads obtained by the method of moments are smaller than those obtained by Lin et al. This is because they neglect the higher order terms in the current distribution which is based on the modified two-term method by King and Wu⁽³⁴⁾.

Tables 3.1 to 3.3 show the input impedance of the antenna loaded with optimum load at different locations along its arms. The current distributions are shown in figures 3.4 to 3.6. Each figure shows the current distribution for the antenna loaded at different locations with the optimum load. The normalized radiation patterns are shown in figures 3.7 to 3.9 for three different lengths of the dipole. In each figure the normalized radiation patterns of the antenna loaded at different locations with the optimum load are also shown. The significance of these results is discussed in Chapter 7.

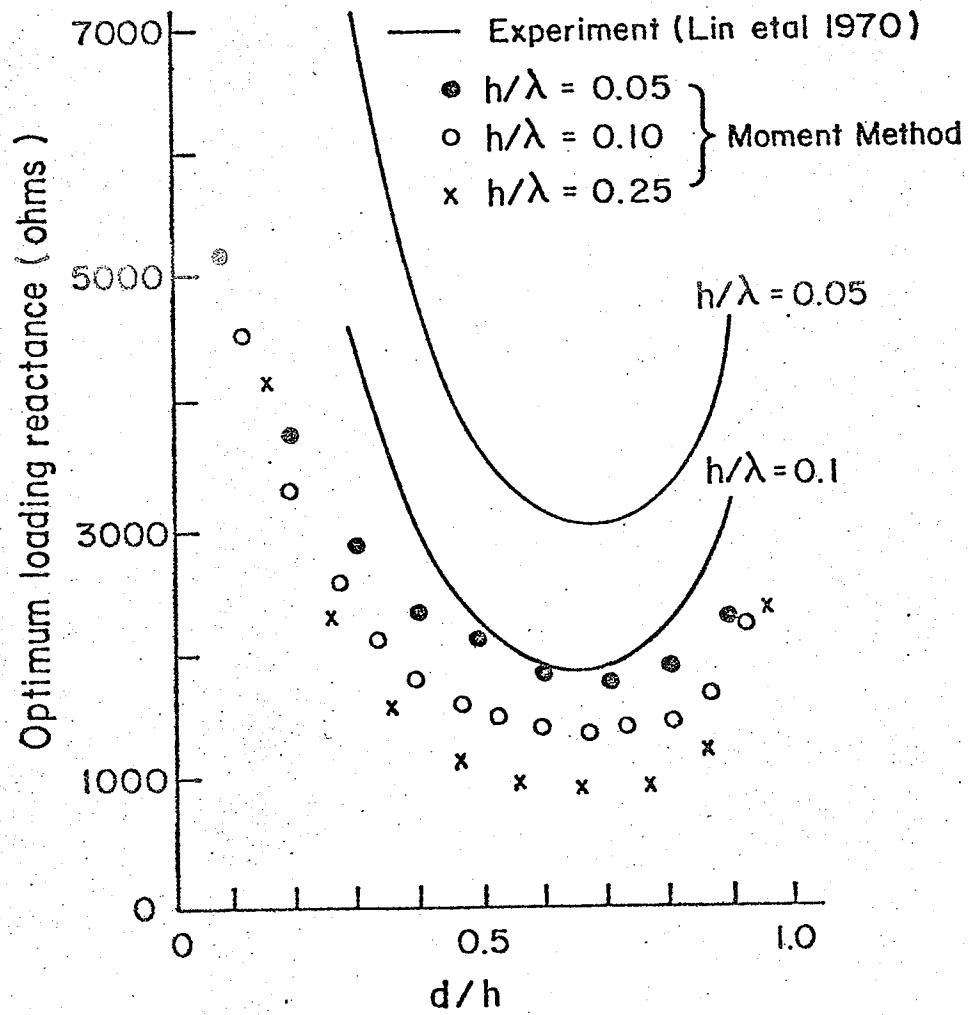


Fig. 3.3 Optimum loading impedances as functions of d/h for various h/λ .

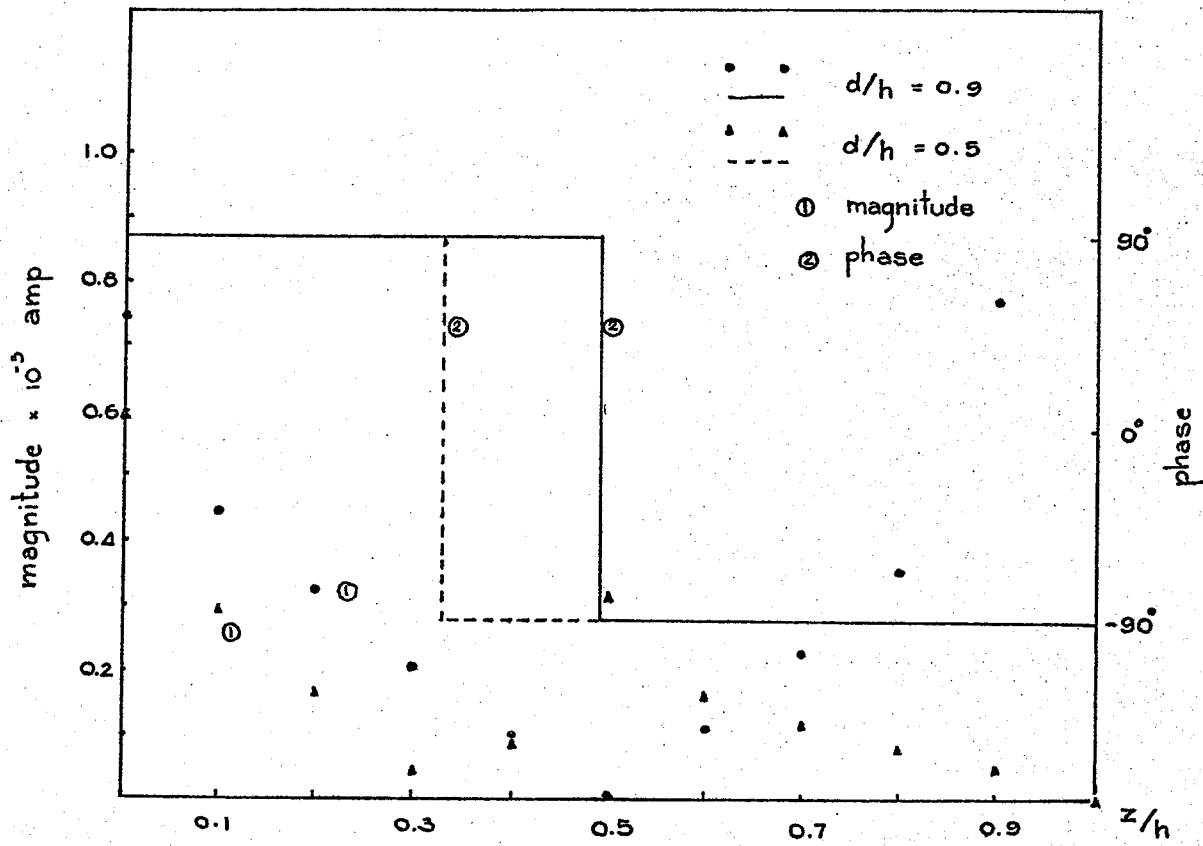


Fig. 3.4 Current distribution for $L/\lambda = 0.1$ dipole loaded with optimum load for maximum directivity.

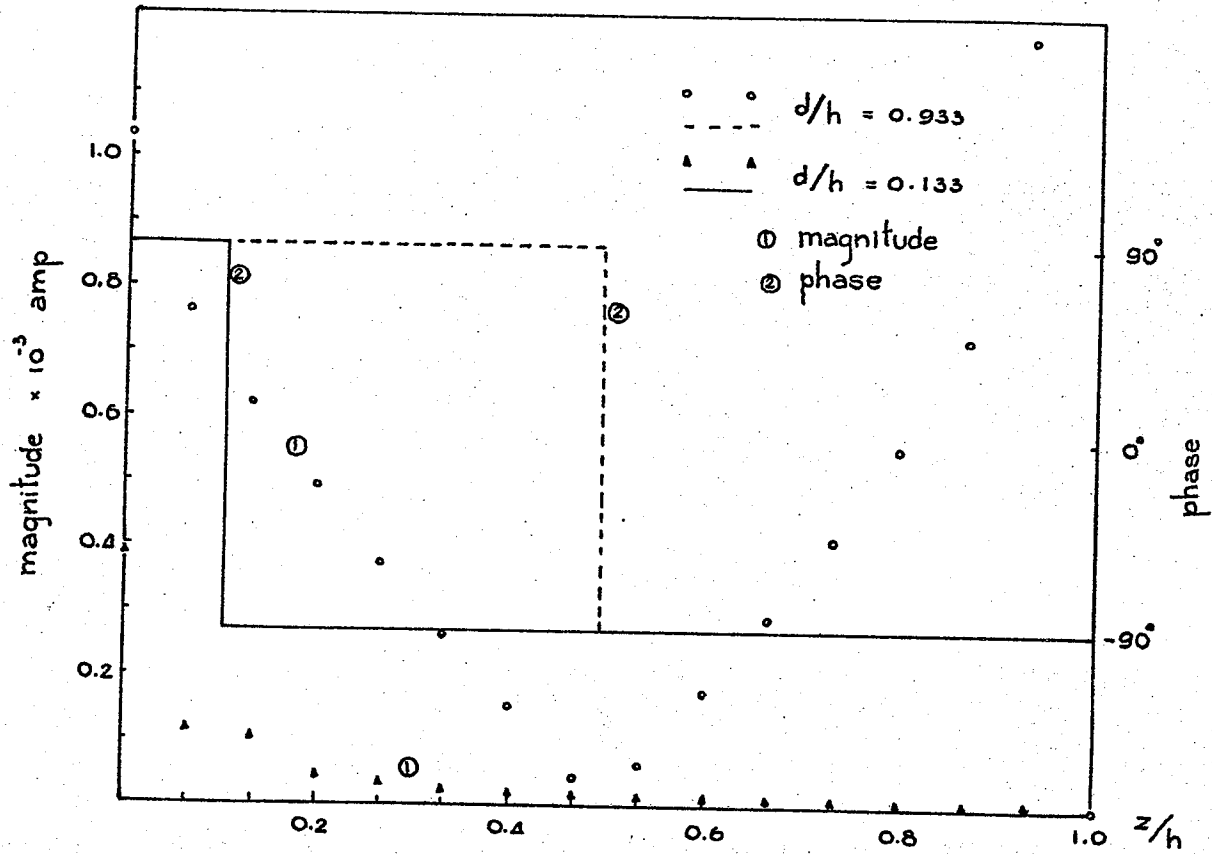


Fig. 3.5 Current distribution for $L/\lambda = 0.2$ dipole loaded with optimum load for maximum directivity.

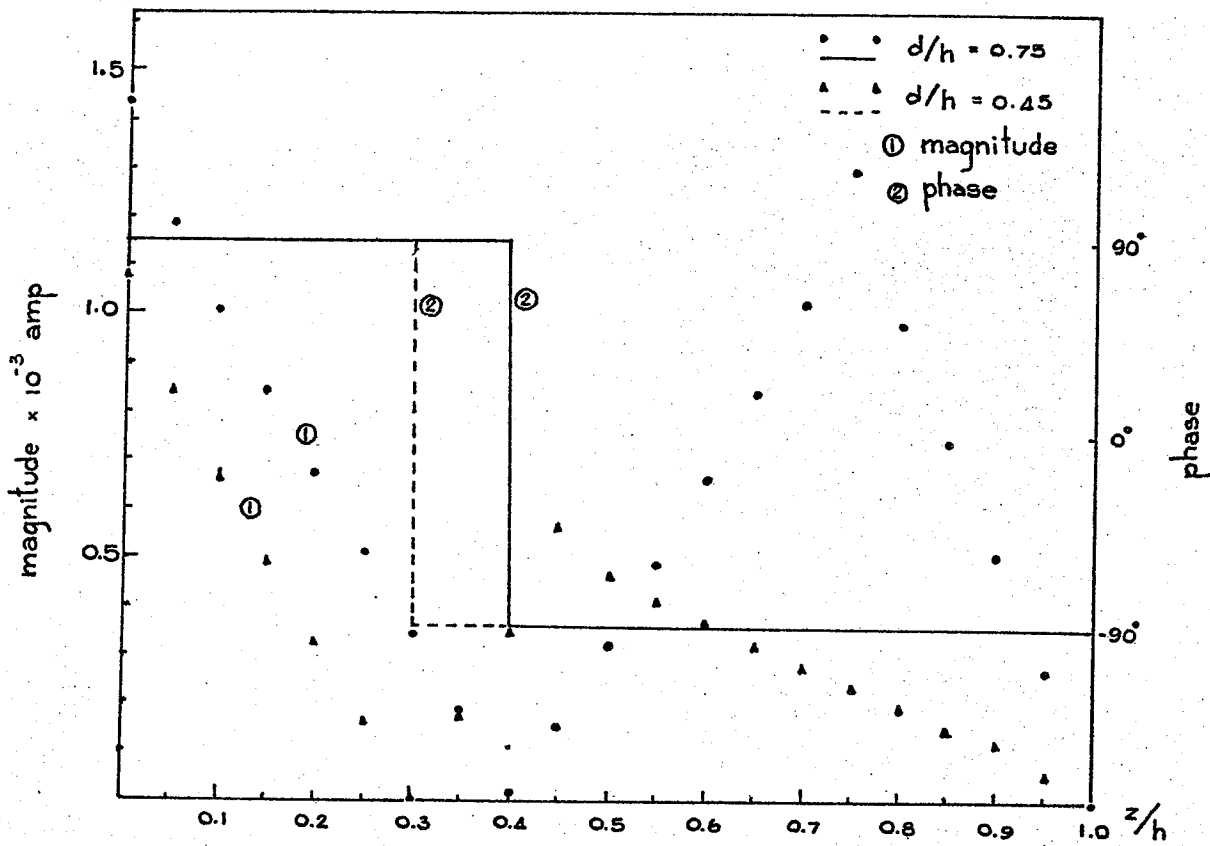


Fig. 3.6 Current distribution for half-wave dipole loaded with optimum load for maximum directivity.

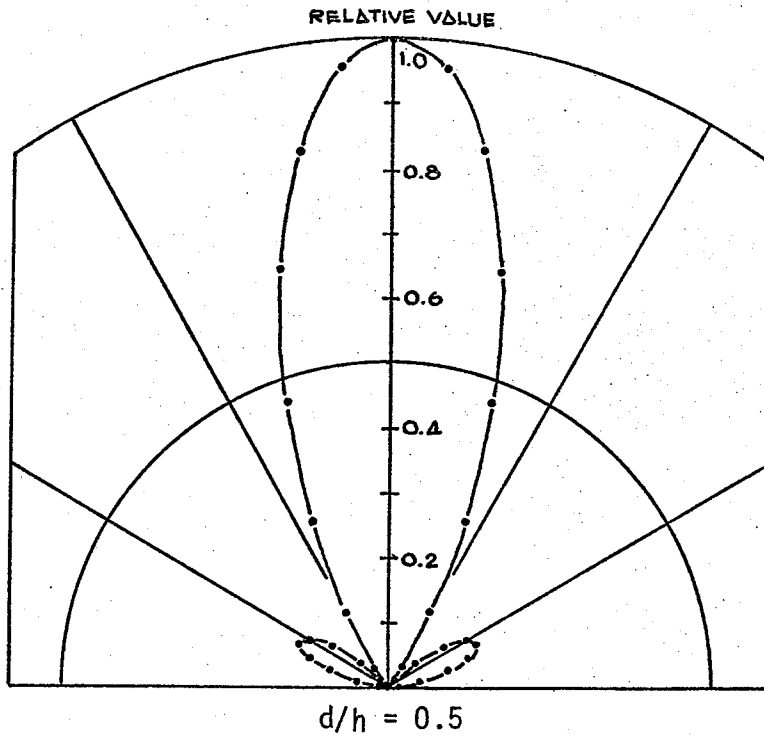
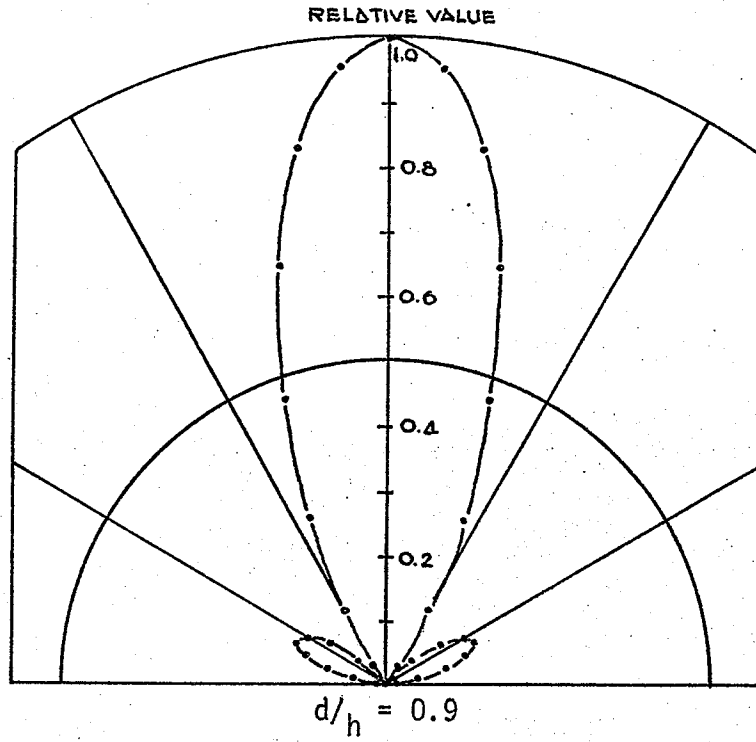
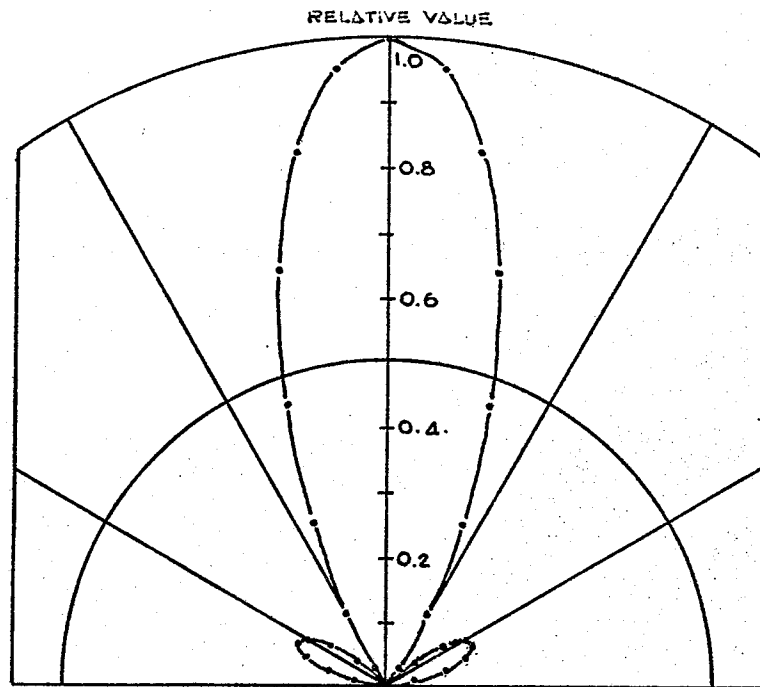
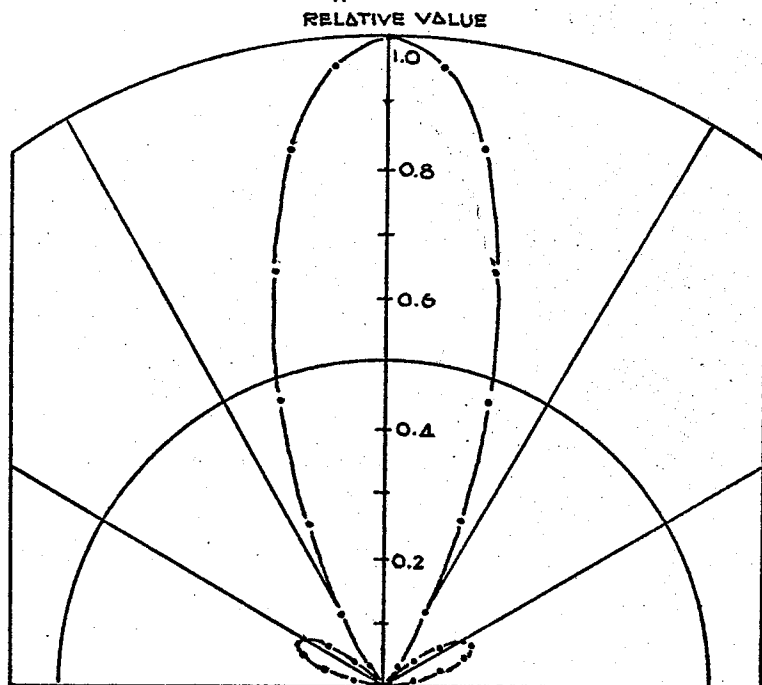


Fig. 3.7 Normalized radiation pattern for $L/\lambda = 0.1$ dipole loaded with optimum load for maximum directivity



$$d/h = 0.933$$



$$d/h = 0.133$$

Fig. 3.8 Normalized radiation pattern for $L/\lambda = 0.2$ dipole loaded with optimum load for maximum directivity

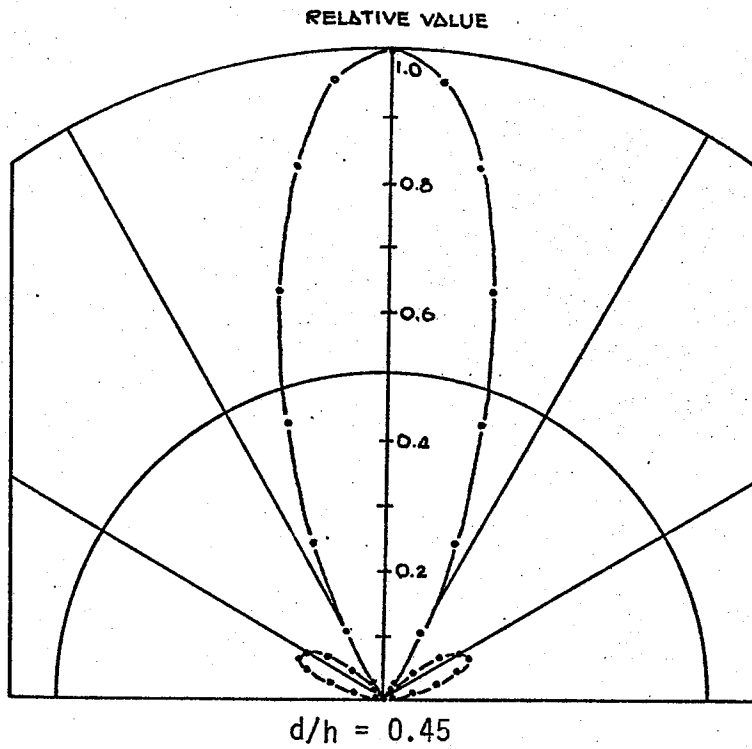
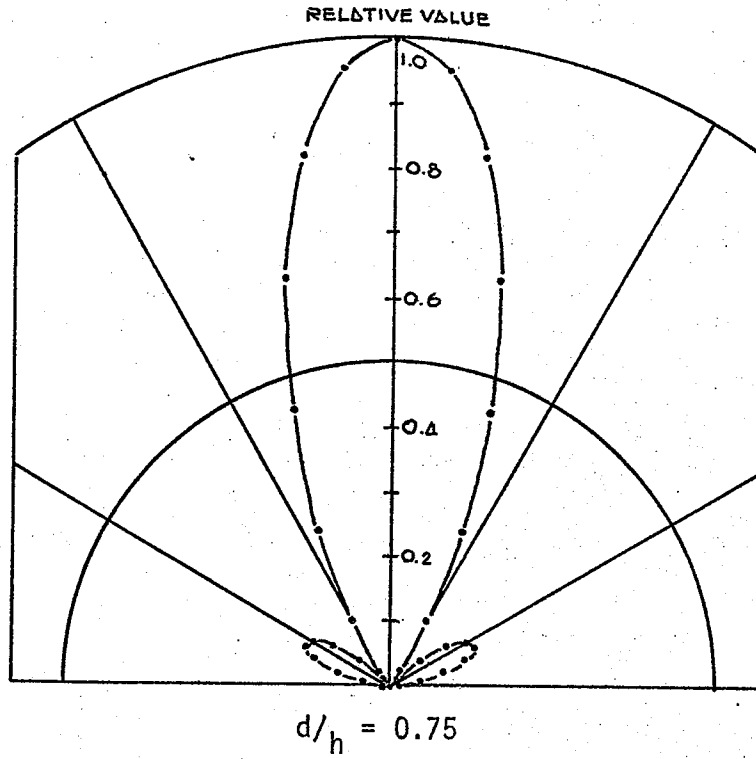


Fig. 3.9 Normalized radiation pattern for half-wave dipole loaded with optimum load for maximum directivity

Table 3.1

Relationships of load impedance, antenna input impedance and directivity at various loading points for $L/\lambda = 0.1$ dipole

d/h	Z_L OHMS	Z_{IN} OHMS		DIRECTIVITY
		R_{in}	X_{in}	
0.1	j5197.99	2.68×10^{-8}	-3414.625	2.813
0.2	j3726.67	2.35×10^{-7}	-2522.096	2.813
0.3	j2836.08	8.23×10^{-7}	-2095.581	2.813
0.4	j2323.70	2.03×10^{-6}	-1848.210	2.813
0.5	j2012.76	4.15×10^{-6}	-1683.543	2.814
0.6	j1836.69	7.63×10^{-6}	-1564.943	2.814
0.7	j1775.34	1.33×10^{-5}	-1474.750	2.814
0.8	j1857.12	2.02×10^{-5}	-1403.048	2.814
0.9	j2230.09	3.03×10^{-5}	-1342.120	2.815

Table 3.2

Relationships of load impedance, antenna input impedance and directivity at various loading points for $L/\lambda = 0.2$ dipole

d/h	Z_L OHMS	Z_{IN} OHMS		DIRECTIVITY
		R_{in}	X_{in}	
0.933	j7337.565	0.899×10^{-6}	-3818.404	2.820
0.867	j4589.930	0.650×10^{-5}	-2567.721	2.820
0.800	j3331.452	0.213×10^{-4}	-2044.707	2.820
0.733	j2611.747	0.484×10^{-4}	-1748.975	2.820
0.667	j2151.716	0.952×10^{-4}	-1555.732	2.821
0.600	j1842.181	0.162×10^{-3}	-1418.255	2.821
0.533	j1629.554	0.260×10^{-3}	-1314.920	2.822
0.467	j1485.539	0.397×10^{-3}	-1234.111	2.823
0.400	j1395.358	0.575×10^{-3}	-1168.931	2.824
0.333	j1353.318	0.794×10^{-3}	-1115.055	2.825
0.267	j1362.719	0.112×10^{-2}	-1069.903	2.826
0.200	j1443.180	0.144×10^{-2}	-1030.868	2.827
0.133	j1655.851	0.188×10^{-2}	-996.988	2.828
0.067	j2260.289	0.244×10^{-2}	-966.485	2.829

Table 3.3

Relationships of load impedance, antenna input impedance and directivity at various loading points for half-wave dipole

d/h	Z_L OHMS	Z_{IN} OHMS		DIRECTIVITY
		R_{in}	X_{in}	
0.05	j13357.58	2.81×10^{-4}	-4311.575	2.865
0.15	j 4195.75	4.49×10^{-3}	-1910.677	2.866
0.25	j 2288.64	1.73×10^{-2}	-1344.414	2.868
0.35	j 1518.09	4.34×10^{-2}	-1080.482	2.871
0.45	j 1144.51	8.85×10^{-2}	-925.597	2.875
0.55	j 957.75	1.59×10^{-1}	-823.094	2.880
0.65	j 885.82	2.64×10^{-1}	-750.005	2.885
0.75	j 919.59	4.14×10^{-1}	-695.243	2.892
0.85	j1138.96	6.25×10^{-1}	-652.621	2.900
0.95	j2313.07	9.15×10^{-1}	-618.361	2.909

CHAPTER 4

OPTIMIZATION OF RADIATED POWER

It is already known that the dipole antenna is a poor radiator, especially for short lengths when the input impedance consists of a very small resistive part and a very large capacitive part. Even with their poor radiated power, dipole antennas have been employed in many applications, such as in the field of radio communications where extended coverage can be achieved and with matching networks sensing to minimize the effects of the large capacitive reactance.

The radiated power of a dipole antenna can be easily calculated if its input current and radiation resistance are known. Usually with only a knowledge of the current distribution, the radiated power can also be determined. It was already shown in Chapter 2 that the modification of current distribution can be realized with lumped impedance loading in series with the arms. Hence a modification of radiated power is implied. It is the purpose of this chapter to find the proper connected load for maximum radiated power.

4.1 Optimization Procedure

The total power input to the antenna is equal to the radiated power plus the dissipated power in the conductor and the power loss due to the resistive part of connected load. Thus the radiated power can be determined from the relation

$$P_r = P_{in} - P_\ell \quad (4.1.1)$$

Where

P_r = radiated power

P_{in} = input power to the antenna

P_ℓ = power loss in the antenna.

For antennas made up of perfect conductors, this term represents loss due to resistive part of connected load.

P_{in} and P_ℓ can be determined from the relations

$$P_{in} = |I_{in}|^2 R_{in} \quad (4.1.2)$$

$$P_\ell = |I_\ell|^2 R_\ell \quad (4.1.3)$$

Where

I_{in} = current at the input terminal

I_ℓ = current at the load point

R_{in} = input resistance

R_ℓ = resistive part of the connected load

Thus

$$P_r = |I_{in}|^2 R_{in} - |I_{\ell}|^2 R_{\ell} \quad (4.1.4)$$

From this equation it is found that the radiated power can be obtained if the values of I_{in} and I_{ℓ} can be found. The accuracy of this equation depends on the accuracy of I_{in} and I_{ℓ} . Because of the difficulty in obtaining the very accurate values of I_{in} and I_{ℓ} , the radiated power is determined from the Poynting vector method⁽²⁸⁾. The Poynting vector method consists of the following steps:

- (i) the calculation of the distant field produced by the resulting current distribution;
- (ii) the calculation of the complex Poynting vector and its real part which represents the average flow of power per unit area;
- (iii) the integration of the Poynting vector over a closed surface which is usually chosen to be an infinitely large sphere. Because the amplitude of the distant field varies as $1/r$, for this reason it is convenient to multiply the Poynting vector by r^2 and thus obtain the radiation intensity Φ which is independent of r . Hence the radiated power can be expressed as

$$P_r = \int_0^{2\pi} \int_0^{\pi} \Phi(\theta, \phi) \sin\theta \, d\theta \, d\phi \quad (4.1.5)$$

Where $\Phi(\theta, \phi)$ is the radiation intensity and is given in equation (3.1.10). As it was pointed out by Schellkunoff and Friis⁽²⁹⁾ that the accuracy of $\Phi(\theta, \phi)$ is insensitive to small errors in current distribution, it is expected that the accuracy of equation (4.1.5) is better than equation (4.1.4).

By using $\Phi(\theta, \phi)$ as given in equation (3.1.10), equation (4.1.5) can be written in a matrix form as

$$P_r = \frac{60}{(\sin k\Delta z)^2} [\tilde{V}]^* [\tilde{Y}]^* [U] [Y] [V] \quad (4.1.6)$$

The elements of matrix [U] are given in Appendix A.

By using equations (3.2.2) and (3.2.3), P_r can be expressed as a function of connected load as

$$P_r = \frac{60}{(\sin k\Delta z)^2} \left[\frac{\alpha_1 + \alpha_2 \{x^2(1) + x^2(2)\} + \alpha_3 x(1) + \alpha_4 x(2)}{x^2(1) + x^2(2)} \right] \quad (4.1.7)$$

Equation (4.1.7) is maximized, using Rosenbrock's method of hill climbing⁽³⁰⁾, with respect to $x(1)$ and $x(2)$ under the conditions

- i that $x(1)$ and $x(2)$ must be real;
- ii that $x(1) \geq \text{Re}(y_{jj}) + \text{Re}(y_{jk})$, $x(2)$ arbitrary.

Thus the value of optimum load can be obtained from equations (3.2.5), (3.2.6) and (3.2.3).

4.2 Numerical Results

Three different lengths of the dipole are arbitrarily chosen for study.

The ratios of L/λ under consideration are 0.1, 0.2 and 0.5. All dipoles are centre-driven with a source of voltage V_0 and are loaded with the optimum load impedance at equidistance from the centre along both arms. The results shown in figure 4.1 are the variation of optimum load with the position of loading for the three different lengths of dipole. The input impedances and directivity corresponding to each position of loading are shown in tables 4.1 to 4.3. The resulting current distributions and normalized radiation patterns are shown in figures 4.2 to 4.11.

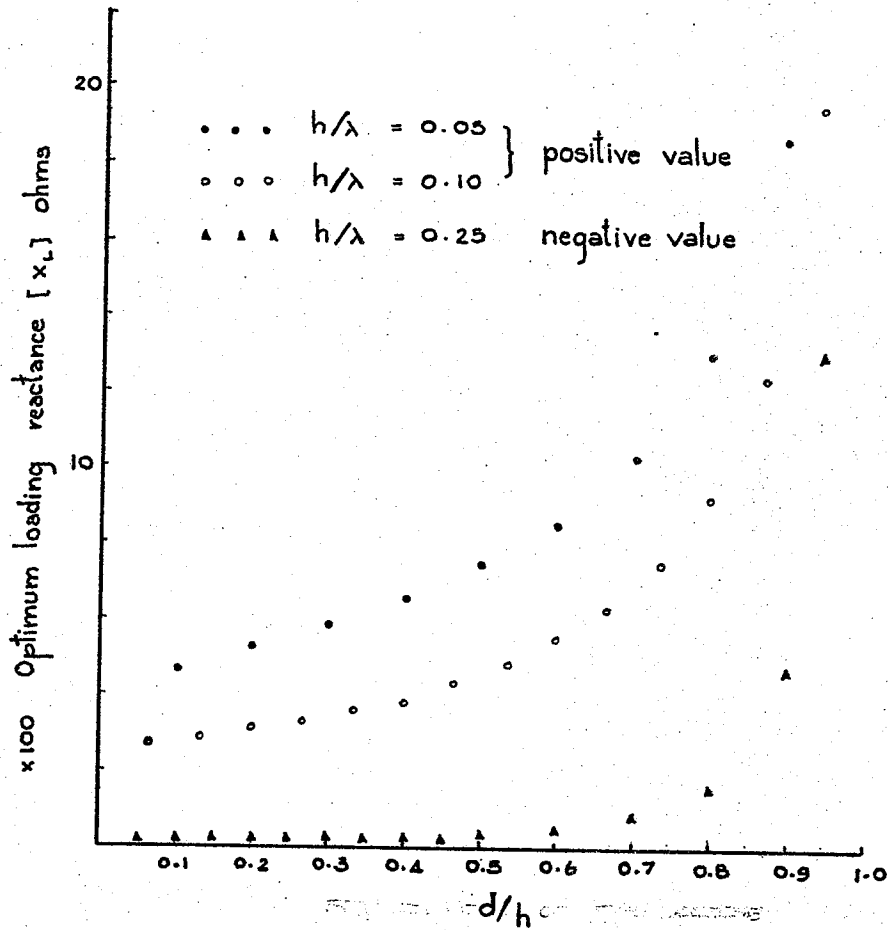


Fig. 4.1 Optimum loading impedances for enhanced radiation as functions of d/h for various h/λ .

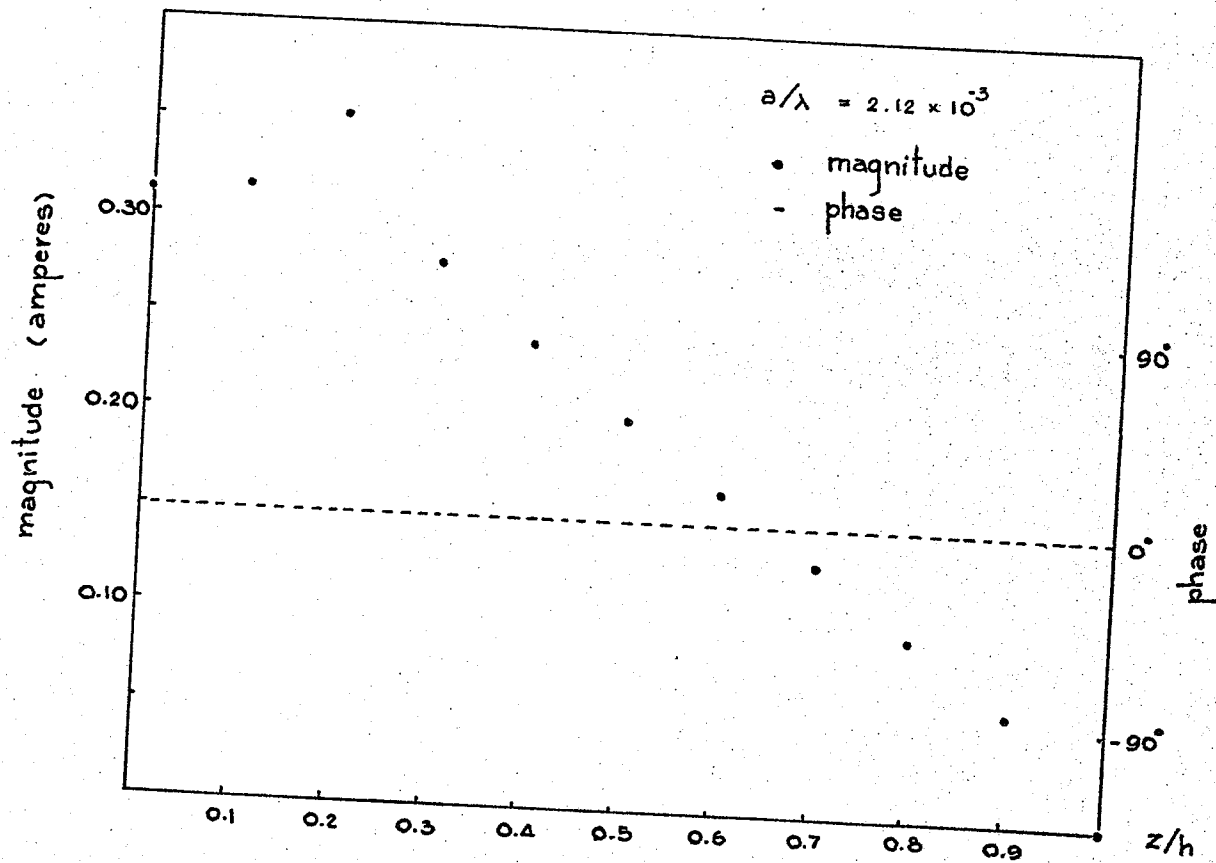


Fig. 4.2 Current distribution for $L/\lambda = 0.1$ dipole loaded at $d/h = 0.2$ with optimum load for enhanced radiation.

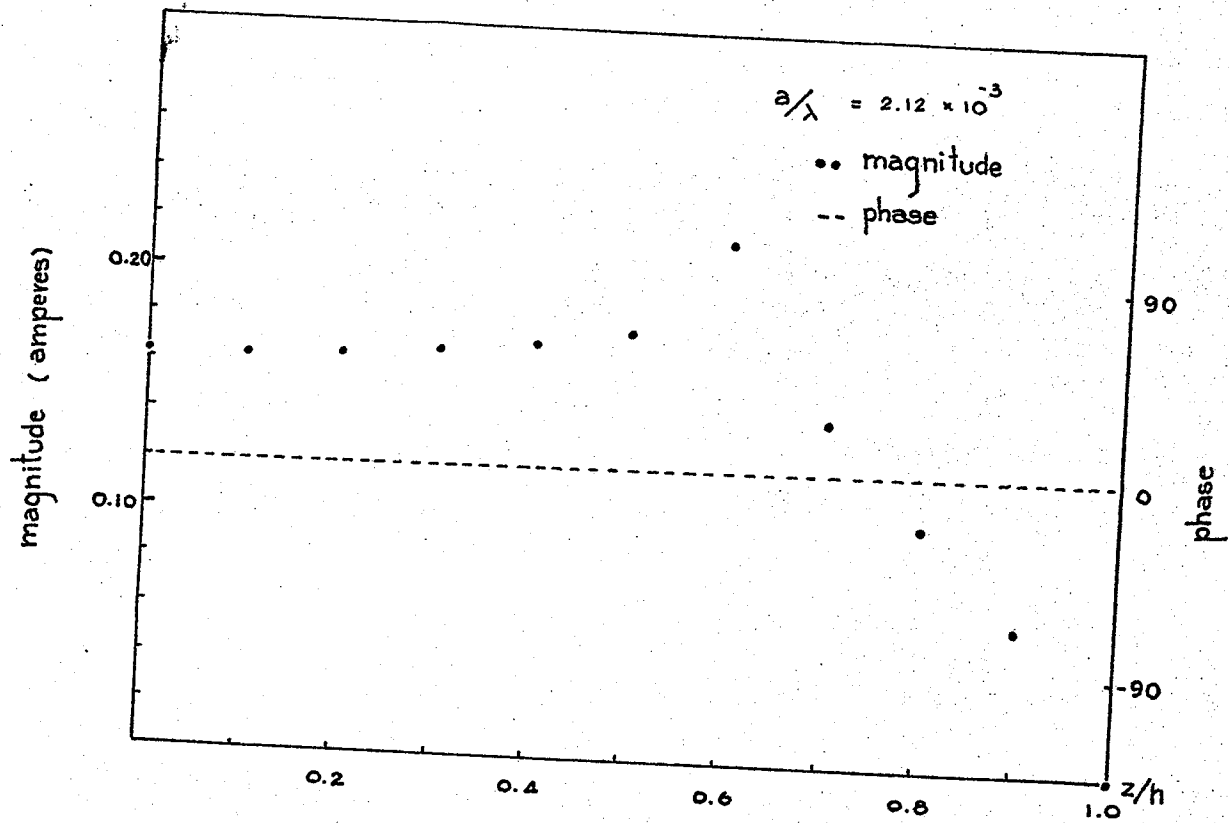


Fig. 4.3 Current distribution for $L/\lambda = 0.1$ dipole loaded at $d/h = 0.6$ with optimum load for enhanced radiation.

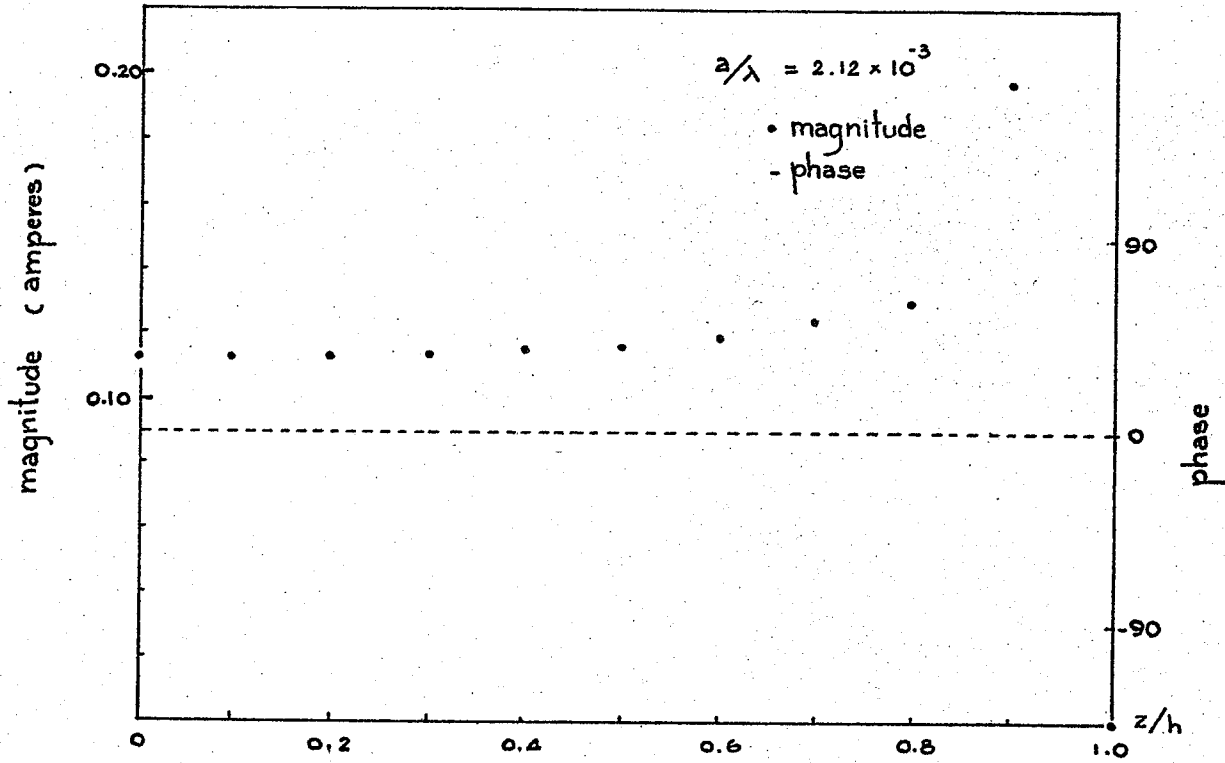


Fig. 4.4 Current distribution for $L/\lambda = 0.1$ dipole loaded at $d/h = 0.9$ with optimum load for enhanced radiation.

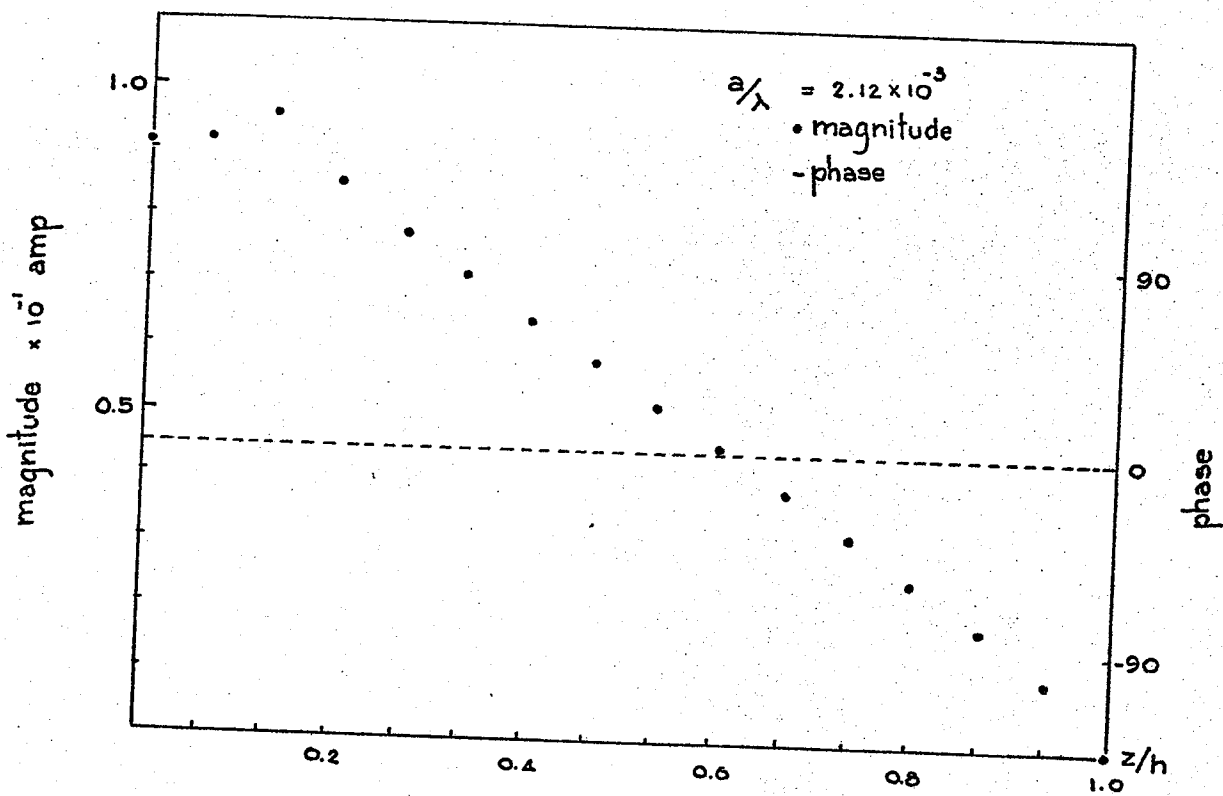


Fig. 4.5 Current distribution for $L/\lambda = 0.2$ dipole loaded at $d/h = 0.133$ with optimum load for enhanced radiation.

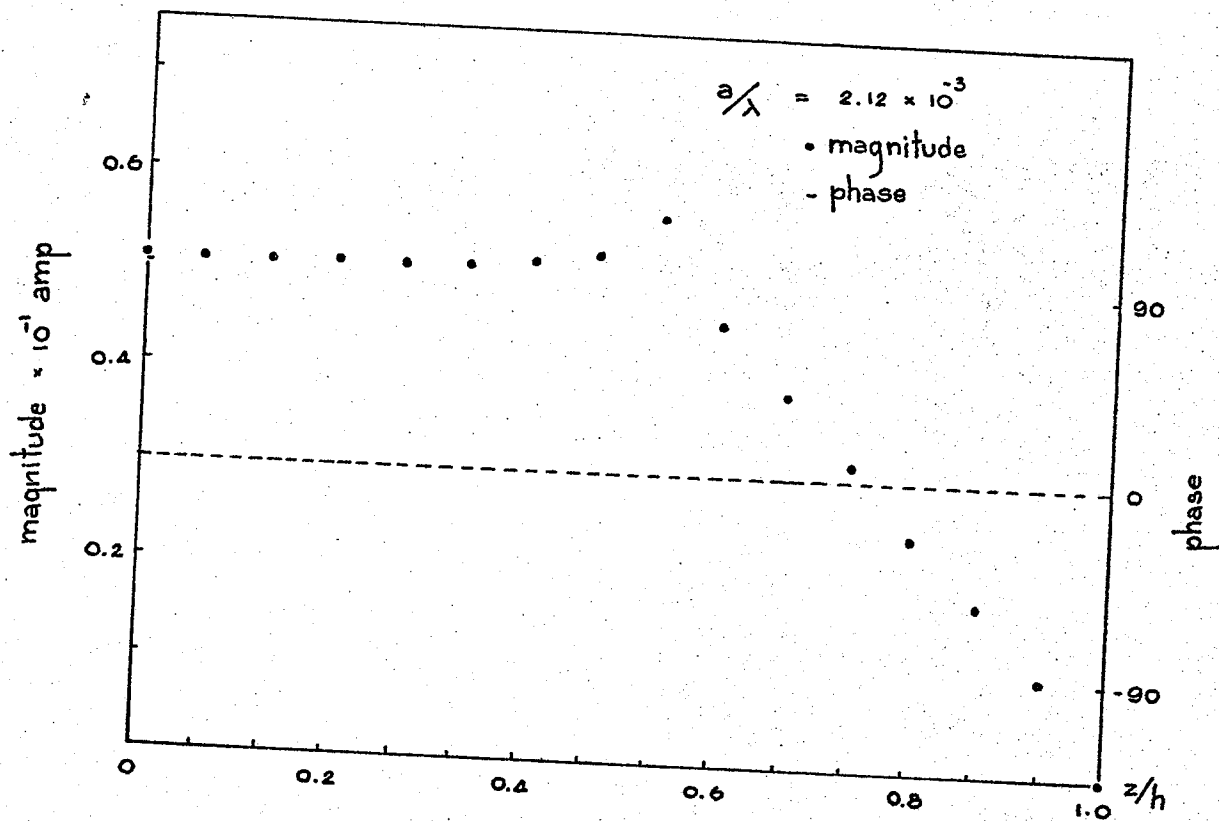


Fig. 4.6 Current distribution for $L/\lambda = 0.2$ dipole loaded at $d/h = 0.533$ with optimum load for enhanced radiation.

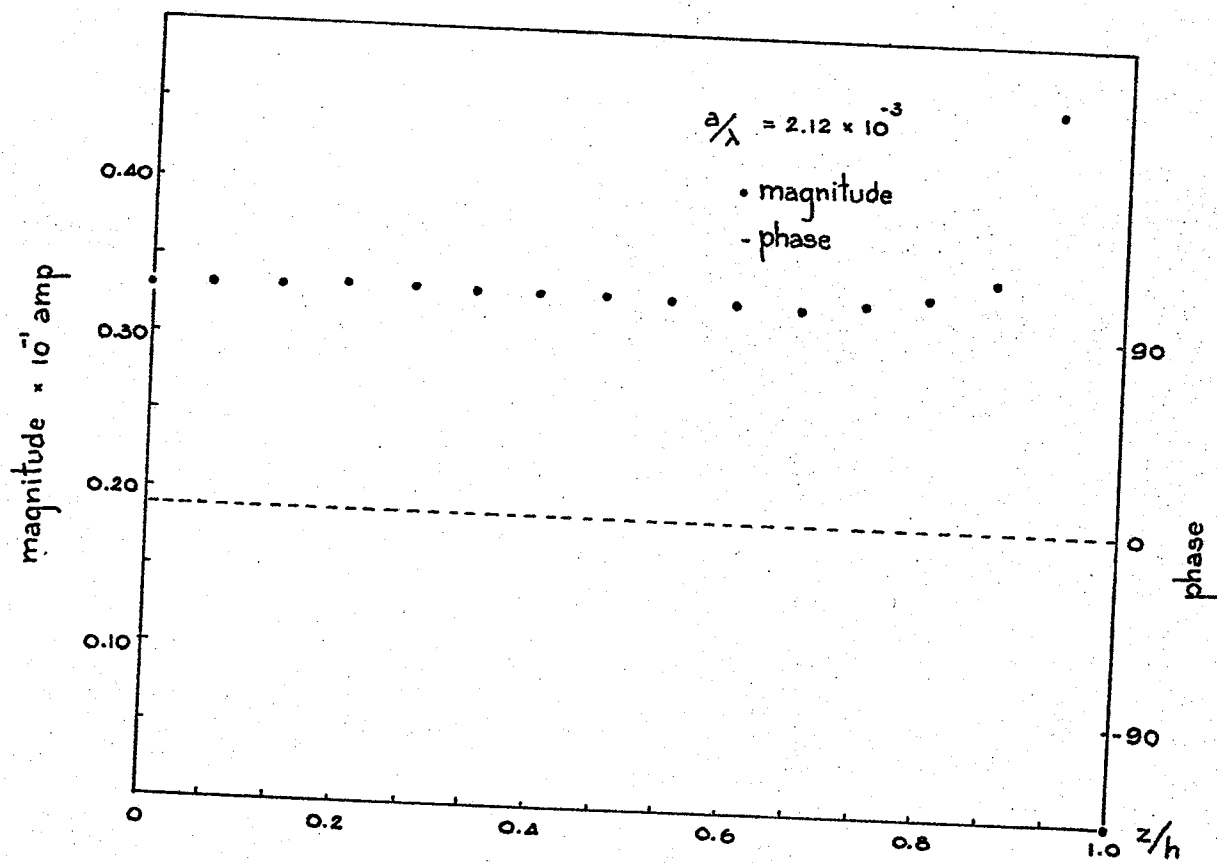


Fig. 4.7 Current distribution for $L/\lambda = 0.2$ dipole loaded at $d/h = 0.933$ with optimum load for enhanced radiation.

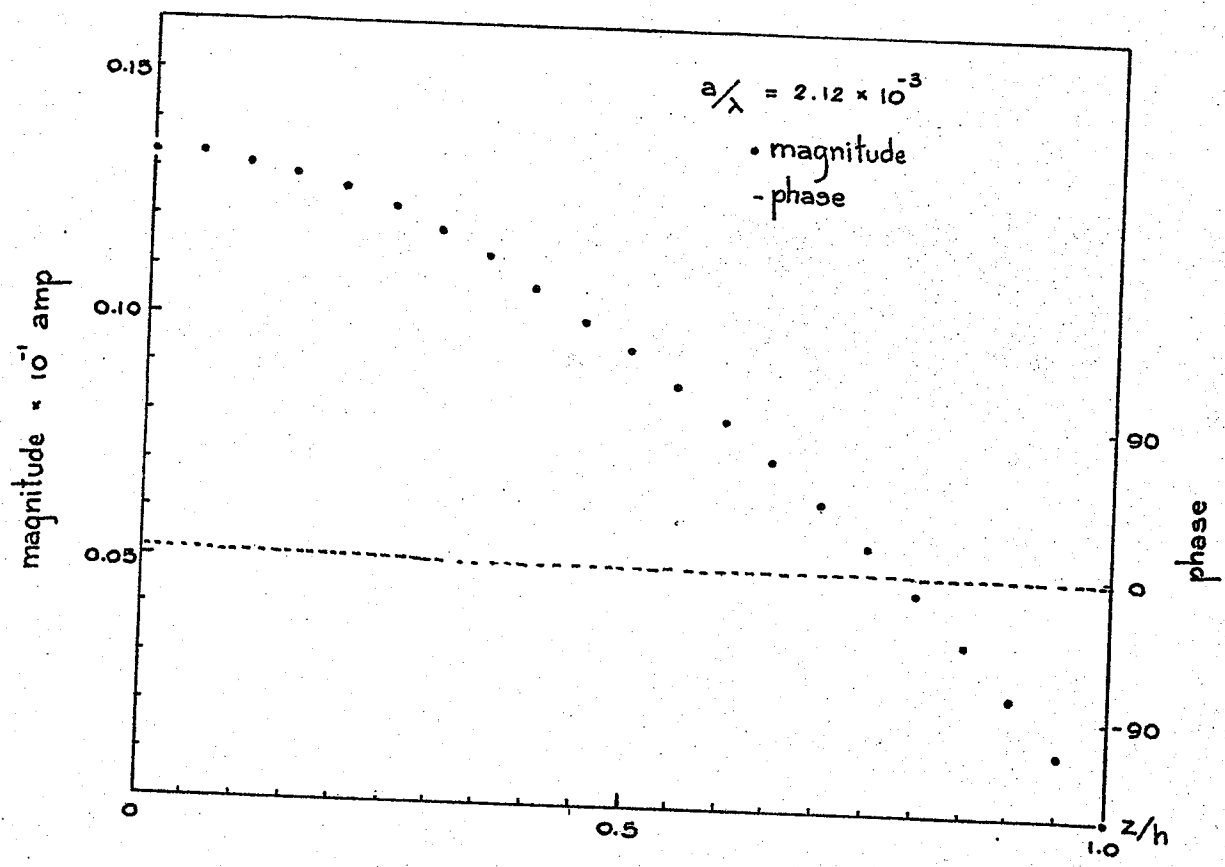


Fig. 4.8 Current distribution for half-wave dipole loaded at $d/h = 0.45$ with optimum load for enhanced radiation.

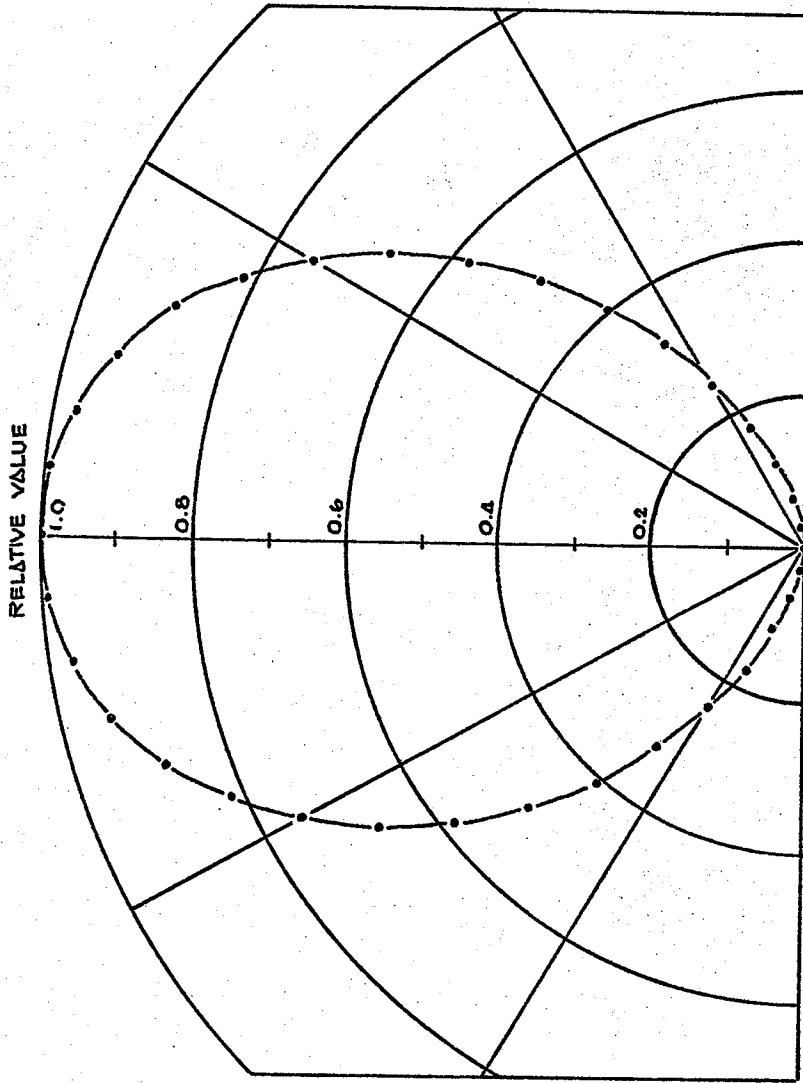


Fig. 4.9 Normalized radiation pattern for $L/\lambda = 0.1$ dipole loaded with optimum load for enhanced radiation.

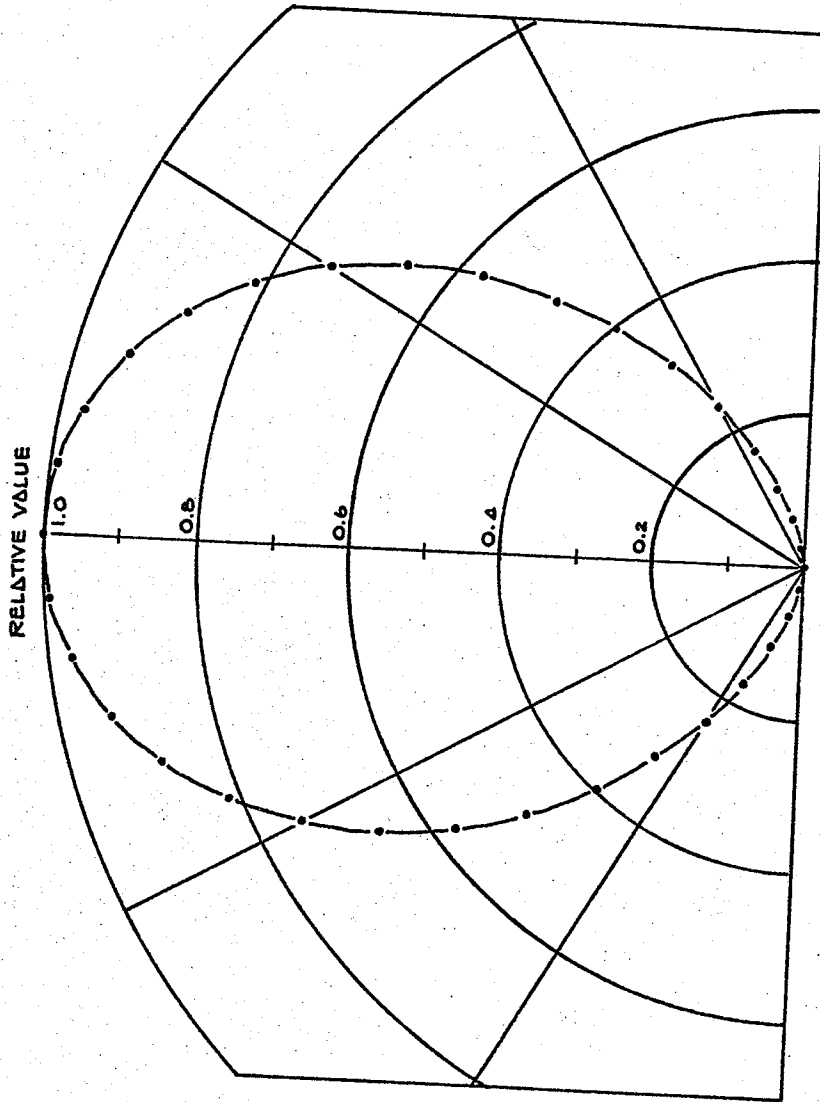


Fig. 4.10 Normalized radiation pattern for $L/\lambda = 0.2$ dipole loaded with optimum load for enhanced radiation.

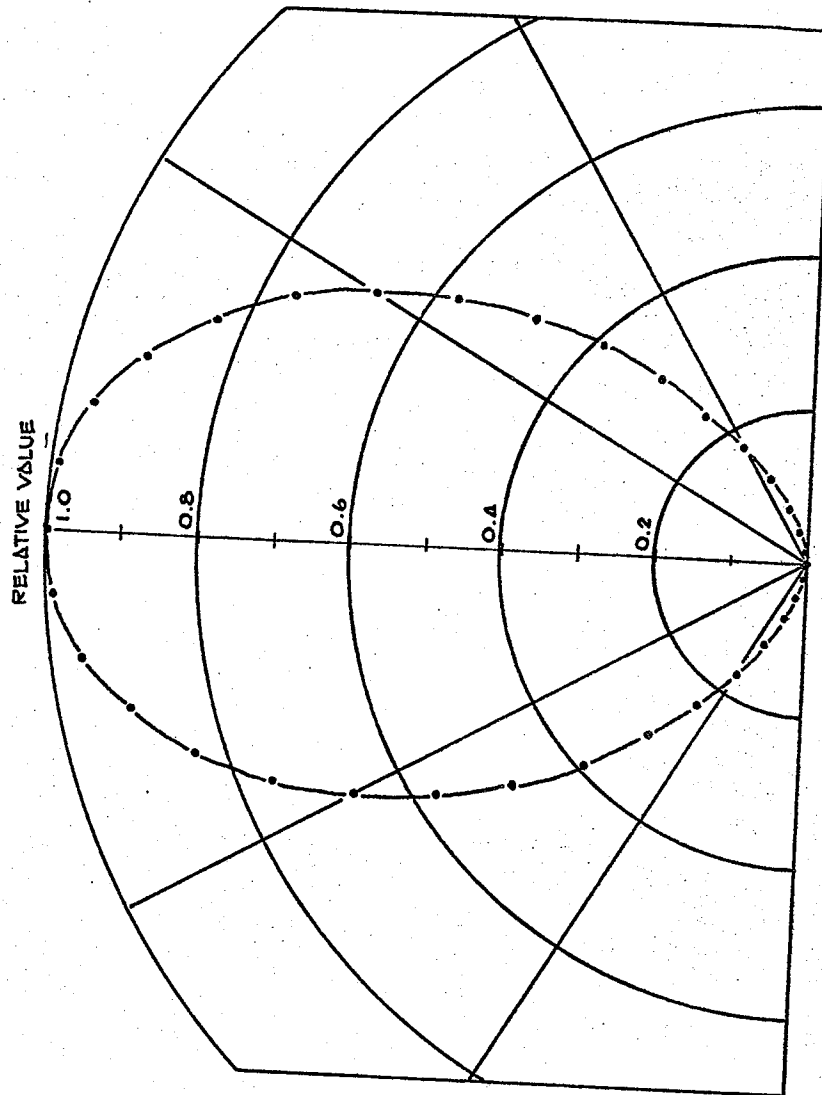


Fig. 4.11 Normalized radiation pattern for half-wave dipole loaded with optimum load for enhanced radiation.

Table 4.1

Antenna input impedance and directivity at various loading points for $L/\lambda = 0.1$ dipole loaded with optimum load for enhanced radiation

d/h	Z_{IN} OHMS		DIRECTIVITY
	R	X	
0.9	8.854	-0.058	1.510
0.8	7.851	-0.044	1.509
0.7	6.954	-0.033	1.508
0.6	6.116	-0.024	1.507
0.5	5.326	-0.017	1.507
0.4	4.580	-0.011	1.506
0.3	3.871	-0.007	1.506
0.2	3.188	-0.004	1.505
0.1	2.548	-0.002	1.505

Table 4.2

Antenna input impedance and directivity at various loading points for $L/\lambda = 0.2$ dipole loaded with optimum load for enhanced radiation

d/h	Z_{IN} OHMS		DIRECTIVITY
	R	X	
0.933	29.512	-0.908	1.539
0.867	27.716	-0.787	1.536
0.800	26.020	-0.660	1.534
0.733	24.378	-0.560	1.532
0.667	22.775	-0.467	1.530
0.600	21.212	-0.387	1.528
0.533	19.682	-0.315	1.527
0.467	18.182	-0.252	1.525
0.400	16.709	-0.197	1.524
0.333	15.259	-0.150	1.523
0.267	13.827	-0.109	1.522
0.200	12.402	-0.075	1.522
0.133	10.962	-0.047	1.521
0.067	9.458	-0.023	1.521

Table 4.3

Antenna input impedance and directivity at various loading points for half-wave dipole loaded with optimum load for enhanced radiation

d/h	Z _{IN} OHMS		DIRECTIVITY
	R	X	
0.90	70.24	-8.50	1.635
0.85	70.69	-8.31	1.637
0.75	71.62	-7.89	1.640
0.65	72.61	-7.42	1.643
0.55	73.68	-6.88	1.645
0.45	74.84	-6.25	1.647
0.35	76.14	-5.47	1.648
0.25	77.60	-4.52	1.649
0.15	79.30	-3.32	1.650
0.05	81.46	-1.53	1.650

CHAPTER 5

INPUT IMPEDANCE OF LOADED DIPOLE

Antenna impedance is defined as the ratio of excitation voltage to input current. It was already found that the current distribution can be modified by lumped impedance loading along the antenna arms. Thus the modification of antenna impedance is implied. In this chapter the antenna impedance as a function of connected load impedance will be derived.

5.1 Antenna Impedance

It was already shown in Chapter 2 that

$$[J] = [Y][V] \quad (5.1.1)$$

Where

$$[Y] = [Z]^{-1} = \text{inverse of the generalized impedance matrix}$$

$$[V] = \text{excitation matrix}$$

When the antenna is excited with the voltage source at z_i and is loaded at z_j and z_k with lumped impedance Z_L , $[V]$ can be written as

$$[V] = [V_0] + [V_L] \quad (5.1.2)$$

Where V_0 is the excitation matrix with all elements equal to zero except at i th row which is equal to V_0 , thus

$$[V_0] = \begin{bmatrix} 0 \\ \vdots \\ V_0 \\ \vdots \\ 0 \end{bmatrix} \quad (5.1.3)$$

$$[V_L] = -[Z_L][J] \quad (5.1.4)$$

Where $[Z_L]$ is the diagonal load impedance matrix with all elements, except Z_{jj} and Z_{kk} , equal to zero, thus equation (5.1.4) reduces to

$$[V_L] = \begin{bmatrix} 0 \\ \vdots \\ V_{Lj} \\ 0 \\ \vdots \\ V_{Lk} \\ \vdots \\ 0 \end{bmatrix} \quad (5.1.5)$$

Substituting equations (5.1.5) and (5.1.3) into equation (5.1.2) which is substituted into equation (5.1.1), we obtain

$$\begin{bmatrix} J_j \\ J_i \\ J_k \end{bmatrix} = \begin{bmatrix} y_{jj} & y_{ji} & y_{jk} \\ y_{ij} & y_{ii} & y_{ik} \\ y_{kj} & y_{ki} & y_{kk} \end{bmatrix} \begin{bmatrix} V_{Lj} \\ V_0 \\ V_{Lk} \end{bmatrix} \quad (5.1.6)$$

From which the input current is found to be

$$J_i = y_{ij} V_{Lj} + y_{ii} V_0 + y_{ik} V_{Lk} \quad (5.1.7)$$

Where

J_i = input current at z_i

V_0 = applied voltage

V_{Lj} and V_{Lk} = voltage drops due to connected load impedance at z_j and z_k , respectively.

From equation (3.2.2) we have

$$V_{Lj} = V_{Lk} = \frac{-y_{ji}}{y_{Lj} + y_{jj} + y_{jk}} V_i \quad (5.1.8)$$

Where

$$V_i = V_0$$

Substituting equation (5.1.8) into equation (5.1.7) we obtain

$$J_i = [y_{ii} - \frac{y_{ij}y_{ji} + y_{ik}y_{ji}}{y_{Lj} + y_{jj} + y_{jk}}]V_0 \tag{5.1.9}$$

Thus

$$Y_{in} = \frac{J_i}{V_0} = y_{ii} - \frac{y_{ij}y_{ji} + y_{ik}y_{ji}}{y_{Lj} + y_{jj} + y_{jk}} \tag{5.1.10}$$

$$Z_{in} = \frac{1}{Y_{in}} = \frac{y_{Lj} + y_{jj} + y_{jk}}{y_{ii}(y_{Lj} + y_{jj} + y_{jk}) - y_{ij}y_{ji} - y_{ik}y_{ji}} \tag{5.1.11}$$

Letting $Y_{Lj} = x'(1) + jx'(2)$, equation (5.1.11) can be further simplified to

$$Z_{in} = \frac{x(1) + jx(2)}{F_1[x(1), x(2)] + jF_2[x(1), x(2)]} \tag{5.1.12}$$

Where

$$x(1) = x'(1) + \text{Re}(y_{jj}) + \text{Re}(y_{jk}) \tag{5.1.13}$$

$$x(2) = x'(2) + \text{Im}(y_{jj}) + \text{Im}(y_{jk}) \tag{5.1.14}$$

$$F_1[x(1), x(2)] = x(1)\text{Re}(y_{ii}) - x(2)\text{Im}(y_{ii}) - \text{Re}(y_{ji})[\text{Re}(y_{ij}) + \text{Re}(y_{ik})] + \text{Im}(y_{ji})[\text{Im}(y_{ij}) + \text{Im}(y_{ik})] \tag{5.1.15}$$

$$\begin{aligned}
F_2[x(1), x(2)] &= x(1) \operatorname{Im}(y_{ji}) + x(2) \operatorname{Re}(y_{ji}) - \operatorname{Im}(y_{ji}) [\operatorname{Re}(y_{ij}) \\
&\quad + \operatorname{Re}(y_{ik})] - \operatorname{Re}(y_{ij}) [\operatorname{Im}(y_{ij}) + \operatorname{Im}(y_{ik})] \quad (5.1.16)
\end{aligned}$$

Thus, the input resistance and reactance can be written as

$$R_{in} = \operatorname{Re}(Z_{in})$$

$$= \frac{x(1) F_1[x(1), x(2)] + x(2) F_2[x(1), x(2)]}{F_1^2[x(1), x(2)] + F_2^2[x(1), x(2)]} \quad (5.1.17)$$

$$X_{in} = \operatorname{Im}(Z_{in})$$

$$= \frac{x(2) F_1[x(1), x(2)] - x(1) F_2[x(1), x(2)]}{F_1^2[x(1), x(2)] + F_2^2[x(1), x(2)]} \quad (5.1.18)$$

5.2 Optimization of $|\operatorname{Im}(Z_{in})|$

The optimization, using Rosenbrock's method of hill climbing, is performed to obtain the optimum load for the minimum of $|\operatorname{Im}(Z_{in})|$. Since the minimum of $|\operatorname{Im}(Z_{in})|$ is equal to zero, this optimization is equivalent to finding the load which resonates the dipole antenna.

From equation (5.1.18) we have

$$|\text{Im}(Z_{in})| = |X_{in}| = \frac{x(2) F_1[x(1), x(2)] - x(1) F_2[x(1), x(2)]}{F_1^2[x(1), x(2)] + F_2^2[x(1), x(2)]}$$

(5.2.1)

Where $F_1[x(1), x(2)]$ and $F_2[x(1), x(2)]$ are given in equations (5.1.15) and (5.1.16), Equation (5.2.1) is minimized with the constraints

- (i) $x(1)$ and $x(2)$ are real
- (ii) $x(1) \geq \text{Re}(y_{jj}) + \text{Re}(y_{jk})$, $x(2)$ arbitrary

It should be noted that the resonating load impedance can also be found from Equation (5.1.18) by putting X_{in} equal to zero. From this we have one equation and two unknowns, $X(1)$ and $X(2)$, thus by putting one unknown equal to zero, the other can be found.

5.3 Numerical Results

The three different lengths of dipole under consideration are the same as those in Chapters 2 and 3. In this thesis general expressions of antenna input impedance are only applied to finding the optimum load for resonating the antenna.

The first consideration is not restricted to any particular type of connected load impedance. The results obtained are shown in Tables 5.1 to 5.3 for the optimum load at the different loading

locations and the corresponding input impedances are also given. The second consideration is restricted to the reactive load and the results obtained are shown in Tables 5.4 to 5.6. The resulting current distributions from the two types of loading, with only one position of loading on each arm for each antenna length, are shown in Figures 5.1 to 5.3. The normalized radiation patterns are given in Figures 5.4 to 5.6.

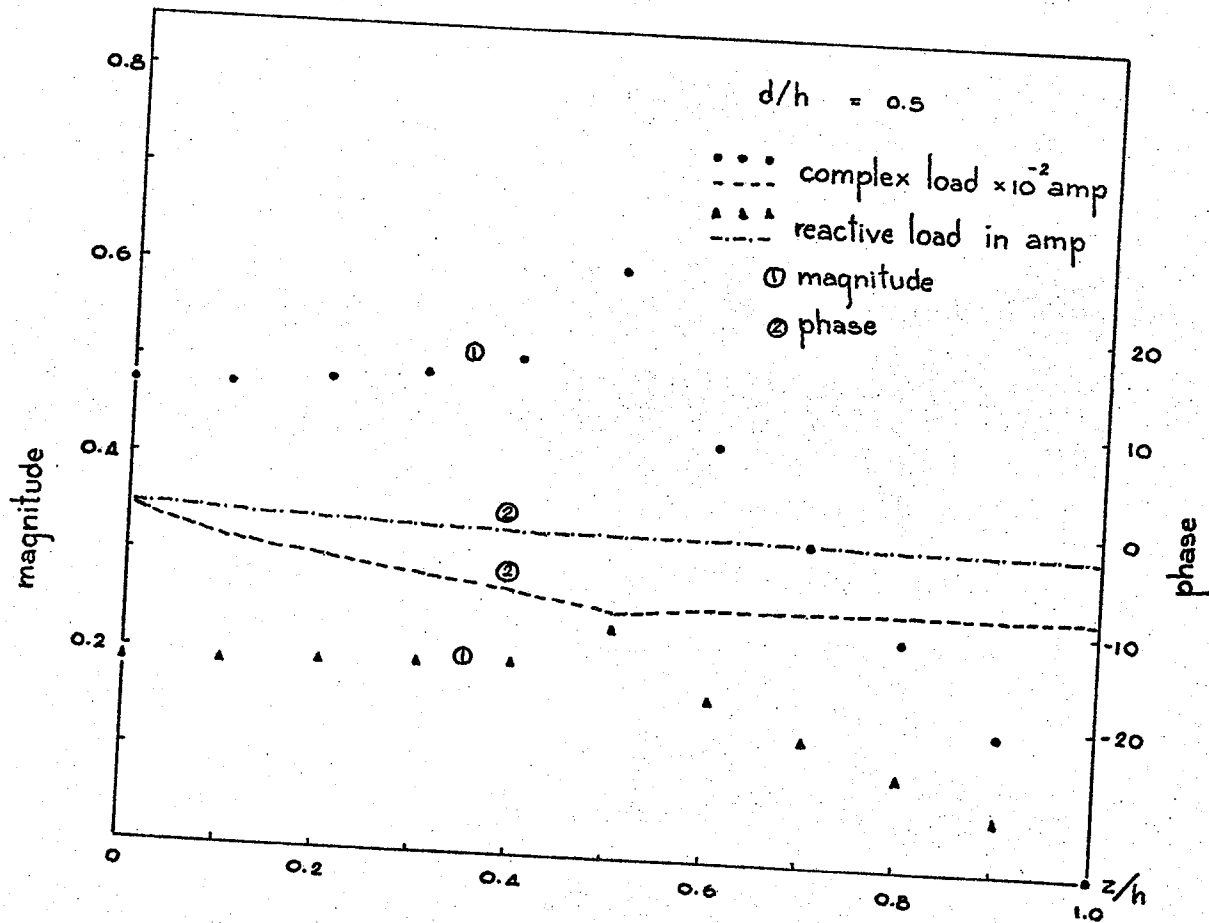


Fig. 5.1 Current distribution for $L/\lambda = 0.1$ dipole loaded with resonating load.

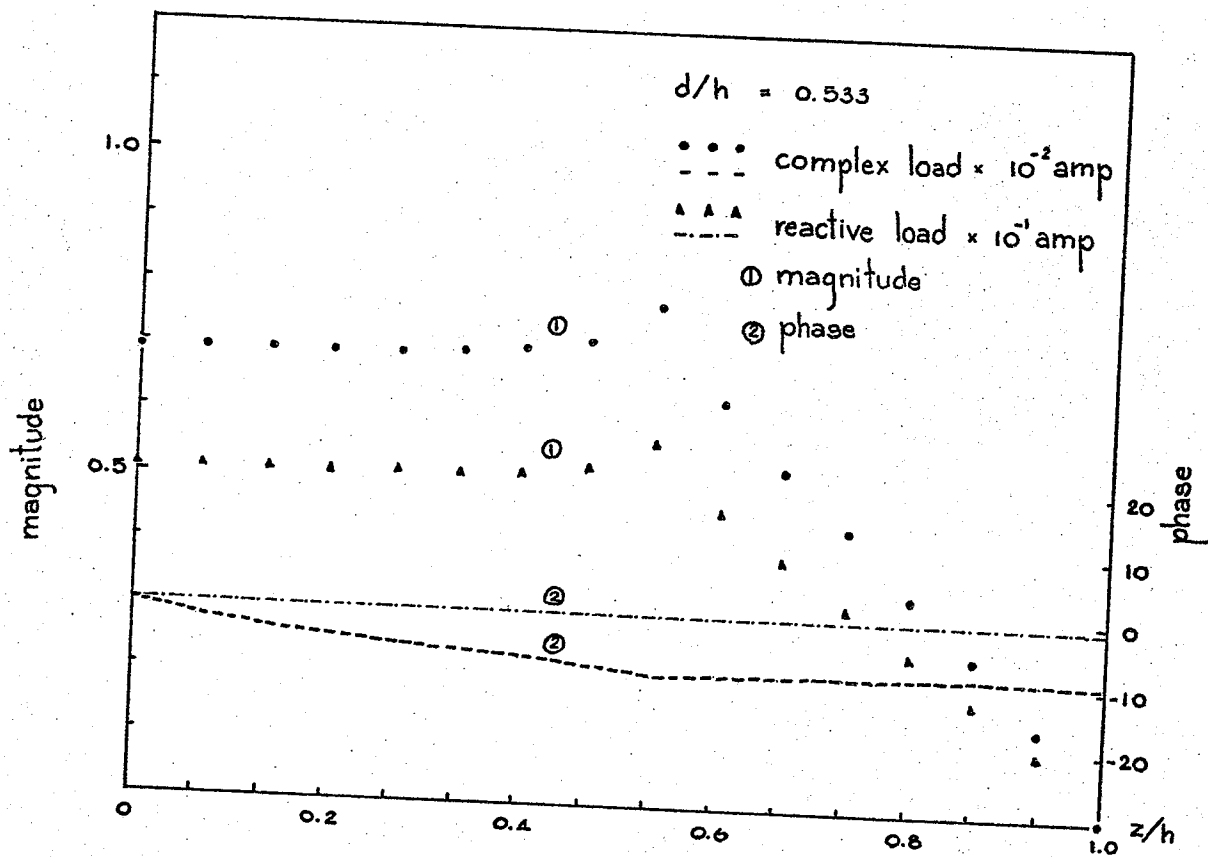


Fig. 5.2 Current distribution for $L/\lambda = 0.2$ dipole loaded with resonating load.

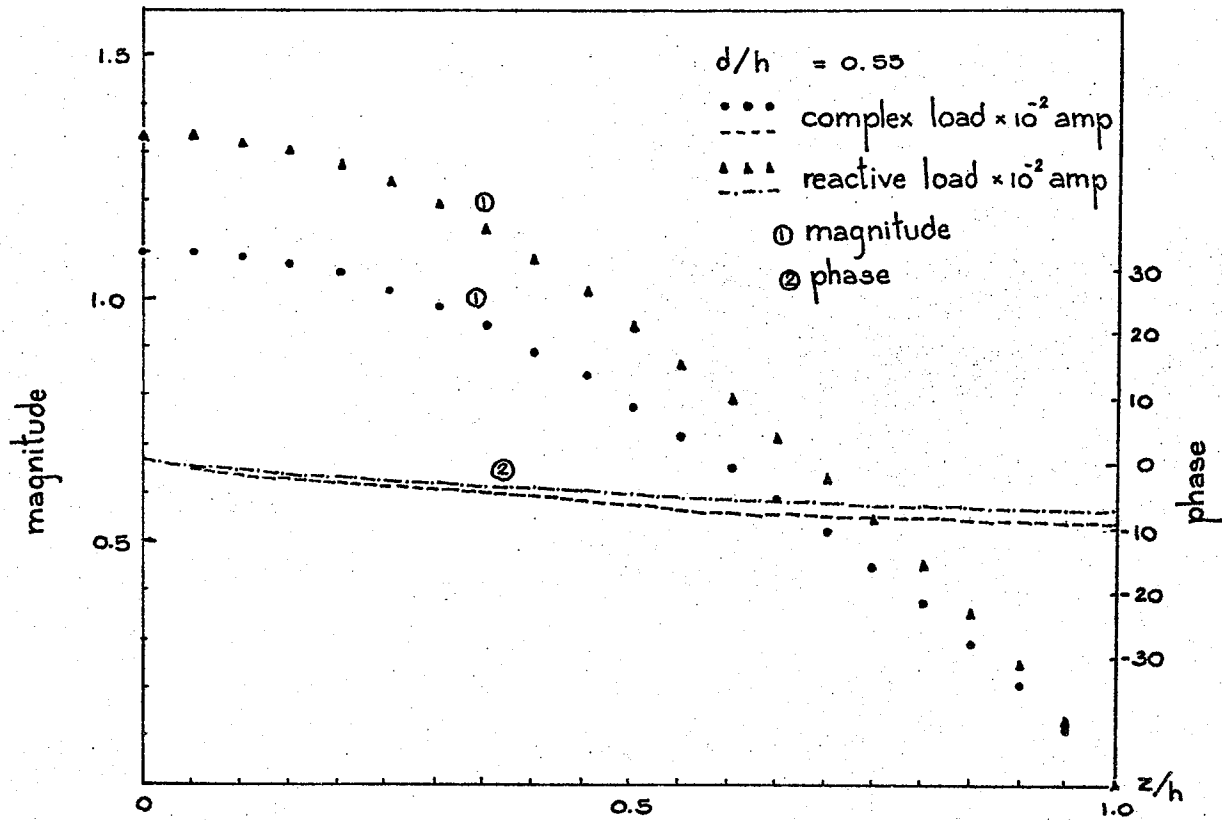


Fig. 5.3 Current distribution for half-wave dipole loaded with resonating load.

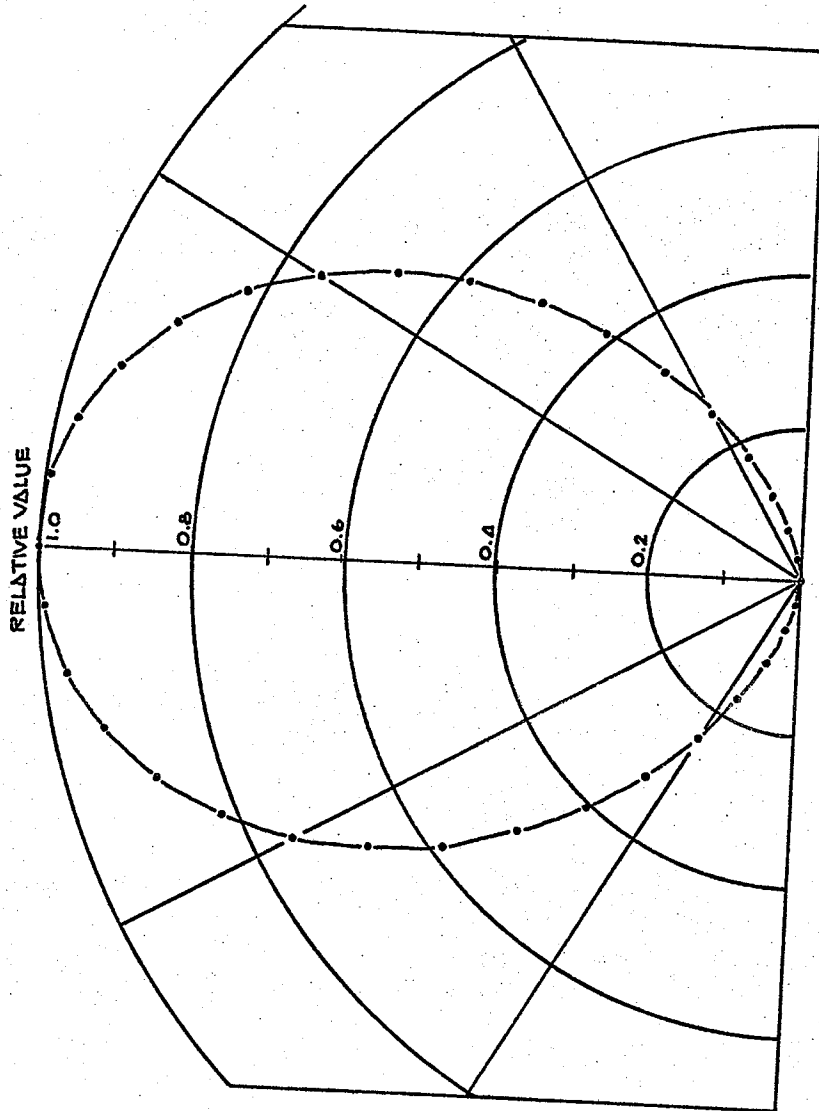


Fig. 5.4 Normalized radiation pattern for $L/\lambda = 0.1$ dipole loaded with resonating load.

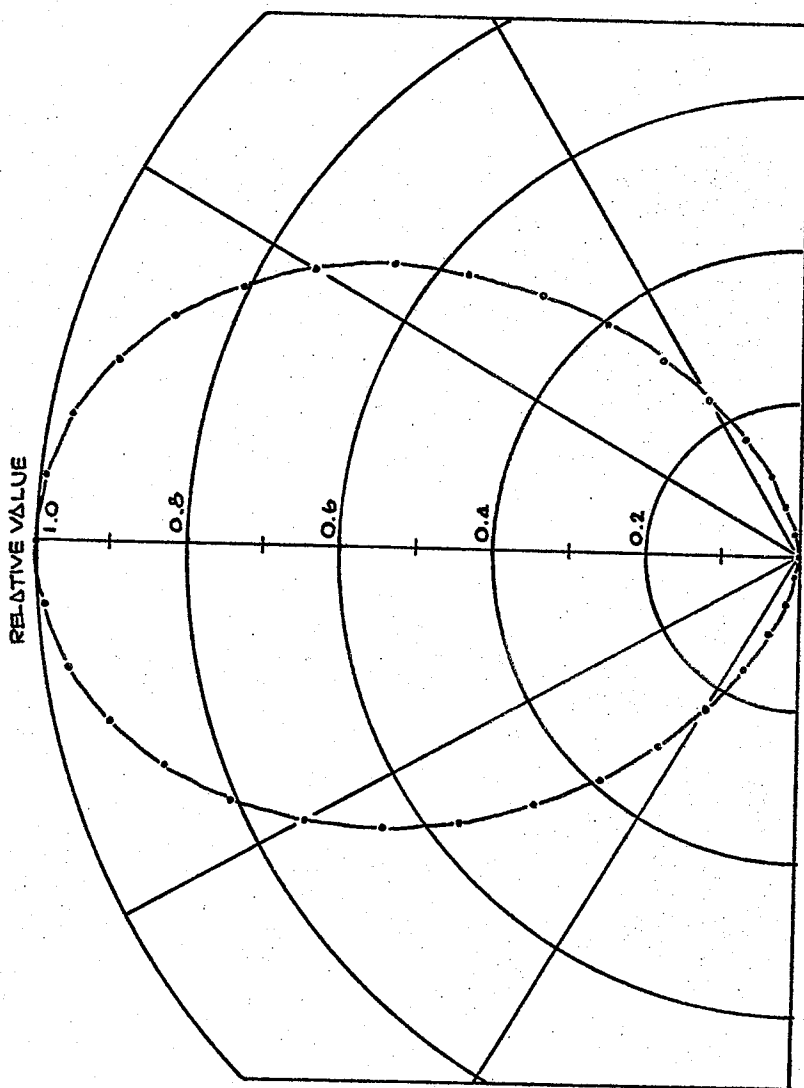


Fig. 5.5 Normalized radiation pattern for $L/\lambda = 0.2$ dipole loaded with resonating load.

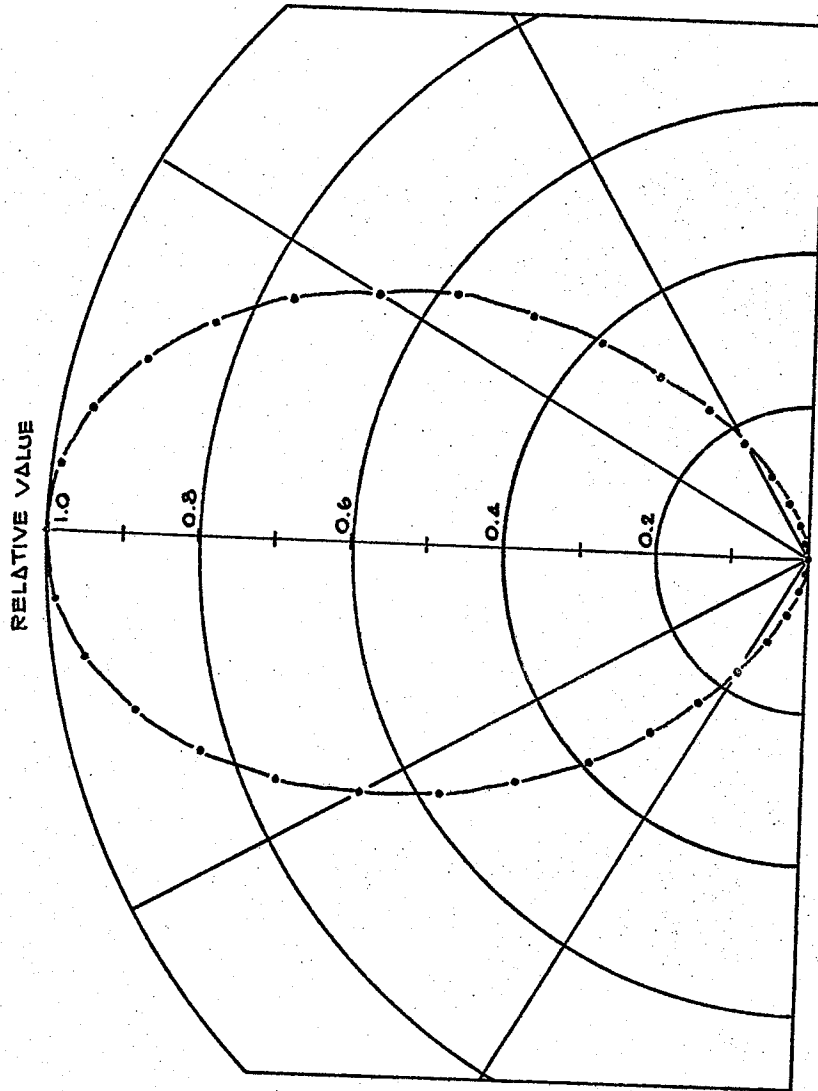


Fig. 5.6 Normalized radiation pattern for half-wave dipole loaded with resonating load.

Table 5.1

Relationships of load impedance, antenna input impedance and directivity at various loading points for $L/\lambda = 0.1$ dipole loaded with complex resonating load

d/h	Z_L OHMS		Z_{IN} OHMS		DIRECTIVITY
	R_L	X_L	R_{IN}	X_{IN}	
0.1	83.496	478.972	202.580	0.0	1.505
0.2	75.792	532.479	197.608	0.0	1.505
0.3	72.547	591.712	204.975	0.0	1.506
0.4	96.520	672.735	301.302	0.0	1.506
0.5	62.872	749.163	210.470	0.0	1.507
0.6	78.472	876.490	299.403	0.0	1.507
0.7	121.213	1118.912	773.909	0.0	1.509
0.8	92.800	1367.497	663.394	0.0	1.510
0.9	67.377	1924.152	792.895	0.0	1.511

Table 5.2

Relationships of load impedance, antenna input impedance and directivity at various loading points for $L/\lambda = 0.2$ dipole loaded with complex resonating load

d/h	Z_L OHMS		Z_{IN} OHMS		DIRECTIVITY
	R_L	X_L	R_{IN}	X_{IN}	
0.067	226.518	308.477	507.588	0.0	1.521
0.133	203.542	339.575	486.695	0.0	1.522
0.200	55.036	315.758	137.970	0.0	1.522
0.267	50.299	339.572	131.200	0.0	1.523
0.333	48.454	367.688	130.654	0.0	1.523
0.400	45.838	400.830	127.876	0.0	1.524
0.467	41.169	440.482	119.616	0.0	1.525
0.533	49.428	493.746	145.003	0.0	1.527
0.600	120.345	616.215	414.693	0.0	1.529
0.667	43.895	642.569	139.710	0.0	1.530
0.733	65.808	774.836	218.669	0.0	1.532
0.800	100.020	1017.051	506.071	0.0	1.536
0.867	82.156	1302.967	422.211	0.0	1.538
0.933	66.397	2018.681	508.272	0.0	1.542

Table 5.3

Relationships of load impedance, antenna input impedance and directivity at various loading points for half-wave dipole loaded with complex resonating load

d/h	Z_L OHMS		Z_{IN} OHMS		DIRECTIVITY
	R_L	X_L	R_{IN}	X_{IN}	
0.05	1.405	-20.677	84.307	0.0	1.650
0.15	6.398	-20.965	91.682	0.0	1.649
0.25	3.426	-23.199	83.994	0.0	1.649
0.35	9.454	-25.863	90.830	0.0	1.648
0.45	6.264	-32.899	83.233	0.0	1.647
0.55	18.734	-41.714	91.130	0.0	1.646
0.65	8.736	-68.152	78.931	0.0	1.644
0.75	51.509	-114.184	88.256	0.0	1.642
0.85	196.138	-278.814	91.587	0.0	1.640
0.95	4789.726	-2521.833	84.150	0.0	1.637

Table 5.4

Relationships of load impedance, antenna input impedance and directivity at various loading points for $L/\lambda = 0.1$ dipole loaded with reactive resonating load

d/h	Z_L OHMS		Z_{IN} OHMS		DIRECTIVITY
	R_L	X_L	R_{IN}	X_{IN}	
0.1	0.0	472.472	2.548	0.0	1.505
0.2	0.0	524.631	3.188	0.0	1.505
0.3	0.0	582.105	3.871	0.0	1.506
0.4	0.0	650.900	4.580	0.0	1.506
0.5	0.0	737.900	5.326	0.0	1.507
0.6	0.0	854.392	6.116	0.0	1.507
0.7	0.0	1022.764	6.955	0.0	1.508
0.8	0.0	1299.180	7.851	0.0	1.509
0.9	0.0	1860.497	8.855	0.0	1.510

Table 5.5

Relationships of load impedance, antenna input impedance and directivity at various loading points for $L/\lambda = 0.2$ dipole loaded with reactive resonating load

d/h	Z_L OHMS		Z_{IN} OHMS		DIRECTIVITY
	R_L	X_L	R_{IN}	X_{IN}	
0.067	0.0	270.330	9.458	0.0	1.521
0.133	0.0	289.884	10.962	0.0	1.521
0.200	0.0	310.697	12.403	0.0	1.522
0.267	0.0	334.274	13.829	0.0	1.522
0.333	0.0	361.806	15.262	0.0	1.523
0.400	0.0	394.671	16.713	0.0	1.524
0.467	0.0	434.712	18.188	0.0	1.525
0.533	0.0	484.607	19.692	0.0	1.527
0.600	0.0	548.510	21.225	0.0	1.528
0.667	0.0	633.353	22.794	0.0	1.530
0.733	0.0	751.844	24.401	0.0	1.532
0.800	0.0	930.655	26.052	0.0	1.534
0.867	0.0	1239.534	27.760	0.0	1.536
0.933	0.0	1952.557	29.568	0.0	1.539

Table 5.6

Relationships of load impedance, antenna input impedance and directivity at various loading points for half-wave dipole loaded with reactive resonating load

d/h	Z_L OHMS		Z_{IN} OHMS		DIRECTIVITY
	R_L	X_L	R_{IN}	X_{IN}	
0.05	0.0	-20.731	81.518	0.0	1.650
0.15	0.0	-21.552	79.575	0.0	1.650
0.25	0.0	-23.624	78.122	0.0	1.649
0.35	0.0	-27.423	76.924	0.0	1.648
0.45	0.0	-34.046	75.893	0.0	1.647
0.55	0.0	-46.025	74.980	0.0	1.646
0.65	0.0	-70.118	74.156	0.0	1.644
0.75	0.0	-129.730	73.397	0.0	1.642
0.85	0.0	-362.493	72.687	0.0	1.639
0.95	0.0	-10899.82	72.010	0.0	1.636

CHAPTER 6

EXTENSION TO DIPOLE LOADED WITH FINITE SIZE LOAD IMPEDANCES

The dipole antenna considered in the previous chapters was assumed to be very thin in order that the thin wire approximation can be applied. The dipole is then loaded with a load impedance of infinitesimal size on each arm. This loading, for example, by using coaxial transmission line of proper value of characteristic impedance and length⁽¹⁵⁾. In this chapter the effect of finite size of load which may be obtained by coating the dipole with an impedance surface, is studied. The results obtained are then compared with those of the dipole loaded with a load impedance of infinitesimal size. Only two values of finite size load impedance are considered, one is equal to the optimum delta load impedance for maximum directive gain in the vertical plane, the other is the optimum finite size load impedance obtained by optimizing the directive gain in the vertical plane.

6.1 Dipole Loaded with Finite Size Load Impedance

The dipole antennas considered in this section are also made very thin in order that the thin wire approximation can still be applied.

The integral equation for the current distribution as derived in chapter 2 is

$$E_z^s = \frac{-j}{4\pi\omega\epsilon} \left(\frac{d^2}{dz^2} + k^2 \right) \int_0^L I(z') \frac{e^{-jkr''}}{r''} dz' \quad (6.1.1)$$

Where

$$r'' = \sqrt{a^2 + (z - z')^2}$$

The boundary condition for the tangential electric field on the surface of the antenna requires that

$$E_z^i + E_z^s = E_z^t \quad (6.1.2)$$

Where E_z^i , E_z^s and E_z^t are incident, scattered and transmitted fields, respectively. On the portion of the antenna which is a perfect conductor, we have

$$E_z^t = 0 \quad (6.1.3)$$

While on the portion of antenna coated with Z^i as surface impedance per unit length, as shown by King⁽³¹⁾, we have

$$E_z^t = Z^i I(z) \quad (6.1.4)$$

Thus equation (6.1.1) can be written as

$$E_z^i - Z^i I(z) = \frac{j}{4\pi\omega\epsilon} \left(\frac{d^2}{dz^2} + k^2 \right) \int_0^L I(z') \frac{e^{-jkr''}}{r''} dz' \quad (6.1.5)$$

This integral equation is solved numerically by Galerkin's version of the method of moments⁽³²⁾. By using a subsectional base technique, the current distribution along the antenna length is written as the sum of triangular sinusoidal pulses of the form (re Figure 2.2)

$$J_i \frac{\sin k[\Delta z - (z' - i\Delta z)]}{\sin k\Delta z} ; i\Delta z \leq z' \leq (i+1)\Delta z$$

$$I_i = J_i \frac{\sin k[\Delta z + (z' - i\Delta z)]}{\sin k\Delta z} ; (i-1)\Delta z \leq z' \leq i\Delta z$$

$$0 \quad \text{otherwise} \quad (6.1.6)$$

Thus the current distribution along the antenna is given by

$$I = \sum_{i=1}^{N-1} I_i \quad (6.1.7)$$

Where N is the number of subsections of the antenna.

By substituting the current distribution given by Equation (6.1.6) in (6.1.5), and following the procedure described in Chapter 2, E_z^i can be reduced to the form

$$E_z^i - Z^i \sum_{i=1}^{N-1} I_i = \left(\frac{30j}{\sin k\Delta z} \right) \sum_{i=1}^{N-1} J_i \left(\frac{e^{-jkr_1}}{R_1} + \frac{e^{-jkr_2}}{R_2} - 2 \cos k\Delta z \right) \frac{e^{-jkr}}{r} \quad (6.1.8)$$

Where

$$R_1 = \sqrt{a^2 + \{z - (i + 1) \Delta Z\}^2}$$

$$R_2 = \sqrt{a^2 + \{z - (i - 1) \Delta Z\}^2}$$

$$r = \sqrt{a^2 + (z - i\Delta Z)^2}$$

For a dipole antenna fed at i th segment and loaded at the j th and k th segments, Equation (6.1.8) can be written, after applying Galerkin's method, in the matrix form as

$$[V_0] - [Z_L] [J] = [Z] [J] \quad (6.1.9)$$

$$[V] = [Z] [J] \quad (6.1.10)$$

Where

$$[V_0] = \begin{bmatrix} 0 \\ \vdots \\ 0 \\ V_i \\ V_{i-1} \\ 0 \\ \vdots \\ \vdots \\ 0 \end{bmatrix} = \begin{bmatrix} 0 \\ \vdots \\ 0 \\ V_0 \\ V_0 \\ 0 \\ \vdots \\ \vdots \\ 0 \end{bmatrix} \quad (6.1.11)$$

[Z] = generalized impedance matrix, its element at m row and n column is given by

$$Z_{mn} = \sum_{i=n}^{n+2} j \left(\frac{30 k \Delta z}{\sin k \Delta z} \right) \left(\frac{e^{-jk\sqrt{a^2 + ((m-i+1)\Delta z)^2}}}{1 - \cos k \Delta z} \right)$$

$$[k(1 + jk\sqrt{a^2 + ((m-i+1)\Delta z)^2}) \{ (\Delta z (i-m))$$

$$\ln \left(\frac{(m-i+1)\Delta z + \sqrt{((m-i+1)\Delta z)^2 + a^2}}{(m-i)\Delta z + \sqrt{((m-i)\Delta z)^2 + a^2}} \right) + (2+m-i)$$

$$\Delta z \ln \left(\frac{(2+m-i)\Delta z + \sqrt{((2+m-i)\Delta z)^2 + a^2}}{(m-i+1)\Delta z + \sqrt{((m-i+1)\Delta z)^2 + a^2}} \right) \}$$

$$+ k(1 + jk\sqrt{a^2 + ((m-i+1)\Delta z)^2}) \{ 2\sqrt{a^2 + ((m-i+1)\Delta z)^2}$$

$$- \sqrt{a^2 + ((m-i)\Delta z)^2} - \sqrt{a^2 + ((2+m-i)\Delta z)^2}$$

$$- j(k\Delta z)^2]$$

(6.1.12)

The equation (6.1.12) is obtained under the condition that $k\Delta z \ll 1$.

The load impedance matrix is given by

$$[Z_L] = \begin{array}{c} 0 \\ 0 \quad Z_{j-1,j-1} \quad Z_{j-1,j} \\ \quad Z_{j,j-1} \quad Z_{j,j} \\ \\ \\ 0 \quad \quad \quad Z_{k-1,k-1} \quad Z_{k-1,k} \\ \quad \quad \quad Z_{k,k-1} \quad Z_{k,k} \end{array}$$

$$Z_{j,j} = \frac{Z^i}{\sin k\Delta z} \left(\frac{k\Delta z}{1 - \cos k\Delta z} \right) \int_{(j-1)\Delta z}^{j\Delta z} \sin^2 k(\Delta z + (z - j\Delta z)) dz$$

(6.1.13)

$$Z_{j,j-1} = \frac{Z^i}{\sin k\Delta z} \left(\frac{k\Delta z}{1 - \cos k\Delta z} \right) \int_{(j-1)\Delta z}^{j\Delta z} \sin k(\Delta z + (z - j\Delta z)) \cdot \sin k(\Delta z - (z - (j-1)\Delta z)) dz$$

(6.1.14)

$$Z_{j-1,j} = \frac{Z^i}{\sin k\Delta z} \left(\frac{k\Delta z}{1 - \cos k\Delta z} \right) \int_{(j-1)\Delta z}^{j\Delta z} \sin k(\Delta z - (z - (j-1)\Delta z)) \cdot \sin k(\Delta z + (z - j\Delta z)) dz$$

(6.1.15)

$$Z_{j-1,j-1} = \frac{Z^i}{\sin k\Delta z} \left(\frac{k\Delta z}{1 - \cos k\Delta z} \right) \int_{(j-1)\Delta z}^{j\Delta z} \sin^2 k(\Delta z - (z - (j-1)\Delta z)) dz$$

(6.1.16)

$Z_{k,k}$, $Z_{k,k-1}$, $Z_{k-1,k}$ and $Z_{k-1,k-1}$ can also be determined from the four equations above by replacing j by k .

6.2 Optimization for Directive Gain in the Vertical Plane

It was already shown in Chapter 3 that the directive gain in the vertical plane can be written in the matrix form

$$D = 2 (1 - \cos k\Delta z)^2 \frac{\begin{matrix} \sim^* & \sim^* & \sim^* \\ [V] & [Y] & [A] \\ \sim^* & \sim^* & \end{matrix} \begin{matrix} [A] & [Y] & [V] \\ [V] & [Y] & [U] \\ [Y] & [U] & [V] \end{matrix}}{\begin{matrix} [V] & [Y] & [U] \\ [Y] & [U] & [V] \end{matrix}} \quad (6.2.1)$$

For a dipole loaded with surface impedance Z^i per unit length in the j^{th} and k^{th} segments and fed in the i^{th} segment, we have

$$[V] = \begin{pmatrix} 0 \\ \cdot \\ V_{j-1} \\ V_j \\ 0 \\ V_{i-1} \\ V_i \\ 0 \\ \cdot \\ V_{k-1} \\ V_k \\ \cdot \\ 0 \end{pmatrix} \quad (6.2.2)$$

Where

$$V_{j-1} = V_k$$

$$V_j = V_{k-1}$$

$$V_{i-1} = V_i = V_0$$

V_{j-1} and V_j can be written as a function of surface impedance as

$$V_{j-1} = -Z^i (\beta_1 J_{j-1} + \beta_2 J_j) \quad (6.2.3)$$

$$V_j = -Z^i (\beta_2 J_{j-1} + \beta_1 J_j) \quad (6.2.4)$$

where

$$\beta_1 = \frac{1}{\sin k\Delta z} \left(\frac{k\Delta z}{1 - \cos k\Delta z} \right) \int_{(j-1)\Delta z}^{j\Delta z} \sin^2 k(\Delta z + (z - j\Delta z)) dz$$

$$\beta_2 = \frac{1}{\sin k\Delta z} \left(\frac{k\Delta z}{1 - \cos k\Delta z} \right) \int_{(j-1)\Delta z}^{j\Delta z} \sin k(\Delta z + (z - j\Delta z)) \sin k .$$

$$(\Delta z - (z - (j - 1)\Delta z)) dz$$

From equations (6.2.3) and (6.2.4) it can be shown that

$$J_{j-1} = -\frac{1}{\Delta Z^i} (\beta_1 V_{j-1} - \beta_2 V_j) \quad (6.2.5)$$

$$J_j = -\frac{1}{\Delta Z^i} (-\beta_2 V_{j-1} + \beta_1 V_j) \quad (6.2.6)$$

where

$$\Delta = \beta_1^2 - \beta_2^2$$

By using equations (6.1.10), (6.2.5) and (6.2.6) V_{j-1} and V_j can be written as

$$V_{j-1} = -\frac{\Delta}{c} y_3 (Y^i \beta_1 + \Delta Y_5) + y_6 (Y^i \beta_2 - \Delta Y_2) \quad (6.2.7)$$

$$V_j = -\frac{\Delta}{c} y_3 (Y^i \beta_2 - \Delta Y_4) + y_6 (Y^i \beta_1 + \Delta Y_1) \quad (6.2.8)$$

where

$$y^i = 1/Z^i$$

$$Y_1 = y_{j-1, j-1} + y_{j-1, k}$$

$$Y_2 = y_{j-1, j} + y_{j-1, k-1}$$

$$Y_3 = y_{j-1, i-1} + y_{j-1, i}$$

$$Y_4 = y_{j, j-1} + y_{j, k}$$

$$Y_5 = y_{j, j} + y_{j, k-1}$$

$$Y_6 = y_{j, i-1} + y_{j, i}$$

$$c = (Y_1 \beta_1 + \Delta Y_5)(Y_{\ell} \beta_1 + \Delta Y_1) - (Y_{\ell} \beta_2 - \Delta Y_2) \cdot \\ (Y_1 \beta_2 - \Delta Y_2)(Y_{\ell} \beta_2 - Y_4)$$

Letting $[B] = [A] [Y]$, the numerator of equation (6.2.1) can be written as

$$[V] [Y] [A] [A] [Y] [V] = [(B_{j-1} + B_k)V_{j-1} + (B_j + B_{k-1})V_j \\ + (B_i + B_{i-1})V_0][(B_{j-1} + B_k)V_{j-1} \\ + (B_j + B_{k-1})V_j + (B_i + B_{i-1})V_0] \quad (6.2.9)$$

And by letting $[E] = [Y] [U] [Y]$, the denominator can be written as

$$[V] [Y] [U] [Y] [V] = V^*(E_1 V_{j-1} + E_2 V_j + E_3 V_0) \\ + V^*(E_4 V_{j-1} + E_5 V_j + E_6 V_0) \\ + V_0^*(E_7 V_{j-1} + E_8 V_j + E_9 V_0) \quad (6.2.10)$$

Where

$$E_1 = e_{j-1, j-1} + e_{j-1, k} + e_{k, j-1} + e_{k, k}$$

$$E_2 = e_{j-1, j} + e_{j-1, k-1} + e_{k, j} + e_{k, k-1}$$

$$E_3 = e_{j-1, i-1} + e_{j-1, i} + e_{k, i-1} + e_{k, i}$$

$$E_4 = e_{j, j-1} + e_{j, k} + e_{k-1, j-1} + e_{k-1, k}$$

$$E_5 = e_{j, j} + e_{j, k-1} + e_{k-1, j} + e_{k-1, k-1}$$

$$E_6 = e_{j, i-1} + e_{j, i} + e_{k-1, i-1} + e_{k-1, i}$$

$$E_7 = e_{i-1, j-1} + e_{i-1, k} + e_{i, j-1} + e_{i, k}$$

$$E_8 = e_{i-1, j} + e_{i-1, k-1} + e_{i, j} + e_{i, k-1}$$

$$E_9 = e_{i-1, i-1} + e_{i-1, i} + e_{i, i-1} + e_{i, i}$$

The computer program is listed in Appendix C.

6.3 Numerical Results

The dipole selected for study is a short dipole of $L/\lambda = 0.1$. The short dipole is first loaded with finite size load impedance of the same value as the optimum delta load impedance for maximum directive gain in the vertical plane. The dipole is then loaded with the optimum finite size load impedance for maximum directive gain in the vertical plane. Figure 6.1 shows the resulting current distributions. The current distribution of the dipole loaded with optimum delta load is also shown in figure 6.1 for comparison. The normalized radiation patterns are shown in figures 6.2, 6.3 and 6.4.

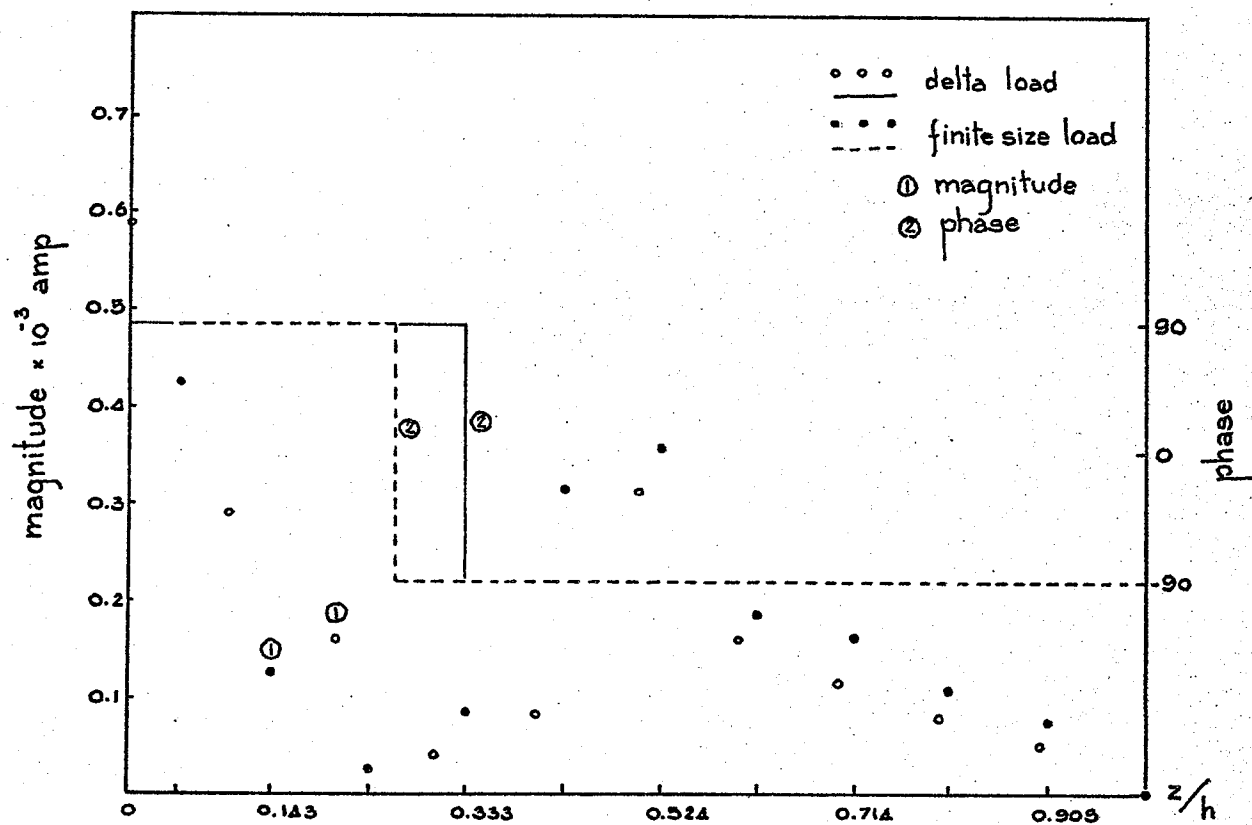


Fig. 6.1 Current distribution for short dipole loaded with finite size inductive load

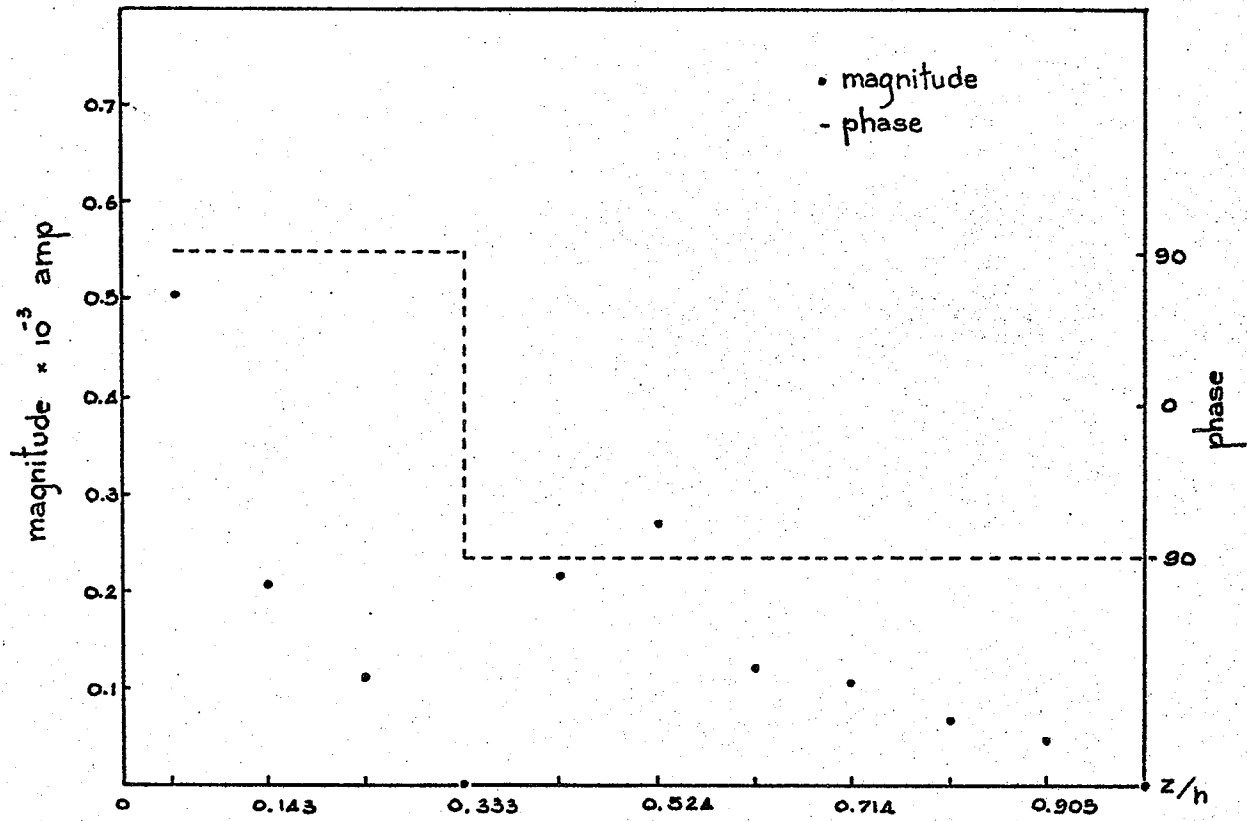


Fig. 6.2 Current distribution for short dipole loaded with finite size optimum load impedance for maximum directivity

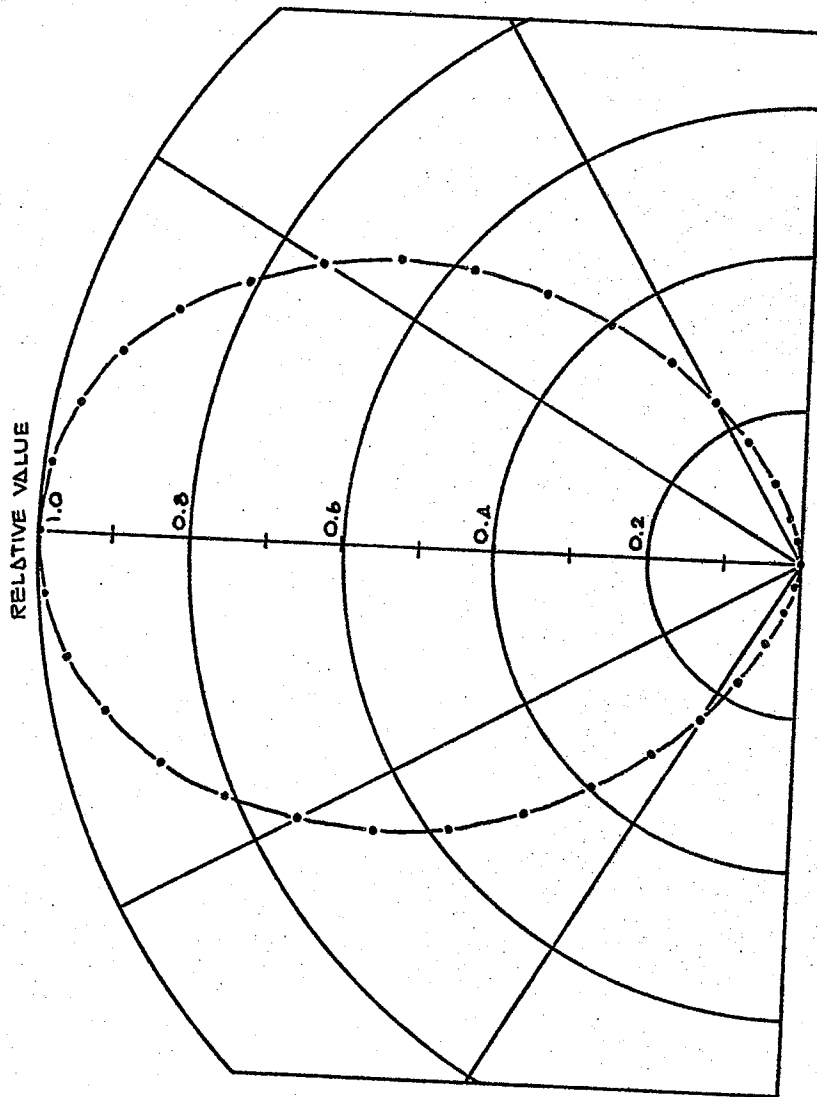


Fig. 6.3 Normalized radiation pattern for short dipole loaded with finite size inductive load

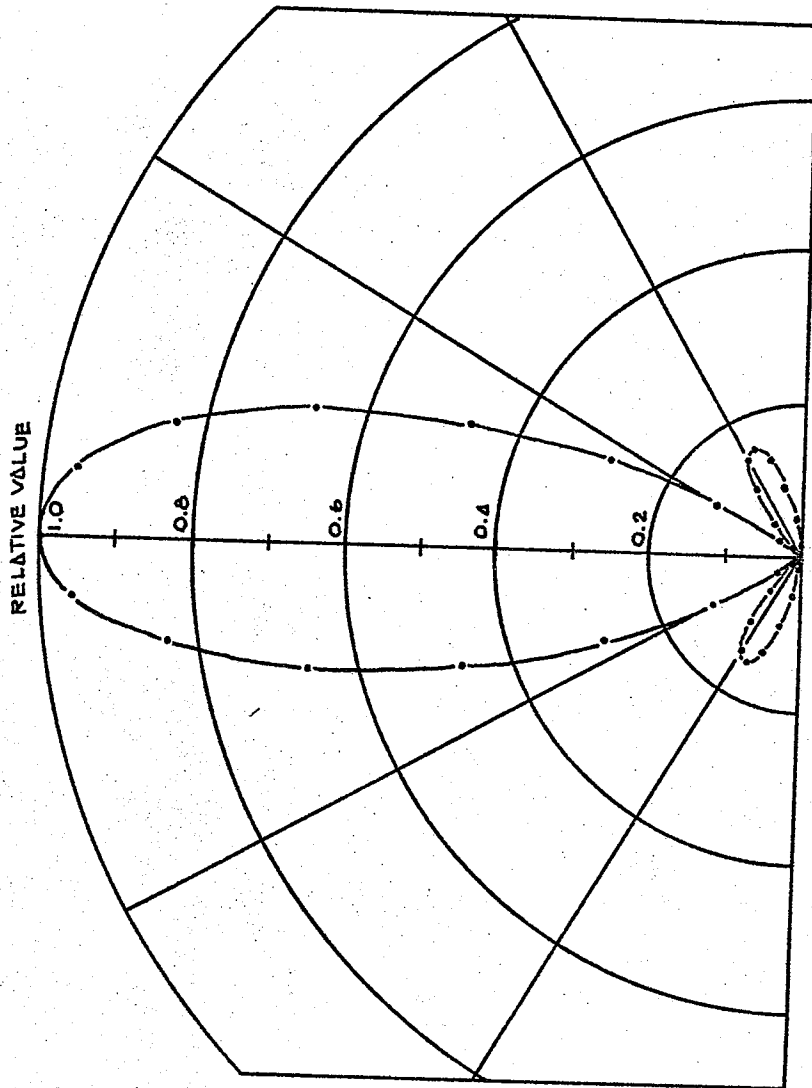


Fig. 6.4 Normalized radiation pattern for short dipole loaded with finite size optimum load impedance for maximum directivity

CHAPTER 7

DISCUSSION AND CONCLUSION

The study of a conventional dipole loaded with a lumped impedance in series with each arm has been the main focus of this thesis. The current distribution, using Pocklington's integral equation, for the unloaded dipole is solved by the method of moments. This solution is then modified to include the effect of the lumped load impedance which makes it possible to write the current distribution as a function of connected load impedance. By applying the calculated current distribution as function of connected load impedance, the expressions for directive gain, radiated power and antenna input impedance as a function of load impedance are determined. Attempt is then made to find the optimum loads for maximum directive gain in the vertical plane, maximum radiated power and for cancelling the input reactance in order to resonate the dipole. The results of the study are shown in Chapters 3, 4, 5 and 6. In this chapter a discussion of the results is presented and certain conclusions are made.

7.1 Discussion

The results obtained when the antenna is loaded with the optimum load for maximum directive gain in the vertical plane are shown in Chapter 3. It is found that all the optimum loads are inductive. The value of load is quite high when placed at the outer open ends of the antenna arms. As the load is moved towards the source at the centre, the value of the optimum load becomes smaller until it reaches a minimum value at some point along

the wire and then it starts increasing again as the load approaches the feed gap. Let us take $L/\lambda = 0.1$ for example, the value of optimum load is 2230.09 ohms at $d/h = 0.9$, it then decreases to 1775.34 ohms at $d/h = 0.7$ and increases to 5197.99 ohms at $d/h = 0.1$. It is also found that at the same ratio of d/h for antennas of different lengths, the optimum load for a short antenna is more inductive than that for the longer antenna, as shown in figure 3.3. Examination of the calculated current distribution indicates that the real part is very much smaller than the imaginary part. The magnitude and phase of the current distribution are shown in figures 3.4 to 3.6 for different antenna lengths. For antennas of the same length which are loaded with the optimum loads at different positions, the current distributions are obviously different. The phase distribution is almost constant at $\pi/2$ except for a 180° reversal at the point where the imaginary current becomes negative. Because of the drastic reduction in the magnitude of the current when the antenna is loaded with the optimum load, as compared to that of the unloaded antenna, the radiated power is very poor. This can also be seen from tables 3.1 to 3.3 which show the input impedance of the antenna consists of a very small resistive part and a very large capacitive part. The resistive part is the input resistance of the antenna which is equal to the radiation resistance because the antenna is perfectly conducting and is loaded with a purely inductive load. From these results it can be seen that the dipole loaded with an optimum load, based on maximum directivity, radiates no-power compared to the unloaded case. The radiation patterns are shown in figures 3.7 to 3.9. For the three different antenna lengths the radiation patterns are almost the same. All the radiation patterns consist of one main lobe and two small side lobes. The beamwidths obtained are about the same and equal to 38° . Though the radiation patterns are almost the same, the radiated power for the

antenna of longer length is larger than that of the shorter length. This can also be seen from tables 3.1 to 3.3 which show that the input impedance of the longer antenna consists of larger radiation resistance and smaller input reactance. For the antenna of the same length loaded at different positions with optimum loads, the radiated power is larger for the antenna with the load position close to the end. This can also be seen from tables 3.1 to 3.3.

The results for maximum radiated power are shown in Chapter 4. Figure 4.1 shows the variation of optimum load for maximum radiated power with its location. It is found that the optimum load for maximum radiated power is quite large at the open end of the antenna arms and becomes smaller as it is moved closer to the centre (take $L/\lambda = 0.1$ for example. The optimum load is 1860.49 ohms at $d/h = 0.9$ and is 472.47 ohms at $d/h = 0.1$). It is also found that the optimum load for a dipole of $L/\lambda = 0.1$ is larger than the optimum load for dipole of $L/\lambda = 0.2$ when the antennas are loaded at the same d/h . But for these two cases the optimum load is inductive. The optimum load for a $\lambda/2$ dipole is found to be capacitive. Thus it can be concluded that the unloaded dipole with higher capacitive input reactance will require optimum load of higher inductive reactance and vice versa. The input impedances shown in tables 4.1 to 4.3 have a very small reactive component and thus the optimum load will almost resonate the antenna. This result is more pronounced for the short dipole. Tables 4.1 and 4.2 show that the modification of the input impedance for a short dipole is very large but from table 4.3, it is seen that the optimum load does not have much effect on the half-wave dipole.

With regard to the input resistance, which is equal to the radiation resistance in these cases (because the optimum load is purely reactive and

the dipole is perfectly conducting), it is larger when the location of load is closer to the open ends. This is true for the unloaded dipole with capacitive input reactance but, when the input reactance of the unloaded dipole is inductive, the radiation resistance is larger when the loading position is closer to the centre. The current distributions are shown in figures 4.2 to 4.8. The modification of the current distribution is very large for short dipoles, as shown in figures 4.2 to 4.7 for different load locations. From these results, the magnitude of the current distribution is almost constant from the source to the point of loading and then it decreases after the point of loading to zero at the end. However it should be noted that there is a jump in the current at the loading point. For a half-wave dipole the magnitude of the current distribution is still sinusoidal as shown in figure 4.8. In all cases the real component of the current distribution is very much larger than its imaginary component, i.e. the phase distribution is almost constant at zero. The normalized radiation patterns are shown in figures 4.9 to 4.11 and they are almost the same as the pattern of the corresponding unloaded cases. It is also found that the variation of loading position does not appreciably change the normalized radiation pattern but it does change the magnitude of radiation intensity. Again for a half-wave dipole, this change is not large compared with the unloaded case. From these results it can be concluded that the improvement of radiated power is very large for short dipoles. For half-wave dipoles, it appears that they radiate almost maximum radiated power and thus no loading is required. In all cases the directivity does not appreciably change from the corresponding unloaded cases.

The results when the antenna is loaded with a resonating load are

shown in Chapter 5. From tables 5.1 to 5.3 it is found that the resonating load is complex. In the presence of resistive part, the input resistance obtained is not equal to the radiation resistance because of the losses in the load. Since the resistive part of the connected load means power loss, the resonating load which is purely reactive, is also determined and the results are shown in tables 5.4 to 5.6. The radiation resistance obtained in this case, i.e. when the resonating load is purely reactive, is almost the same as the radiation resistance obtained when the antenna is loaded for maximum radiated power. It is found in all cases that the connected load reactance is inductive for the unloaded dipole with capacitive input reactance and is capacitive for the unloaded dipole with inductive input reactance. The variation of the reactive part of the connected load with the loading position is such that it is large at the open end of the antenna arms and becomes smaller as it is moved towards the centre (for $L/\lambda = 0.1$, the load reactance is 1860.50 ohms at $d/h = 0.9$ and is 472.47 ohms at $d/h = 0.1$).

The current distribution when the antenna is loaded with the resonating load is shown in figures 5.1 to 5.3. In each figure the current distribution of the antenna loaded with purely reactive load is compared with the antenna loaded with complex load. The difference between these two cases is quite large for short antennas but for a half-wave dipole it is quite small. The magnitude of the current distribution in the first case is larger than in the latter case. The phase distribution in the first case is almost constant at zero while in the latter case it deviates appreciably from zero. The magnitude of the current distribution as shown is almost constant from the source to the loading position and then it decreases, after the loading point, and tends to zero at the open end. For half-wave dipole case the current distribution is still sinusoidal. It

is noted that the current suffers a jump discontinuity at the loading point. The current distribution when the antenna is loaded with a purely reactive load is almost the same as the current distribution for the case when maximum power is radiated.

The normalized radiation patterns are shown in figures 5.4 to 5.6. These patterns are almost the same as the corresponding unloaded antennas. The directive gain in the vertical plane is almost the same as in the unloaded case.

The numerical results for resonating the antenna shown have served as good examples of the transformation of the antenna input impedance. In general the antenna input impedance can be transformed to arbitrary values by using equations (5.10) and (5.11). From these two equations the value of the connected load can be determined.

When the size of the load is taken into consideration the results are given in Chapter 6. It is found that the current distribution, as shown in figure 6.1, is larger when the dipole is loaded with a finite size load of the same value on each arm as when it is loaded with a delta load for maximum directive gain in the vertical plane. The normalized radiation pattern, as shown in figure 6.3, in this case does not change much from that of the unloaded dipole and thus it indicates that the optimum value of load for maximum directive gain in the vertical plane changes when it is of finite size. It is found that the optimum load in this case is larger than the optimum delta load and amounts to 1.25 times for the short dipole case investigated.

The current distribution and radiation pattern (fig. 6.1, 6.2 and 6.4) of the dipole loaded with this new optimum load for maximum directive gain in the vertical plane which is of finite size are almost the same as when the dipole is loaded with the optimum delta load for maximum directive gain in the vertical plane. However, the current distribution, input impedance, radiation pattern and gain are significantly altered when the load is of finite size and not optimized for maximum directive gain in the vertical plane.

7.2 Conclusion

When the dipole is loaded with an optimum load for maximum directive gain in the vertical plane, it is found that the optimum load is purely inductive. The current distribution has a very small real component and a very large imaginary component. The input impedance consists of a very small resistive part and a very large capacitive part. This means that the antenna will almost radiate no power at all.

When the antenna is loaded with the optimum load for maximum radiated power, it is found for the unloaded antenna with capacitive input reactance, that the optimum load is inductive, and for inductive unloaded input reactance, the optimum load is capacitive. For a half-wave dipole, the improvement is very small, thus the loading is not necessary. For a short dipole, the improvement is quite large, thus the radiated power of a short dipole can be enhanced by proper impedance loading.

For transformation of the antenna input impedance, only the case of a resonating load is determined. For a short dipole loaded with a purely reactive resonating load, maximum power is radiated. For a half-

wave dipole, the improvement in radiated power is small. In general with the proper value of connected load, the antenna impedance can be transformed to almost any arbitrary value.

7.3 Suggestions for Future Research

In the course of this thesis, emphasis has been placed on a dipole antenna which is assumed to be very thin in order that the thin wire approximation can be applied. As the antenna diameter becomes larger and larger, this approximation is no longer applicable and the optimum loads which are obtained for the thin dipole antenna will not be the same as for the fat dipole antenna. It would therefore be interesting to extend this study to take into account the effect of antenna wire diameter. This could be achieved by replacing the thin-wire kernel by the exact kernel, as shown in equation (2.1.15). It is shown by Pearson⁽³²⁾ that this exact kernel consists of singularity in logarithmic term, which is integrable and the non-singular terms can be evaluated numerically.

Another assumption made in this study is regarding the electric field in the feed gap region. It is assumed for simplicity that the excitation field in the gap region is constant. This assumption gives a reasonable accuracy for the current distribution away from the feed region. However, in order to improve the accuracy, a more precise impressed field should be employed. By taking into account the effect of antenna feeder, Popovic⁽³³⁾ showed that the impressed field can be written in terms of a cosine function which exists over a narrow feed

region. For a larger size feed region, the gap may be taken into account by our method by simply considering it to be a one or more segment of the dipole using Galerkin's version of the moment method⁽²²⁾. It is expected that the effect of a large feed gap is on the input impedance since the region becomes effectively a parallel plate capacitor shunted across the feed line and the antenna itself.

APPENDIX A

DERIVATION OF MATRIX [U]

The total radiated power as given in equation (3.1.11) is

$$P_r = \int_0^{2\pi} \int_0^{\pi} \Phi(\theta, \phi) \sin\theta \, d\theta \, d\phi \quad (\text{A.1})$$

Where $\Phi(\theta, \phi)$ is the radiation intensity and is given

$$\Phi(\theta, \phi) = \frac{120}{4\pi(\sin k\Delta z)^2} \left[\frac{\cos(k\Delta z \cos\theta) - \cos k\Delta z}{\sin\theta} \right]^2$$

$$\begin{matrix} \sim^* & \sim^* & \sim^* \\ [V] & [Y] & [A] \end{matrix} [A] [Y] [V] \quad (\text{A.2})$$

Where [A] is given by

$$[A] = [e^{jk\Delta z \cos\theta} \quad e^{2jk\Delta z \cos\theta} \quad \dots \quad e^{(N-1)jk\Delta z \cos\theta}] \quad (\text{A.3})$$

Substituting equation (A.2) into equation (A.1), we obtain

$$P_r = \frac{60}{(\sin k\Delta z)^2} \int_0^{\pi} \left[\frac{\cos(k\Delta z \cos\theta) - \cos k\Delta z}{\sin\theta} \right]^2 \begin{matrix} \sim^* & \sim^* & \sim^* \\ [V] & [Y] & [A] \end{matrix} [A] [Y] [V] \, d\theta \quad (\text{A.4})$$

From which the matrix [U] is defined

$$[U] = \int_0^{\pi} \frac{[\cos(k\Delta z \cos\theta) - \cos k\Delta z]^2}{\sin\theta} [A][A]^* d\theta \quad (A.5)$$

By using the matrix [A] as given in (A.3), the elements of matrix [U] are given by

$$U_{mn} = \int_0^{\pi} \frac{[\cos(k\Delta z \cos\theta) - \cos(k\Delta z)]^2}{\sin\theta} e^{jk\Delta z(n-m)\cos\theta} d\theta \quad (A.6)$$

Where m and n represent row and column of the element.

APPENDIX B

All the constants are derived for the thin cylindrical antenna fed at z_i by a delta voltage source and loaded at z_j and z_k by identical lumped impedance of infinitesimal dimension. In dealing with the resulting matrices, the subscripted letters represent the position of the element of the matrix. $\text{Re} []$ and $\text{Im} []$ represent the real and imaginary part, respectively, of the complex number in the square bracket and $| |$ represents the amplitude.

The matrix $[Y]$ is defined as

$$[Y] = [Z]^{-1}$$

The matrix $[B]$ is defined as

$$[B] = [N][Y]$$

where $[N]$ is a row matrix with unity elements.

The constants γ_1 , γ_2 , γ_3 and γ_4 are then defined as

$$\gamma_1 = |y_{ji}|^2 [\{\text{Re}(B_j) + \text{Re}(B_k)\}^2 + \{\text{Im}(B_j) + \text{Im}(B_k)\}^2]$$

$$\gamma_2 = |B_i|^2$$

$$\gamma_3 = -2[\text{Re}(y_{ji})\text{Re}(B_j)\text{Re}(B_i) + \text{Re}(y_{ji})\text{Im}(B_j)\text{Im}(B_i) + \text{Im}(y_{ji})$$

$$\text{Re}(B_j)\text{Im}(B_i) - \text{Im}(y_{ji})\text{Re}(B_i)\text{Im}(B_j) + \text{Re}(y_{ji})\text{Re}(B_i)$$

$$\text{Re}(B_k) + \text{Re}(y_{ji})\text{Im}(B_i)\text{Im}(B_k) - \text{Im}(y_{ji})\text{Re}(B_i)\text{Im}(B_k)$$

$$+ \text{Im}(y_{ji})\text{Re}(B_k)\text{Im}(B_i)]$$

$$\gamma_4 = 2[\text{Re}(y_{ji})\text{Re}(B_j)\text{Im}(B_i) - \text{Re}(y_{ji})\text{Re}(B_i)\text{Im}(B_j) - \text{Im}(y_{ji})\text{Re}(B_j)$$

$$\text{Re}(B_i) - \text{Im}(y_{ji})\text{Im}(B_j)\text{Im}(B_i) - \text{Re}(y_{ji})\text{Re}(B_i)\text{Im}(B_k)$$

$$+ \text{Re}(y_{ji})\text{Re}(B_k)\text{Im}(B_i) - \text{Im}(y_{ji})\text{Re}(B_k)\text{Re}(B_i) - \text{Im}(y_{ji})\text{Im}(B_i)$$

$$\text{Im}(B_k)]$$

The matrix [F] is defined as

$$[F] = [Y] [U] [Y]^*$$

Because of symmetric property of the matrix [Y], [F] can be written as

$$[F] = [Y]^* [U] [Y]$$

Then α_1 , α_2 , α_3 and α_4 can be defined as

$$\alpha_1 = \operatorname{Re}(F_{jj} + F_{jk} + F_{kj} + F_{kk}) |y_{ji}|^2$$

$$\alpha_2 = \operatorname{Re}(F_{ii})$$

$$\alpha_3 = -2[\operatorname{Re}(F_{ji} + F_{ki})\operatorname{Re}(y_{ji}) + \operatorname{Im}(F_{ji} + F_{ki})\operatorname{Im}(y_{ji})]$$

$$\alpha_4 = -2[\operatorname{Re}(F_{ji} + F_{ki})\operatorname{Im}(y_{ji}) - \operatorname{Im}(F_{ji} + F_{ki})\operatorname{Re}(y_{ji})]$$

APPENDIX C

COMPUTER PROGRAMS

The computer programs are separately written for the wire antenna loaded with delta and finite size load impedances.

(I) The dipole loaded with delta load impedance

The following computer programs are written

- (a) The computer program for determining the parameters for optimization.
- (b) Optimization program, using the subroutine 'CLIMBD' of the University of Waterloo WATFIV library programs.
- (c) The computer program for determining the current distribution and radiation pattern of loaded dipole.

\$\$\$JOB WATFIV A. ITTIPI800N

THE INTEGRAL EQUATION OF POCKLINGTON TYPE IS USED IN ANALYSING
LOADED DIPOLE ANTENNA. IN THIS PROGRAM THIN WIRE APPROXIMATION
IS USED.

IMPLICIT REAL*8 (A-H,O-Z)
COMPLEX*16 DCMLX,COMP,CDEXP,CMLXA,CMLXB,CMLXC,
*Z,NMTRA,NMTRB,NMTRC,DET,DCONJG,XVAR,FARFLD
COMPLEX*16 YAD,BE,BE1
COMPLEX*16 FIELD,EXP1,EXP2,EXP3,NRFLD
COMPLEX*16 SUMY,ZLOAD
COMPLEX*16 KS,EM,CONST1,EX,CONST2,EXCTN
COMPLEX*16 API(40,40)
REAL*8 LENGTH,LAMDA
DIMENSION YAD(40,40),BE(40),KS(42),EXCTN(40)
DIMENSION AMG(40)
DIMENSION EM(19,19),Z(19,19),IC(19),IR(19)
EQUIVALENCE(EM,Z)

RADIUS = RADIUS OF WIRE ANTENNA
LENGTH = TOTAL LENGTH OF ANTENNA
NSEG = NUMBER OF SEGMENTS ALONG THE WIRE ANTENNA
LAMDA = WAVE LENGTH OF OPERATING FREQUENCY

DAIMAG(XVAR) = ((0.D0,-1.D0)*XVAR+DCONJG((0.D0,-1.D0)*XVAR))/2.D0
DREAL(XVAR) = (XVAR+DCONJG(XVAR))/2.D0

READ, LAMDA,LENGTH,RADIUS,NSEG

PRINT101
FORMAT('1')

READ01

PRINT, 'LAMDA', LAMDA, 'LENGTH', LENGTH, 'RADIUS', RADIUS, 'N', NSEG
N = NSEG

PI = 3.141592654
BETA = 2.D0*PI/LAMDA
DELTAZ = LENGTH/NSEG
RADIAN = BETA*DELTAZ
SINN = DSIN(RADIAN)
COSS = DCOS(RADIAN)
COMP = DCMLX(0.D0,30.D0/SINN)
CCNST = 120.D0*((1-COSS)/SINN)**2
PRINT, COMP
NUMBER = NSEG-1
N1 = NUMBER-1

GENERALIZED IMPEDANCE IS DETERMINED

M = 1
DO 1 I = 1,NUMBER
DENMTA = (RADIUS**2+((M-I-1)*DELTAZ)**2)**(1./2.)
EXPTNA = BETA*DENMTA
DENMTB = (RADIUS**2+((M-I+1)*DELTAZ)**2)**(1./2.)
EXPTNB = BETA*DENMTB
DENMTC = (RADIUS**2+((M-I)*DELTAZ)**2)**(1./2.)
EXPTNC = BETA*DENMTC
CMLXA = DCMLX(0.D0,-EXPTNA)
NMTRA = CDEXP(CMLXA)
CMLXB = DCMLX(0.D0,-EXPTNB)
NMTRB = CDEXP(CMLXB)
CMLXC = DCMLX(0.D0,-EXPTNC)
NMTRC = 2.D0*COSS*CDEXP(CMLXC)
Z(1,I) = COMP * (NMTRA/DENMTA + NMTRB/DENMTB - NMTRC/DENMTC)
Z(1,I) = Z(1,I) * DELTAZ * 10.00-05
CONTINUE
DO 2 JCOUNT = 2,NUMBER

```

2      Z(JCOUNT,JCOUNT) = Z(1,1)
      DO 3 JB = 2,NUMBER
          JA = 1
          NCCOUNT = JB
4      Z(NCCOUNT,JA) = Z(JA,NCCOUNT)
          JA = JA+1
          NCCOUNT = NCCOUNT+1
          IF( NCCOUNT .GT. NUMBER ) GO TO 3
          Z(JA,NCCOUNT) = Z(1,JB)
          GO TO 4
3      CONTINUE
      CALL MINVCD(Z,NUMBER,NUMBER,DET,IR,IC)
      DO107 J = 1,NUMBER
      DO107 I = 1,NUMBER
517     YAD(J,I) = Z(J,I) * 10.0D-05
      MCOL = NSEG/2
513     DO513 IAC = 1,NUMBER
          PRINT,' COLUMN',MCOL,' ROW',IAC,YAD(IAC,MCOL)
          RIN = DREAL(YAD(MCOL,MCOL))/CDABS(YAD(MCOL,MCOL))**2
          RTCEIN = -DAIMAG(YAD(MCOL,MCOL))/CDABS(YAD(MCOL,MCOL))**2
          PRINT,' INPUT RESISTANCE =',RIN
          PRINT,' INPUT REACTANCE =',RTCEIN
          DO 514 JCNT = 1,NUMBER
              AMG(JCNT) = CDABS(YAD(JCNT,MCOL))
              AIM = DAIMAG(YAD(JCNT,MCOL))
              REP = DREAL(YAD(JCNT,MCOL))
              PS = DATAN2(AIM,REP)
              PHASE = PS*180.0D/PI
514     PRINT,' ',AMG(JCNT),' ',PHASE
              SUMY = (0.0D0,0.0D0)
              DO112 KNT = 1,NUMBER
                  SUMY = SUMY + YAD(KNT,MCOL)
                  ABSUMY = SUMY * DCONJG(SUMY)
C
C      DETERMINATION OF THE MATRIX EM.
C
      NR = 1
      DO701 JC = 1,NUMBER
          IN = JC-NR
          RL = COSINE(DELTAZ,IN,BETA)
          AG = SINE(DELTAZ,IN,BETA)
          EM(NR,JC) = DCMPLX(RL,AG)
701     CONTINUE
      DO702 LA = 1,NUMBER
702     EM(LA,LA) = EM(1,1)
      DO703 JB = 2,NUMBER
          JA = 1
          NCCOUNT = JB
720     EM(NCCOUNT,JA) = DCONJG(EM(JA,NCCOUNT))
          JA = JA+1
          NCCOUNT = NCCOUNT+1
          IF( NCCOUNT.GT.NUMBER ) GO TO 703
          EM(JA,NCCOUNT) = EM(1,JB)
          GO TO 720
703     CONTINUE
      DO704 I = 1,NUMBER
          EXP1 = (0.0D0,0.0D0)
      DO705 J = 1,NUMBER
705     EXP1 = EXP1 + EM(I,J)*YAD(J,MCOL)
      KS(I) = EXP1
704     CONTINUE
      PRAD = (0.0D0,0.0D0)
      DO706 J = 1,NUMBER
706     PRAD = PRAD + DCONJG(YAD(J,MCOL))*KS(J)
      PRAD = (60.0D0/SINN**2)*PRAD
      DGAIN = ( CONST*ABSUMY )/PRAD

```

PRINT, :
PRINT, :
RADIATED POWER, PRAD
GAIN * .DGAIN

C
C

```

732 DO730 I = 1,NUMBER
      DO731 J = 1,NUMBER
      EXP2 = (0.00,0.00)
      DO732 L = 1,NUMBER
      EXP2 = EXP2 + EM(I,L)*YAD(L,J)
731 API(I,J) = EXP2
730 CONTINUE
      CONTINUE
C
      DO733 I = 1,NUMBER
      DO734 J = 1,NUMBER
      EXP3 = (0.00,0.00)
735 DO735 L = 1,NUMBER
      EXP3 = EXP3 + DCONJG(YAD(I,L))*API(L,J)
      EM(I,J) = EXP3
      IF( J.EQ.I ) GO TO 734
      EM(J,I) = DCONJG(EM(I,J))
734 CONTINUE
733 CONTINUE
      DO108 J = 1,NUMBER
      BE1 = (0.00,0.00)
      DO 109 I = 1,NUMBER
      BE1 = BE1+YAD(I,J)
109 CONTINUE
      BE(J) = BE1
108 CONTINUE
      I11 = NSEG / 2
      MCNT = I11 - 1
      DO105 IN = 1,MCNT
      J1J = IN
      K1K = NSEG - IN
      REYJJ = DREAL(YAD(J1J,J1J))
      AIYJJ = DAIMAG(YAD(J1J,J1J))
      REYJK = DREAL(YAD(J1J,K1K))
      AIYJK = DAIMAG(YAD(J1J,K1K))
      REYII = DREAL(YAD(I11,I11))
      AIYII = DAIMAG(YAD(I11,I11))
      REYJI = DREAL(YAD(J1J,I11))
      AIYJI = DAIMAG(YAD(J1J,I11))
      REYKI = DREAL(YAD(K1K,I11))
      AIYKI = DAIMAG(YAD(K1K,I11))
      REYKK = DREAL(YAD(K1K,K1K))
      AIYKK = DAIMAG(YAD(K1K,K1K))
      REBEJ = DREAL(BE(J1J))
      AIBEJ = DAIMAG(BE(J1J))
      REBEI = DREAL(BE(I11))
      AIBEI = DAIMAG(BE(I11))
      REBEK = DREAL(BE(K1K))
      AIBEK = DAIMAG(BE(K1K))
      GRAND1 = REYJI**2+AIYJI**2
      GAMMA1 = GRAND1*((REBEJ+REBEK)**2+(AIBEJ+AIBEK)**2)
      GAMMA2 = REBEI**2+AIBEI**2
      GRAND2 = REYJI*REBEJ+REBEI*REYJI+AIYJI*REBEJ+AIBEI*
      *AIYJI*REBEI+AIBEJ
      GRAND3 = REYJI*REBEJ*AIBEI-REYJI*REBEI*AIBEJ-AIYJI*REBEJ*REBEI-
      *AIYJI*AIYJI*AIBEI
      GRAND4 = REYJI*REBEI*REBEK+REYJI*AIYJI*AIBEK-AIYJI*REBEI*AIBEK+
      *AIYJI*REBEK*AIBEI
      GRAND5 = REYJI*REBEI*AIYJI*REBEK-REYJI*REBEK*AIBEI+AIYJI*REBEK
      *REBEI+AIYJI*AIYJI*AIBEK
      GAMMA3 = -2.*(GRAND2+GRAND4)
      GAMMA4 = 2.*(GRAND3-GRAND5)

```

```

EXP1 = EM(J1J,J1J)+EM(J1J,K1K)+EM(K1K,J1J)+EM(K1K,K1K)
EXP2 = EM(J1J,I1I)+EM(K1K,I1I)
ECON = DREAL(EXP1)*( CDABS(YAD(J1J,I1I))**2)
EMCOL = DREAL(EM(I1I,I1I))
EMA = DREAL(EXP2)*DREAL(YAD(J1J,I1I))+DAIMAG(EXP2)*DAIMAG(YAD(J1J
*I1I))
EMB = DREAL(EXP2)*DAIMAG(YAD(J1J,I1I))-DREAL(YAD(J1J,I1I))*DAIMAG
*(EXP2)
CONST = 2.00*(1.00-COSS)**2
PRINT106
FORMAT('0:')
106 PRINT,CONST = *,CONST
PRINT,GAMMA1 = *,GAMMA1
PRINT,GAMMA2 = *,GAMMA2
PRINT,GAMMA3 = *,GAMMA3
PRINT,GAMMA4 = *,GAMMA4
PRINT,ECON = *,ECON
PRINT,EMCOL = *,EMCOL
PRINT,EMA = *,EMA
PRINT,EMB = *,EMB
PRINT,REYJI = *,REYJI
PRINT,REYKI = *,REYKI
PRINT,AIYJI = *,AIYJI
PRINT,AIYKI = *,AIYKI
PRINT,REYJJ = *,REYJJ
PRINT,REYJK = *,REYJK
PRINT,AIYJJ = *,AIYJJ
PRINT,AIYJK = *,AIYJK
PRINT,REYII = *,REYII
105 CONTINUE
STOP
END

REAL FUNCTION SINE*B(DZ,IN,BETA)
IMPLICIT REAL*8(A-H,O-Z)
C = BETA*DZ
A = 0.00
R = 3.141592654
TOL = 0.00
NORDER = 5
K = 0
1 CALL GAUQUUD(A,B,FX,X,TOL,NORDER,K)
K = K+1
IF( K.LE. 0 ) GO TO 2
FX = (1.00/DSIN(X))*(DCOS(C*DCOS(X))-DCOS(C))**2*DSIN(C*IN*
*DCOS(X))
GO TO 1
2 SINE = FX
RETURN
END

REAL FUNCTION COSINE*B(DZ,IN,BETA)
IMPLICIT REAL*8(A-H,O-Z)
C = BETA*DZ
A = 0.00
R = 3.141592654
TOL = 0.00
NORDER = 5
K = 0
1 CALL GAUQUUD(A,B,FX,X,TOL,NORDER,K)
K = K+1
IF( K.LE. 0 ) GO TO 2
FX = (1.00/DSIN(X))*(DCOS(C*DCOS(X))-DCOS(C))**2*DCOS(C*IN*
*DCOS(X))
GO TO 1
2 COSINE = FX
RETURN
END
$ ENTRY

```

```

SJOB WATFIV ITTIPIBOON APISAK
C OPTIMIZATION OF THE RADIATED POWER.
  IMPLICIT REAL*8(A-H,O-Z)
  COMPLEX*16 DCONJG,X,IR
  COMPLEX*16 YII,YIJ,YJI,YIK,YJJ,YJK,YIN,ZIN
  DIMENSION X(2),G(2),H(2),S(14)
  COMMON GAMMA1,GAMMA2,GAMMA3,GAMMA4,CONST,ECON,EMCOL,EMA,EMB,REYII
  EXTERNAL SUB
  DREAL(XVAR) = (XVAR+DCONJG(XVAR))/2.D0
  DAIMAG(XVAR) = ((0.D0,-1.D0)*XVAR+DCONJG((0.D0,-1.D0)*XVAR))/2.D0
  READ,CONST,GAMMA1,GAMMA2,GAMMA3,GAMMA4,ECON,EMCOL,EMA,EMB,REYJI,
  *REYKI,AIYJI,AIYKI,REYJJ,REYJK,AIYJJ,AIYJK,REYII,AIYII,CDS
  KWRT = 1
  INDEX = 2
  G(1) = REYJJ+REYJK
  G(2) = -10.0**(30)
  H(1) = 10.0D 20
  H(2) = 10.C**(30)
  X(1) = REYJJ+REYJK+0.00001D0
  X(2) = 0.329681914162D-01
  NVR = +2
  NFIG = 16
  NCON = 2
  NTRIPV = 700
  L = 14
  PRINT,00
  FORMAT('1')
  DO1 I=1,10
  CALL CLIMBD(NVR,X,NCON,P,NFIG,S,L,KWRT,G,H,INDEX,NTRIPV,SUB)
  PRD = CDS*P
  PRINT,' MAXIMUM RADIATED POWER = ',PRD
  ADMTCE = X(1)-REYJJ-REYJK
  SUSTCE = X(2)-AIYJJ-AIYJK
  YLOAD = DCVPLX(ADMTCE,SUSTCE)
  ZLOAD = 1.D0/YLOAD
  PRINT,' CONNECTED LOAD
  WY = ( GAMMA1+GAMMA2*(X(1)**2+X(2)**2)+GAMMA3*X(1)+GAMMA4*X(2) ) /
  * ( ECON+EMCOL*(X(1)**2+X(2)**2)-2.D0*EMA*X(1)-2.D0*EMB*X(2) )
  PRINT,' GAIN
  AMGTDE = CDARS(ZLOAD)
  REZO = DREAL(ZLOAD)
  AIMZO = DAIMAG(ZLOAD)
  PHASE = DATAN2(AIMZO,REZO)
  ANGLE = 180.D0*PHASE/3.1416D0
  PRINT,' MAGNITUDE OF CONNECTED LOAD
  PRINT,' PHASE OF CONNECTED LOAD
  YII = DCVPLX(REYII,AIYII)
  YIJ = DCVPLX(REYJI,AIYJI)
  YJI = YIJ
  YIK = DCVPLX(REYKI,AIYKI)
  YIN = YII-(YIJ*YJI+YIK*YJI)/DCVPLX(X(1),X(2))
  ZIN = 1.D0/YIN
  PRINT,' INPUT IMPEDANCE
  CONTINUE
  STOP
  END
  =',ZLOAD
  =',WY
  =',AMGTDE
  =',ANGLE
  =',ZIN

SUBROUTINE SUB(NVAR,X,NCON,P,G,H)
  IMPLICIT REAL*8(A-H,O-Z)
  DIMENSION X(2),G(2),H(2)
  COMMON GAMMA1,GAMMA2,GAMMA3,GAMMA4,CONST,ECON,EMCOL,EMA,EMB,REYII
  P = ( ECON+EMCOL*(X(1)**2+X(2)**2)-2.D0*EMA*X(1)-2.D0*EMB*X(2) ) /
  * ( X(1)**2+X(2)**2 )
  RETURN
  END
$ENTRY

```

```

$JOB WATFIV ITTIPIBOON APISAK
      IMPLICIT REAL*8(A-H,O-Z)
      COMPLEX*16 DCONJG,XVAR
      COMPLEX*16 DCMPLX,YLOAD,ZLOAD
      DIMENSION X(2),G(2),H(2),S(14)
      COMMON GAMMA1,GAMMA2,GAMMA3,GAMMA4,CONST,ECON,EMCOL,EMA,EMB,REYII
      EXTERNAL SUB
      DREAL(XVAR) = (XVAR+DCONJG(XVAR))/2.D0
      DAIMAG(XVAR) = ((C.D0,-1.D0)*XVAR+DCONJG((0.D0,-1.D0)*XVAR))/2.D0
      READ,CONST,GAMMA1,GAMMA2,GAMMA3,GAMMA4,ECON,EMCOL,EMA,EMB,REYJI,
      *REYKI,AIYJI,AIYKI,REYJJ,REYJK,AIYJJ,AIYJK,REYII,AIYII,CDS
      KWRT = 0
      INDEX = 2
      G(1) = REYJJ+REYJK
      G(2) = -10.0**(30)
      H(1) = 10.0D 20
      H(2) = 10.0**(30)
      X(1) = 0.191455793537D-01
      X(2) = -0.100344324131D-01
      NVR = +2
      NFIG = 16
      NCON = 2
      NTRIPV = 700
      L = 14
      PRINT100
      FORMAT('1')
      DO1 I=1,10
      CALL CLIMBD(NVR,X,NCON,W,NFIG,S,L,KWRT,G,H,INDEX,NTRIPV,SUB)
      W = CONST*W
      PRINT,'MAXIMUM GAIN = ',W
      ADMTCE = X(1)-REYJJ-REYJK
      SUSTCF = X(2)-AIYJJ-AIYJK
      YLOAD = DCMPLX(ADMTCE,SUSTCF)
      ZLOAD = 1.D0/YLOAD
      PRINT,' CONNECTED LOAD = ',ZLOAD
      XSTO = X(1)
      X(1) = REYJJ+REYJK
      WY = ( GAMMA1+GAMMA2*(X(1)**2+X(2)**2)+GAMMA3*X(1)+GAMMA4*X(2) ) /
      *( ECON+EMCOL*(X(1)**2+X(2)**2)-2.D0*EMA*X(1)-2.D0*EMB*X(2) )
      WY = CONST*WY
      PRINT,' GAIN WHEN R IS EQUAL TO ZERO = ',WY
      AMGTDE = CDABS(ZLOAD)
      REZD = DREAL(ZLOAD)
      AIMZD = DAIMAG(ZLOAD)
      PHASE = DATAN2(AIMZD,REZD)
      ANGLE = 180.D0*PHASE/3.1416D0
      PRINT,' MAGNITUDE OF CONNECTED LOAD = ',AMGTDE
      PRINT,' PHASE OF CONNECTED LOAD = ',ANGLE
      X(1) = XSTO
      CONTINUE
      STOP
      END

      SUBROUTINE SUB(NVAR,X,NCON,W,G,H)
      IMPLICIT REAL*8(A-H,O-Z)
      DIMENSION X(2),G(2),H(2)
      COMMON GAMMA1,GAMMA2,GAMMA3,GAMMA4,CONST,ECON,EMCOL,EMA,EMB,REYII
      W = ( GAMMA1+GAMMA2*(X(1)**2+X(2)**2)+GAMMA3*X(1)+GAMMA4*X(2) ) /
      *( ECON+EMCOL*(X(1)**2+X(2)**2)-2.D0*EMA*X(1)-2.D0*EMB*X(2) )
      RETURN
      END

```

\$ENTRY

```

$JOB C WATFIV A ITTIPB00N
OPTIMIZATION OF ABSOLUTE VALUE OF INPUT REACTANCE.
IMPLICIT REAL*8(A-H,O-Z)
COMPLEX*16 DCONJG,XVAR
COMPLEX*16 YII,YIJ,YJI,YIK,YJJ,YJK,YIN,ZIN
COMPLEX*16 DCPLX,YLOAD,ZLOAD
DIMENSION X(2),G(2),H(2),S(14)
COMMON REYII,AIYII,REYJI,REYKI,AIYJI,AIYKI
EXTERNAL SUB
DREAL(XVAR) = (XVAR+DCONJG(XVAR))/2.D0
DAIMAG(XVAR) = ((0.D0,-1.D0)*XVAR+DCONJG((0.D0,-1.D0)*XVAR))/2.D0
READ,CONST,GAMMA1,GAMMA2,GAMMA3,GAMMA4,ECON,EMCOL,EMA,EMB,REYJI,
*REYKI,AIYJI,AIYKI,REYJJ,REYJK,AIYJJ,AIYJK,REYII,AIYII,CDS
KWRT = 0
INDEX = 2
G(1) = REYJJ+REYJK
G(2) = -10.0**(30)
H(1) = G(1)+0.1D-10
H(2) = 10.0**(30)
X(1) = G(1)+0.1D-11
X(2) = 0.378378727895D-01
NVR = -2
NFIG = 16
NCON = 2
NTRIPV = 700
L = 14
PRINT100
FORMAT('1')
DC1 I=1,10
CALL CLIMBD(NVR,X,NCON,T,NFIG,S,L,KWRT,G,H,INDEX,NTRIPV,SUB)
PRINT,' INPUT REACTANCE =',T
P = (ECON+EMCOL*(X(1)**2+X(2)**2)-2.D0*EMA*X(1)-2.D0*EMB*X(2)) /
*(X(1)**2+X(2)**2)
PRD = CDS*P
PRINT,' RADIATED POWER =',PRD
ADMTCE = X(1)-REYJJ-REYJK
SUSTCE = X(2)-AIYJJ-AIYJK
YLOAD = DCPLX(ADMTCE,SUSTCE)
ZLOAD = 1.D0/YLOAD
PRINT,' CONNECTED LOAD =',ZLOAD
WY = (GAMMA1+GAMMA2*(X(1)**2+X(2)**2)+GAMMA3*X(1)+GAMMA4*X(2)) /
*(ECON+EMCOL*(X(1)**2+X(2)**2)-2.D0*EMA*X(1)-2.D0*EMB*X(2))
WY = CONST*WY
PRINT,' GAIN =',WY
AMGTDE = CDABS(ZLOAD)
RE7D = DREAL(ZLOAD)
AIMZD = DAIMAG(ZLOAD)
PHASE = DATAN2(AIMZD,RE7D)
ANGLE = 180.D0*PHASE/3.1416D0
PRINT,' MAGNITUDE OF CONNECTED LOAD =',AMGTDE
PRINT,' PHASE OF CONNECTED LOAD =',ANGLE
YII = DCPLX(REYII,AIYII)
YIJ = DCPLX(REYJI,AIYJI)
YJI = YIJ
YIK = DCPLX(REYKI,AIYKI)
YIN = YII-(YIJ*YJI+YIK*YJI)/DCPLX(X(1),X(2))
ZIN = 1.D0/YIN
PRINT,' INPUT IMPEDANCE =',ZIN
CONTINUE
STOP
END

SUBROUTINE SUB(NVAR,X,NCON,T,G,H)
IMPLICIT REAL*8(A-H,O-Z)
DIMENSION X(2),G(2),H(2)
COMMON REYII,AIYII,REYJI,REYKI,AIYJI,AIYKI
F1 = X(1)-REYII-X(2)*AIYII-REYJI*(REYJI+REYKI)+AIYJI*(AIYJI+AIYKI)
F2 = X(1)*AIYII+X(2)*REYII-AIYJI*(REYJI+REYKI)-REYJI*(AIYJI+AIYKI)
T = CDABS(X(2)*F1-X(1)*F2)/(F1**2+F2**2)
RETURN
END

```

\$ENTRY

SJOB WATFIV A. ITTIPOON

THE INTEGRAL EQUATION OF POCKLINGTON TYPE IS USED IN ANALYSING
LOADED DIPOLE ANTENNA. IN THIS PROGRAM THIN WIRE APPROXIMATION
IS USED.

IMPLICIT REAL*8 (A-H,D-Z)
COMPLEX*16 DCMLX,COMP,CDEXP,CMLXA,CMLXB,CMLXC,
*Z,NMTRA,NMTRB,NMTRC,DET,DCONJG,XVAR,FARFLD
COMPLEX*16 YAD,BE,BE1
COMPLEX*16 FIELD,EXPI,EXP2,EXP3,NRFLD
COMPLEX*16 SUMY,ZLOAD
COMPLEX*16 KS,EM,CONST1,EX,CONST2,EXCTN
COMPLEX*16 TOTVAL,BOX1,BOX2,BOX3,BOX4,FIRST,SECOND,VALUE,XXV,CEXP
REAL*8 LENGTH,LAMDA
REAL*8 NORRAD(40)
DIMENSION YAD(40,40),BE(40),KS(42),EXCTN(40)
DIMENSION AMG(40)
DIMENSION RADINS(35),ANGLE(37)
DIMENSION EM(19,19),Z(19,19),IC(19),IR(19)
EQUIVALENCE(EM,Z)
EQUIVALENCE(YAD(1,10),EXCTN)

RADIUS = RADIUS OF WIRE ANTENNA
LENGTH = TOTAL LENGTH OF ANTENNA
NSEG = NUMBER OF SEGMENTS ALONG THE WIRE ANTENNA
LAMDA = WAVE LENGTH OF OPERATING FREQUENCY
RELD = RESISTIVE PART OF THE CONNECTED LOAD IMPEDANCE.
AIMLD = IMAGINARY PART OF THE CONNECTED LOAD IMPEDANCE.
LDATJ,LDATK = THE POSITIONS OF LOAD IMPEDANCE AT ZJ (J*DELTAZ) AND
ZK (K*DELTAZ), RESPECTIVELY.

CEXP(XXV) = CDEXP(XXV)
DAIMAG(XVAR) = ((0.DO,-1.DO)*XVAR+DCONJG((0.DO,-1.DO)*XVAR))/2.DO
DREAL(XVAR) = (XVAR+DCONJG(XVAR))/2.DO

READ, LAMDA,LENGTH,RADIUS,NSEG
READ,RELD,AIMLD,LDATJ,LDATK

READO1
READO2

PRINTIO1
FORMAT('1')
101 PRINT, 'LAMDA', LAMDA, 'LENGTH', LENGTH, 'RADIUS', RADIUS, 'N', NSEG
N = NSEG
PI = 3.141592654
BETA = 2.00*PI/LAMDA
DELTAZ = LENGTH/NSEG
RADIAN = BETA*DELTAZ
SINN = DSIN(RADIAN)
COSS = DCOS(RADIAN)
COMP = DCPLX(0.DO,30.DO/SINN)
CONST = 120.DO*((1-COSS)/SINN)**2
PRINT, COMP
NUMBER = NSEG-1
N1 = NUMBER-1

GENERALIZED IMPEDANCE IS DETERMINED

M = 1
DO 1 I = 1,NUMBER
DENMTA = (RADIUS**2+((M-I-1)*DELTAZ)**2)**(1./2.)
FXPTNA = BETA*DENMTA
DENMTB = (RADIUS**2+((M-I+1)*DELTAZ)**2)**(1./2.)
FXPTNB = BETA*DENMTB
DENMTC = (RADIUS**2+((M-I)*DELTAZ)**2)**(1./2.)
FXPTNC = BETA*DENMTC
CMLXA = DCMLX(0.DO,-FXPTNA)

```

NMTRA = CDEXP(CMPLXA)
CMPLXB = DCMLPX(0.00,-EXPTNB)
NMTRB = CDEXP(CMPLXB)
CMPLXC = DCMLPX(0.00,-EXPTNC)
NMTRC = 2.00*COSS*CDEXP(CMPLXC)
Z(1,1) = COMP * (NMTRA/DENMTA + NMTRB/DENMTB - NMTRC/DENMTC)
Z(1,1) = Z(1,1) * DELTAZ * 10.00-05

```

```

1 CONTINUE
-2 DO 2 JCOUNT = 2,NUMBER
Z(JCOUNT,JCOUNT) = Z(1,1)
DO 3 JB = 2,NUMBER
4 JA = 1
NCOUNT = JB
Z(NCOUNT,JA) = Z(JA,NCOUNT)
JA = JA+1
NCOUNT = NCOUNT+1
IF(NCOUNT GT NUMBER) GO TO 3
3 Z(JA,NCOUNT) = Z(1,JB)
GO TO 4
CONTINUE

```

```

ZLOAD = DCMLPX(RELD,AIMLD)
PRINT, ' ZLOAD = ', ZLOAD
ZLOAD = ZLOAD * 10.0-05
Z(LDATJ,LDATJ) = Z(LDATJ,LDATJ) + ZLOAD
Z(LDATK,LDATK) = Z(LDATK,LDATK) + ZLOAD
CALL MINVCD(Z,NUMBER,NUMBER,DET,IR,IC)
DO 107 J = 1,NUMBER
DO 107 I = 1,NUMBER
107 YAD(J,I) = Z(J,I) * 10.00-05
MCOL = NSEG/2
PRINT, 'YII = ', YAD(MCOL,MCOL)
PRINT, 'YIJ = ', YAD(MCOL,LDATJ)
PRINT, 'YJI = ', YAD(LDATJ,MCOL)
PRINT, 'YIK = ', YAD(MCOL,LDATK)
PRINT, 'YJJ = ', YAD(LDATJ,LDATJ)
PRINT, 'YJK = ', YAD(LDATJ,LDATK)
DO 513 IAC = 1,NUMBER
513 PRINT, 'COLUMN', MCOL, 'ROW', IAC, YAD(IAC,MCOL)
RIN = DREAL(YAD(MCOL,MCOL))/CDABS(YAD(MCOL,MCOL))**2
RTCEIN = -DAIMAG(YAD(MCOL,MCOL))/CDABS(YAD(MCOL,MCOL))**2
PRINT, ' INPUT RESISTANCE = ', RIN
PRINT, ' INPUT REACTANCE = ', RTCEIN
DO 514 JCNT = 1,NUMBER
514 AMG(JCNT) = CDABS(YAD(JCNT,MCOL))
AIM = DAIMAG(YAD(JCNT,MCOL))
REP = DREAL(YAD(JCNT,MCOL))
PS = DATAN2(AIM,REP)
PHASE = PS*180.00/PI
PRINT, ' AMG(JCNT), ' , PHASE
SUMY = (0.000,0.000)
DO 112 KNT = 1,NUMBER
112 SUMY = SUMY + YAD(KNT,MCOL)
ABSUMY = SUMY * DCNJG(SUMY)

```

DETERMINATION OF THE MATRIX EM.

```

C C C
NR = 1
DO 701 JC = 1,NUMBER
701 IN = JC-NR
RL = COSINE(DELTAZ,IN,BETA)
AG = SINE(DELTAZ,IN,BETA)
EM(NR,JC) = DCMLPX(RL,AG)
CONTINUE
702 DO 702 LA = 1,NUMBER
EM(LA,LA) = EM(1,1)
703 DO 703 JB = 2,NUMBER

```

```

JA = 1
NCCOUNT = JB
720 EM(NCCOUNT,JA) = DCONJG(EM(JA,NCCOUNT))
JA = JA+1
NCCOUNT = NCCOUNT+1
IF( NCCOUNT.GT.NUMBER ) GO TO 703
EM(JA,NCCOUNT) = EM(1,JB)
GO TO 720
703 CONTINUE
DO704 I = 1,NUMBER
EXPI = (0.DO,0.DO)
DO705 J = 1,NUMBER
705 EXPI = EXPI + EM(I,J)*YAD(J,MCOL)
704 KS(I) = EXPI
CONTINUE
PRAD = (0.DO,0.DO)
DO706 J = 1,NUMBER
706 PRAD = PRAD + DCONJG(YAD(J,MCOL))*KS(J)
PRAD = (50.DO/SINN**2)*PRAD
DGAIN = (CONST*ABSUMY)/PRAD
PRINT, ' RADIATED POWER', PRAD
PRINT, ' GAIN', DGAIN
*****
DETERMINE RADIATION INTENSITY.
0 AND 180 DEGREE ARE EXCLUDED FROM ANGLE.
*****
DO111 JAM=1,35
TOTVAL = (0.DO,0.DO)
ANGLE(JAM)=JAM*5.
ANG=ANGLE(JAM)*3.1416/180
CBSINE = DCOS(ANG)
SBNE = DSIN(ANG)
DO270 JIG = 1,NSEG
BANG = RADIAN * CBSINE
BIG1=BANG*JIG
BIG2=BANG*(JIG-1)
BOX1 = DC*PLX(0.DO,BIG1)
BOX2 = DC*PLX(0.DO,BIG2)
WIN=SINN*CBSINE
BOX3 = DC*PLX(COSS,WIN)
BOX4 = DC*PLX(-COSS,WIN)
IF ( JIG.EQ. 1 ) GO TO 274
IF ( JIG .EQ. NSEG ) GO TO 275
FIRST = ( CEXP(BOX1) - CEXP(BOX2) * BOX 3 ) * EXCTN(JIG-1) / SINN
SECOND = ( CEXP(BOX1) * BOX4 + CEXP(BOX2) ) * EXCTN(JIG) / SINN
GO TO 276
724 FIRST = (0.DO,0.DO)
SECOND = ( CEXP(BOX1) * BOX4 + CEXP(BOX2) ) * EXCTN(1) / SINN
GO TO 276
725 FIRST = ( CEXP(BOX1) - CEXP(BOX2) * BOX3 ) * EXCTN(NSEG-1) / SINN
726 SECOND = (0.DO,0.DO)
VALUE = FIRST+ SECOND
720 TOTVAL = TOTVAL+VALUE
CONTINUE
RADINS(JAM) = (30.DO/(4.DO*3.1416*SBNE**2))*(TOTVAL*
*DCONJG(TOTVAL))
GOTO273
723 IF(JAM.GT.1) GO TO990
RADMAX=RADINS(1)
990 IF(RADINS(JAM).LE.RADMAX) GOTO111
RADMAX=RADINS(JAM)
111 CONTINUE
DO709 JAI=1,35
NORRAD(JAI) = RADINS(JAI) / RADMAX
709 WRITE (6,709) ANGLE(JAI),NORRAD(JAI),RADINS(JAI)
FORMAT(' ',20X,F8.3,10X,F15.7,10X,E15.9)

```

311
708

```

WRITE (6,311) ANGLE(JAI), NORRAD(JAI)
FORMAT(F6.2,10X,F7.5)
CONTINUE
STOP
END

```

```

REAL FUNCTION SINE*8(DZ,IN,BETA)
IMPLICIT REAL*8(A-H,O-Z)

```

```

C = BETA*DZ
A = 0.00
B = 3.141592654
TOL = 0.00
NORDER = 5
K = 0

```

```

1 CALL GAUQUO(A,B,FX,X,TOL,NORDER,K)
  K = K+1
  IF (K.LE. 0) GO TO 2
  FX = (1.00/DSIN(X))*(DCOS(C*DCOS(X))-DCOS(C))**2*DSIN(C*IN*
*DCOS(X))
  GO TO 1
2 SINE = FX
  RETURN
  END

```

```

REAL FUNCTION COSINE*8(DZ,IN,BETA)
IMPLICIT REAL*8(A-H,O-Z)

```

```

C = BETA*DZ
A = 0.00
B = 3.141592654
TOL = 0.00
NORDER = 5
K = 0

```

```

1 CALL GAUQUO(A,B,FX,X,TOL,NORDER,K)
  K = K+1
  IF (K.LE. 0) GO TO 2
  FX = (1.00/DSIN(X))*(DCOS(C*DCOS(X))-DCOS(C))**2*DCOS(C*IN*
*DCOS(X))
  GO TO 1
2 COSINE = FX
  RETURN
  END

```

\$ENTRY

(II) The dipole loaded with finite size load impedance

The following computer programs are written

- (a) The computer program for determining the parameters for optimization
- (b) Optimization program
- (c) The computer program for determining the current distribution and radiation pattern of loaded dipole


```

BRJ = BETA*RJ
C1 = BETA*DCMPLX(1.00, BRJ)
C2 = CDEXP(DCMPLX(0.00, -BRJ))
A(I) = C2*(C1*((ZI-DO)*DLN(D1, DO, ZI, RADIUS)+(D2-ZI)*DLN(D2, D1, ZI,
*RADIUS))+C1*(2.00*SR(RADIUS, D1, ZI)-SR(RADIUS, DO, ZI)-SR(RADIUS, D2,
*ZI))+(0.00, -1.00)*RADIAN**2)

```

```

2 CONTINUE
DO3 I = 1, NUMBER
3 Z(J, I) = C5*(A(I)+A(I+2)-2.00*DCOS(RADIAN)*A(I+1))/C6
DO5 J = 2, NUMBER
5 Z(J, J) = Z(1, 1)
DO6 JB = 2, NUMBER
JA = 1
NCOUNT = JB
7 Z(NCOUNT, JA) = Z(JA, NCOUNT)
JA = JA+1
NCOUNT = NCOUNT+1
IF( NCOUNT. GT. NUMBER ) GO TO 6
Z(JA, NCOUNT) = Z(1, JB)
GO TO 7

```

```

6 CONTINUE
THE EXCITATION MATRIX.
JU = THE SEGMENT CONTAINED AN EXCITATION VOLTAGE.
JL = JU-1

```

```

JU = (NSEG+1)/2
JL = JU-1
DO4 J = 1, NUMBER
4 V(J) = (0.00, 0.00)
V(JL) = (1.00, 0.00)
V(JU) = (1.00, 0.00)
CALL MINVCD(Z, NUMBER, NUMBER, DET, IR, IC)
DO8 J = 1, NUMBER
DO8 I = 1, NUMBER
8 YAD(J, I) = Z(J, I)
DO9 I = 1, NUMBER
9 V(I) = YAD(I, JL)+YAD(I, JU)
PRINT, ' ROW', I, V(I)
RINI = DREAL(V(JL))/CDABS(V(JL))**2
RIN2 = DREAL(V(JU))/CDABS(V(JU))**2
RTCE1 = -DAIMAG(V(JL))/CDABS(V(JL))**2
RTCE2 = -DAIMAG(V(JU))/CDABS(V(JU))**2
PRINT, ' INPUT RESISTANCE = ', RINI, RIN2
PRINT, ' INPUT REACTANCE = ', RTCE1, RTCE2
DO10 J = 1, NUMBER
AMG(J) = CDABS(V(J))
AIM = DAIMAG(V(J))
REP = DREAL(V(J))
PS = DATAN2(AIM, REP)
PHASE = PS*180.00/PI
10 PRINT, ' ', AMG(J), ' ', PHASE
SUMY = (0.00, 0.00)
DO112 KNT = 1, NUMBER
112 SUMY = SUMY+V(KNT)
ABSUMY = SUMY*DCONJG(SUMY)

```

```

C C C
DETERMINATION OF THE MATRIX EM.

```

```

NR = 1
DO701 JC = 1, NUMBER
IN = JC-NR
RL = COSINE(DELTAZ, IN, BETA)
AG = SINE(DELTAZ, IN, BETA)
EM(NR, JC) = DCMPLX(RL, AG)
701 CONTINUE
DO702 LA = 1, NUMBER

```

```

02 EM(LA,LA) = EM(1,1)
DO703 JB = 2,NUMBER
JA = 1
NCCOUNT = JB
EM(NCCOUNT,JA) = DCONJG(EM(JA,NCCOUNT))
JA = JA+1
NCCOUNT = NCCOUNT+1
IF( NCCOUNT.GT.NUMBER ) GO TO 703
EM(JA,NCCOUNT) = EM(1,JB)
GO TO 720
CONTINUE
DO704 I = 1,NUMBER
EXP1 = (0.DO,0.DO)
DO705 J = 1,NUMBER
EXP1 = EXP1+EM(I,J)*V(J)
KS(I) = EXP1
CONTINUE
PRAD = (0.DO,0.DO)
DO706 J = 1,NUMBER
PRAD = PRAD+DCONJG(V(J))*KS(J)
PRAD = (60.DO/SINN**2)*PRAD
DGAIN = (CONST*ABSUMY)/PRAD
PRINT, ' RADIATED POWER', PRAD
PRINT, ' GAIN', DGAIN
DO730 I = 1,NUMBER
DO731 J = 1,NUMBER
EXP2 = (0.DO,0.DO)
DO732 L = 1,NUMBER
EXP2 = EXP2 + EM(I,L)*YAD(L,J)
API(I,J) = EXP2
CONTINUE
CONTINUE
DO733 I = 1,NUMBER
DO734 J = 1,NUMBER
EXP3 = (0.DO,0.DO)
DO735 L = 1,NUMBER
EXP3 = EXP3 + DCONJG(YAD(I,L))*API(L,J)
EM(I,J) = EXP3
IF( J.EQ. I ) GO TO 734
EM(J,I) = DCONJG(EM(I,J))
CONTINUE
CONTINUE
DO108 J = 1,NUMBER
BE1 = (0.DO,0.DO)
DO109 I = 1,NUMBER
BE1 = BE1 + YAD(I,J)
CONTINUE
BE(J) = BE1
CONTINUE
DO905 JK = 2,JL
L = JK
M = N1-JK
L1 = L
LO = L-1
M1 = M
MO = M-1
DETERMINE C10 AND C11.
C10 = SL(BETA,DELTAZ,LO,LO,L,-1,1)/(DS*C6)
C11 = SL(BETA,DELTAZ,L1,LO,L,1,1)/(DS*C6)
PRINT, C10,C11
DETERMINE Y1 TO Y6.
Y1 = YAD(LO,LO)+YAD(LO,M1)
Y2 = YAD(LO,L1)+YAD(LO,MO)
Y3 = YAD(LO,JL)+YAD(LO,JU)
Y4 = YAD(L1,LO)+YAD(L1,M1)
Y5 = YAD(L1,L1)+YAD(L1,MO)

```

```

Y6 = YAD(L1,JL)+YAD(L1,JU)
PRINT,Y1
PRINT,Y2
PRINT,Y3
PRINT,Y4
PRINT,Y5
PRINT,Y6
C DETERMINE B1 TO B3.
B1 = BE(LO)+BE(M1)
B2 = BE(L1)+BE(MO)
B3 = BE(JU)+BE(JL)
PRINT,B1
PRINT,B2
PRINT,B3
C DETERMINE EM1 TO EM9.
EM1 = EM(LO,LO)+EM(LO,M1)+EM(M1,LO)+EM(M1,M1)
EM2 = EM(LO,L1)+EM(LO,MO)+EM(M1,L1)+EM(M1,MO)
EM3 = EM(LO,JL)+EM(LO,JU)+EM(M1,JL)+EM(M1,JU)
EM4 = EM(L1,LO)+EM(L1,M1)+EM(MO,LO)+EM(MO,M1)
EM5 = EM(L1,L1)+EM(L1,MO)+EM(MO,L1)+EM(MO,MO)
EM6 = EM(L1,JL)+EM(L1,JU)+EM(MO,JL)+EM(MO,MO)
EM7 = EM(JL,LO)+EM(JL,M1)+EM(JU,LO)+EM(JU,M1)
EM8 = EM(JL,L1)+EM(JL,MO)+EM(JU,L1)+EM(JU,MO)
EM9 = EM(JL,JL)+EM(JL,JU)+EM(JU,JL)+EM(JU,JU)
PRINT,EM1
PRINT,EM2
PRINT,EM3
PRINT,EM4
PRINT,EM5
PRINT,EM6
PRINT,EM7
PRINT,EM8
PRINT,EM9
05 CONTINUE
STOP
END

```

```

REAL FUNCTION DLN*8(DN,DD,ZI,A)
IMPLICIT REAL*8(A-H,D-Z)
X = DN-ZI
Y = DD-ZI
V = X+(X**2+A**2)**(1/2.D0)
W = Y+(Y**2+A**2)**(1/2.D0)
DLN = DLG(V/W)
RETURN
END

```

```

REAL FUNCTION SR*8(A,D,ZI)
IMPLICIT REAL*8(A-H,D-Z)
X = A**2+(D-ZI)**2
SR = X**(1/2.D0)
RETURN
END

```

```

REAL FUNCTION SL*8(BETA,DZ,NA,NB,L,M,N)
IMPLICIT REAL*8(A-H,D-Z)
RADIAN = BETA*DZ
A = (L-1)*DZ
B = L*DZ
TOL = 0.70
NORDER = 5
K = 0
CALL GAUQUJ(A,B,F,Z,TOL,NORDER,K)
K = K+1
IF (K.LE.0) GO TO 2
F = DSIN(BETA*(DZ+M*(Z-NA*DZ)))*DSIN(BETA*(DZ-N*(Z-NB*DZ)))

```

```

2 GO TO 1
  SL = F
  RETURN
  END

```

```

REAL FUNCTION SINE*8(DZ,IN,BETA)
IMPLICIT REAL*8(A-H,O-Z)

```

```

  C = BETA*DZ
  A = 0.00
  B = 3.141592654
  TOL = 0.00
  NORDER = 5
  K = 0

```

```

1 CALL GAUQUUD(A,B,FX,X,TOL,NORDER,K)

```

```

  K = K+1

```

```

  IF( K.LE. 0 ) GO TO 2

```

```

  FX = (1.00/DSIN(X))*(DCOS(C*DCOS(X))-DCOS(C))**2*DSIN(C*IN*

```

```

  *DCOS(X))

```

```

  GO TO 1

```

```

2 SINE = FX

```

```

  RETURN
  END

```

```

REAL FUNCTION COSINE*8(DZ,IN,BETA)
IMPLICIT REAL*8(A-H,O-Z)

```

```

  C = BETA*DZ
  A = 0.00
  B = 3.141592654
  TOL = 0.00
  NORDER = 5
  K = 0

```

```

1 CALL GAUQUUD(A,B,FX,X,TOL,NORDER,K)

```

```

  K = K+1

```

```

  IF( K.LE. 0 ) GO TO 2

```

```

  FX = (1.00/DSIN(X))*(DCOS(C*DCOS(X))-DCOS(C))**2*DCOS(C*IN*

```

```

  *DCOS(X))

```

```

  GO TO 1

```

```

2 COSINE = FX

```

```

  RETURN
  END

```

ENTRY

SJOB WATFIV A ITTIPIBOON

OPTIMIZATION OF DIRECTIVE GAIN ON HORIZONTAL PLANE.

```

IMPLICIT REAL*8 (A-H,O-Z)
COMPLEX*16 Y1,Y2,Y3,Y4,Y5,Y6,R1,R2,R3,EM1,EM2,EM3,EM4,EM5,EM6
COMPLEX*16 EM7,EM8,EM9,XVAR,DCONJG,DCMPLX,YLOAD,ZLOAD
DIMENSION X(2),G(2),H(2),S(14)
COMMON C10,C11,Y1,Y2,Y3,Y4,Y5,Y6,R1,R2,R3
COMMON EM1,EM2,EM3,EM4,EM5,EM6,EM7,EM8,EM9
EXTERNAL SUB
DREAL(XVAR) = (XVAR+DCONJG(XVAR))/2.D0
DAIMAG(XVAR) = ((0.D0,-1.D0)*XVAR+DCONJG((0.D0,-1.D0)*XVAR))/2.D0
READ,CONST,C10,C11,RY1,RY2,RY3,RY4,RY5,RY6,
*AY6,RR1,AB1,RR2,AB2,RR3,AB3,REM1,AEM1,REM2,AEM2,REM3,AEM3,REM4,
*AEM4,REM5,AEM5,REM6,AEM6,REM7,AEM7,REM8,AEM8,REM9,AEM9
Y1 = DCMPLX(RY1,AY1)
Y2 = DCMPLX(RY2,AY2)
Y3 = DCMPLX(RY3,AY3)
Y4 = DCMPLX(RY4,AY4)
Y5 = DCMPLX(RY5,AY5)
Y6 = DCMPLX(RY6,AY6)
R1 = DCMPLX(RR1,AB1)
R2 = DCMPLX(RR2,AB2)
R3 = DCMPLX(RR3,AB3)
EM1 = DCMPLX(REM1,AEM1)
EM2 = DCMPLX(REM2,AEM2)
EM3 = DCMPLX(REM3,AEM3)
EM4 = DCMPLX(REM4,AEM4)
EM5 = DCMPLX(REM5,AEM5)
EM6 = DCMPLX(REM6,AEM6)
EM7 = DCMPLX(REM7,AEM7)
EM8 = DCMPLX(REM8,AEM8)
EM9 = DCMPLX(REM9,AEM9)
AK = 0.6704396656D 05

```

```

KWRT = 0
INDEX = 2
G(1) = 0.D0
G(2) = -10.0**30
H(1) = 10.0**30
H(2) = 10.0**30
X(1) = 0.1029750911050-09
X(2) = -0.1895070656700-03
NVR = 2
NFIG = 16
NCON = 2
NTRIPV = 700
L = 14
DO1 I = 1,10
CALL CLIMRD(NVR,X,NCON,D,NFIG,S,L,KWRT,G,H,INDEX,NTRIPV,SUB)
D = CONST*D
PRINT,' MAXIMUM DIRECTIVE GAIN ON THE HORIZONTAL PLANE=' ,D
ADMTCE = X(1)
SUSTCE = X(2)
YLOAD = DCMPLX(ADMTCE,SUSTCE)
ZLOAD = 1.D0/YLOAD
RL = DREAL(ZLOAD)
AL = DAIMAG(ZLOAD)
AMTDE = COABS(ZLOAD)
PHASE = DATAN2(AL,RL)
PRINT,'CONNECTED LOAD =' ,ZLOAD
PRINT,'MAGNITUDE OF CONNECTED LOAD =' ,AMTDE
ANGLE = 180.D0+PHASE/3.1416D0
PRINT,'PHASE OF CONNECTED LOAD =' ,ANGLE

```

CONTINUE
 STOP
 END

```

SUBROUTINE SUB(NVAR,X,NFCN,D,G,H)
IMPLICIT REAL*8(A-H,O-Z)
COMPLEX*16 Y1,Y2,Y3,Y4,Y5,Y6,B1,B2,B3
COMPLEX*16 EM1,EM2,EM3,EM4,EM5,EM6,EM7,EM8,EM9
COMPLEX*16 YL,VJ1,VJ,VX,DCONJG,DCMPLX
COMPLEX*16 XVAR,DNTR,NMTR
COMPLEX*16 CD1
DIMENSION X(2),G(2),H(2)
COMMON C10,C11,Y1,Y2,Y3,Y4,Y5,Y6,B1,B2,B3
COMMON EM1,EM2,EM3,EM4,EM5,EM6,EM7,EM8,EM9
DREAL(XVAR) = (XVAR+DCONJG(XVAR))/2.00
CD = C10**2-C11**2
YL = DCMPLX(X(1),X(2))
CD1 = (YL*C10+CD*Y5)*(YL*C10+CD*Y1)-(YL*C11-CD*Y2)*(YL*C11-CD*
*Y4)
VJ1 = -CD*(Y3*(YL*C10+CD*Y5)+Y6*(YL*C11-CD*Y2))/CD1
VJ = -CD*(Y3*(YL*C11-CD*Y4)+Y6*(YL*C10+CD*Y1))/CD1
VX = B1*VJ1+B2*VJ+B3
NMTR = VX*DCONJG(VX)
DNTR = DCONJG(VJ1)*(EM1*VJ1+EM2*VJ+EM3)+DCONJG(VJ)*(EM4*VJ1+EM5*
*VJ+EM6)+EM7*VJ1+EM8*VJ+EM9
D = CDABS(NMTR)/DREAL(DNTR)
RETURN
END

```

5ENTRY

\$\$\$JOB WATFIV A ITTIPIBOON

PROGRAM FOR TREATING DIPOLE WITH FINITE SIZE OF EXCITATION AND
OF LOAD IMPEDANCE.
THE PROGRAM IS BASED ON THE METHOD OF MOMENTS, USING GALERKIN
METHOD.

IMPLICIT REAL*8(A-H,O-Z)
COMPLEX*16 A,XXV,DCONJG,CEXP,CDEXP,XVAR,C1,DCMPLX,C2,C5,V
COMPLEX*16 Z,YAD,DET
COMPLEX*16 ZL
COMPLEX*16 EFIELD
COMPLEX*16 SUMY,EM,EXP1,KS,PRAD,EXCTN
COMPLEX*16 TOTVAL,BOX1,BOX2,BOX3,BOX4,FIRST,SECOND,VALUE
COMPLEX*16 EXP2,EXP3,API,RE,BE1
COMPLEX*16 Y1,Y2,Y3,Y4,Y5,Y6,B1,B2,B3,EM1,EM2,EM3,EM4,EM5,EM6
COMPLEX*16 EM7,EM8,EM9
REAL*8 NORRAD
REAL*8 LAMDA,LENGTH
DIMENSION A(40),V(40),YAD(40,40),AMG(40)
DIMENSION API(20,20),RE(40)
DIMENSION NORRAD(40),RADINS(35),ANGLE(37)
DIMENSION KS(40),EXCTN(40)
DIMENSION EM(20,20),Z(20,20),IR(20),IC(20)
EQUIVALENCE(EM,Z)
EQUIVALENCE(V,EXCTN)
EQUIVALENCE(A,KS)

RADIUS = RADIUS OF THE WIRE ANTENNA.
LENGTH = TOTAL LENGTH OF THE WIRE ANTENNA.
NSEG = TOTAL NUMBER OF SEGMENTS ALONG THE WIRE ANTENNA.
LAMDA = WAVE LENGTH OF THE OPERATING FREQUENCY.
RL, AIL = RESISTIVE AND REACTIVE COMPONENTS OF THE CONNECTED LOAD
IMPEDANCE.
ZL = IMPEDANCE PER UNIT LENGTH.
L AND M ARE THE POSITIONS OF LOADING.

CEXP(XXV) = CDEXP(XXV)
DAIMAG(XVAR) = ((0.D0,-1.D0)*XVAR+DCONJG((0.D0,-1.D0)*XVAR))/2.D0
DREAL(XVAR) = (XVAR+DCONJG(XVAR))/2.D0

READ,LAMDA,LENGTH,RADIUS,NSEG
READ,RL,AIL,L,M
ZL = DCMPLX(RL,AIL)
PRINT,LAMDA,LENGTH,RADIUS,NSEG
PRINT,ZL

DETERMINATION OF THE GENERALIZED IMPEDANCE MATRIX.

PI = 3.141592654D0
HETA = 2.00*PI/LAMDA
DELTAZ = LENGTH/NSEG
RADIAN = HETA*DELTAZ
C4 = (30.D0)/DSIN(RADIAN)
C5 = DCMPLX(0.D0,C4)
C6 = (1.D0-DCOS(RADIAN))/RADIAN
SINN = DSIN(RADIAN)
COSS = DCCS(RADIAN)
CONST = 120.00*((1-COSS)/SINN)**2
CCNST = 2.00*(1.D0-DCOS(RADIAN))**2
PRINT,CCNST
N1 = NSEG+1
N1 = NSEG-1
J = 1

```

D0 = (J-1)*DELTAZ
D1 = J*DELTAZ
D2 = (J+1)*DELTAZ
D02 I = 1,N1
Z1 = (I-1)*DELTAZ
ZJ = J*DELTAZ
RJ = (RADIUS**2+(ZJ-ZI)**2)**(1/2.D0)
BRJ = BETA*RJ
C1 = BETA*DCMPLX(1.D0, BRJ)
C2 = CDEXP(DCMPLX(0.D0, -BRJ))
A(I) = C2*(C1*((Z1-D0)*DLN(D1,D0,ZI,RADIUS)+(D2-ZI)*DLN(D2,D1,ZI,
*RADIUS))+C1*(2.D0*SR(RADIUS,D1,ZI)-SR(RADIUS,D0,ZI)-SR(RADIUS,D2,
*ZI))+(0.D0,-1.D0)*RADIAN**2)
CONTINUE
D03 I = 1,NUMBER
Z(J,I) = C5*(A(I)+A(I+2)-2.D0*DCOS(RADIAN)*A(I+1))/C6
D05 J = 2,NUMBER
Z(J,J) = Z(1,1)
DC6 JB = 2,NUMBER
JA = 1
NCCOUNT = JB
Z(NCCOUNT,JA) = Z(JA,NCCOUNT)
JA = JA+1
NCCOUNT = NCCOUNT+1
IF( NCCOUNT.GT. NUMBER, ) GO TO 6
Z(JA,NCCOUNT) = Z(1,JB)
GO TO 7
CCCONTINUE

```

THE VOLTAGE DROP DUE TO LOAD IMPEDANCE IN THE L TH. SEGMENT.

```

L0 = L-1
L1 = L
DS = DSIN(RADIAN)
ZL = ZL/C6
Z(L0,L0) = Z(L0,L0)+ZL*SL(BETA,DELTAZ,L0,L0,L,-1,1)/DS
Z(L0,L1) = Z(L0,L1)+ZL*SL(BETA,DELTAZ,L1,L0,L,1,1)/DS
Z(L1,L1) = Z(L1,L1)+ZL*SL(BETA,DELTAZ,L1,L1,L,-1,1)/DS
Z(L1,L0) = Z(L1,L0)+ZL*SL(BETA,DELTAZ,L1,L0,L,1,1)/DS

```

THE VOLTAGE DROP DUE TO LOAD IMPEDANCE IN THE M TH. SEGMENT.

```

M0 = M-1
M1 = M
Z(M0,M0) = Z(M0,M0)+ZL*SL(BETA,DELTAZ,M0,M0,M,-1,1)/DS
Z(M0,M1) = Z(M0,M1)+ZL*SL(BETA,DELTAZ,M1,M0,M,1,1)/DS
Z(M1,M1) = Z(M1,M1)+ZL*SL(BETA,DELTAZ,M1,M1,M,-1,1)/DS
Z(M1,M0) = Z(M1,M0)+ZL*SL(BETA,DELTAZ,M1,M0,M,1,1)/DS
PRINT, Z(L0,L0), Z(L0,L0), Z(M0,M0), Z(M0,M0)
PRINT, Z(L0,L1), Z(L0,L1), Z(M0,M1), Z(M0,M1)
PRINT, Z(L1,L1), Z(L1,L1), Z(M1,M1), Z(M1,M1)
PRINT, Z(L1,L0), Z(L1,L0), Z(M1,M0), Z(M1,M0)

```

THE EXCITATION MATRIX.

JU = THE SEGMENT CONTAINED AN EXCITATION VOLTAGE.

JL = JU-1

JU = (NSEG+1)/2

JL = JU-1

D04 J = 1,NUMBER

V(J) = (0.D0,0.D0)

V(JL) = (1.D0,0.D0)

V(JU) = (1.D0,0.D0)

CALL MINVCD(7,NUMBER,NUMBER,DET,IR,IC)

D08 J = 1,NUMBER

D08 I = 1,NUMBER

```

8  YAD(J,I) = Z(J,I)
   DO9 I = 1,NUMBER
   V(I) = YAD(I,JL)+YAD(I,JU)
9  PRINT,' ROW',I,V(I)
   RIN1 = DREAL(V(JL))/CDABS(V(JL))**2
   RIN2 = DREAL(V(JU))/CDABS(V(JU))**2
   RTCE1 = -DAIMAG(V(JL))/CDABS(V(JL))**2
   RTCE2 = -DAIMAG(V(JU))/CDABS(V(JU))**2
   PRINT,' INPUT RESISTANCE = ',RIN1,RIN2
   PRINT,' INPUT REACTANCE = ',RTCE1,RTCE2
   DO10 J = 1,NUMBER
   AMG(J) = CDABS(V(J))
   AIM = DAIMAG(V(J))
   REP = DREAL(V(J))
   PS = DATAN2(AIM,REP)
10  PHASE = PS*180.DO/PI
   PRINT,' ',AMG(J),' ',PHASE
   SUMY = (0.DO,0.DO)
112 DO112 KNT = 1,NUMBER
   SUMY = SUMY+V(KNT)
   ABSUMY = SUMY*DCONJG(SUMY)
C
C
C  DETERMINATION OF THE MATRIX EM.
   NR = 1
   DO701 JC = 1,NUMBER
   IN = JC-NR
   RL = COSINE(DELTAZ,IN,BETA)
   AG = SINE(DELTAZ,IN,BETA)
701 EM(NR,JC) = DCMPLX(RL,AG)
   CONTINUE
702 DO702 LA = 1,NUMBER
   EM(LA,LA) = EM(1,1)
   DO703 JB = 2,NUMBER
   JA = 1
   NCCOUNT = JB
720 EM(NCCOUNT,JA) = DCONJG(EM(JA,NCCOUNT))
   JA = JA+1
   NCCOUNT = NCCOUNT+1
   IF( NCCOUNT.GT.NUMBER ) GO TO 703
   EM(JA,NCCOUNT) = EM(1,JB)
   GO TO 720
703 CONTINUE
   DO704 I = 1,NUMBER
   EXP1 = (0.DO,0.DO)
705 DO705 J = 1,NUMBER
   EXP1 = EXP1+EM(I,J)*V(J)
   KS(I) = EXP1
704 CONTINUE
   PRAD = (0.DO,0.DO)
706 DO706 J = 1,NUMBER
   PRAD = PRAD+DCONJG(V(J))*KS(J)
   PRAD = (60.DO/SIN**2)*PRAD
   DGAIN = (CONST*ABSUMY)/PRAD
   C10 = SL(BETA,DELTAZ,LC,LC,L,-1,1)/(DS*C6)
   C11 = SL(BETA,DELTAZ,L1,L0,L,1,1)/(DS*C6)
   EM7 = -7L*(C10*V(L0)+C11*V(L1))
   EM8 = -7L*(C11*V(L0)+C10*V(L1))
   PRINT,EM7
   PRINT,EM8
   PRINT,' RADIATED POWER',PRAD
   PRINT,' GAIN',DGAIN
   DO730 I = 1,NUMBER
   DO731 J = 1,NUMBER
   EXP2 = (0.DO,0.DO)
   DO732 L = 1,NUMBER

```

```

732 EXP2 = EXP2 + EM(I,L)*YAD(L,J)
API(I,J) = EXP2
731 CONTINUE
730 CONTINUE
DO733 I = 1,NUMBER
DO734 J = 1,NUMBER
EXP3 = (0,00,0,00)
DO735 L = 1,NUMBER
735 EXP3 = EXP3 + DCONJG(YAD(I,L))*API(L,J)
EM(I,J) = EXP3
IF (J.EQ. 1) GO TO 734
EM(J,I) = DCONJG(EM(I,J))
734 CONTINUE
733 CONTINUE
C
C DETERMINE RADIATION INTENSITY.
C 0 AND 180 DEGREE ARE EXCLUDED.
C
DO111 JAM=1,35
TOTVAL = (0,00,0,00)
ANGLE(JAM)=JAM*5.
ANG=ANGLE(JAM)*3.1416/180
CBSINE= DCOSS(ANG)
SBNE = DSIN(ANG)
DO270 JIG = 1,NSEG
BANG = RADIAN * CBSINE
BIG1=BANG*JIG
BIG2=BANG*(JIG-1)
BOX1 = DCMLPX(0,00,BIG1)
BOX2 = DCMLPX(0,00,BIG2)
WIN=SINN*CBSINE
BOX3 = DCMLPX(COSS,WIN)
BOX4 = DCMLPX(-COSS,WIN)
IF ( JIG.EQ. 1 ) GO TO 274
IF ( JIG . EQ . NSEG ) GO TO 275
FIRST = ( CEXP(BOX1) - CEXP(BOX2) * BOX3 ) * EXCTN(JIG-1) / SINN
SECOND = ( CEXP(BOX1) * BOX4 + CEXP(BOX2) ) * EXCTN(JIG) / SINN
GO TO 276
274 FIRST = (0,00,0,00)
SECOND = ( CEXP(BOX1) * BOX4 + CEXP(BOX2) ) * EXCTN(1) / SINN
GO TO 276
275 FIRST = ( CEXP(BOX1) - CEXP(BOX2) * BOX3 ) * EXCTN(NSEG-1) / SINN
SECOND = (0,00,0,00)
276 VALUE = FIRST+ SECOND
TOTVAL = TOTVAL+VALUE
270 CONTINUE
RADINS(JAM) = (30,00/(4,00*3,1416*SBNE**2))* (TOTVAL*
*DCONJG(TOTVAL))
GCTC273
273 IF(JAM.GT.1) GO TO990
RADMAX=RADINS(1)
990 IF(RADINS(JAM).LE.RADMAX) GOTO111
RADMAX=RADINS(JAM)
111 CCNTINUE
DO708 JAI=1,35
NORRAD(JAI) = RADINS(JAI) / RADMAX
WRITE(6,709) ANGLE(JAI),NORRAD(JAI),RADINS(JAI)
709 FORMAT('0',20X,F8,3,10X,F15,7,10X,E15,9)
WRITE(7,311)ANGLE(JAI),NORRAD(JAI)
311 FORMAT(F6,2,10X,F7,5)
708 CCNTINUE
STOP
END
REAL FUNCTION DLN*8(DN,DD,ZI,A)
IMPLICIT REAL*8(A-H,O-Z)

```

```

X = DN-ZI
Y = DD-ZI
V = X+(X**2+A**2)**(1/2.D0)
W = Y+(Y**2+A**2)**(1/2.D0)
DLN = DLOG(V/W)
RETURN
END

```

```

REAL FUNCTION SR*8(A,D,ZI)
IMPLICIT REAL*8(A-H,O-Z)
X = A**2+(D-ZI)**2
SR = X**(1/2.D0)
RETURN
END

```

```

REAL FUNCTION SL*8(BETA,DZ,NA,NB,L,M,N)
IMPLICIT REAL*8(A-H,O-Z)
RADIANT = BETA*DZ
A = (L-1)*DZ
B = L*DZ
TOL = 0.D0
NGRDER = 5
K = 0
1 CALL GAUQUO(A,B,F,Z,TCL,NGRDER,K)
K = K+1
IF (K.LE.0) GO TO 2
F = DSIN(BETA*(DZ+M*(Z-NA*DZ)))*DSIN(BETA*(DZ-N*(7-NB*DZ)))
GO TO 1
2 SL = F
RETURN
END

```

```

REAL FUNCTION SINE*8(DZ,IN,BETA)
IMPLICIT REAL*8(A-H,O-Z)
C = BETA*DZ
A = 0.D0
B = 3.141592654
TOL = 0.D0
NGRDER = 5
K = 0
1 CALL GAUQUO(A,B,FX,X,TCL,NGRDER,K)
K = K+1
IF (K.LE.0) GO TO 2
FX = (1.D0/DSIN(X))*(DCOS(C*DCOS(X))-DCOS(C))**2*DSIN(C*IN*
*DCOS(X))
GO TO 1
2 SINE = FX
RETURN
END

```

```

REAL FUNCTION COSINE*8(DZ,IN,BETA)
IMPLICIT REAL*8(A-H,O-Z)
C = BETA*DZ
A = 0.D0
B = 3.141592654
TOL = 0.D0
NGRDER = 5
K = 0
1 CALL GAUQUO(A,B,FX,X,TCL,NGRDER,K)
K = K+1
IF (K.LE.0) GO TO 2
FX = (1.D0/DSIN(X))*(DCOS(C*DCOS(X))-DCOS(C))**2*DCOS(C*IN*
*DCOS(X))
GO TO 1
2 COSINE = FX
RETURN
END

```

\$ENTRY

BIBLIOGRAPHY

- [1] R.W.P. King, *The Theory of Linear Antennas*, Cambridge, Mass.: Harvard University Press, 1956.
- [2] E. Hallén, "Theoretical investigations into the transmitting and receiving qualities of antennae", *Nova Acta Regiae Soc. Sci. Upsaliensis*, Ser. IV, 11, No. 4, pp. 1-44, 1938.
- [3] R.F. Harrington, "Matrix methods for field problems", *Proc. IEEE*, Vol. 58, pp. 136-149, February 1967.
- [4] M.A.K. Hamid, W.M. Boerner, L. Shafai, S.J. Towaij, W.P. Alsip and G.J. Wilson, "Radiation characteristics of bent-wire antennas", *IEEE Trans. on Electromagnetic Compatibility*, Vol. EMC-12, pp. 106-111, August 1970.
- [5] R.F. Harrington and J. Mautz, "Straight wires with arbitrary excitation and loading", *IEEE Trans. Antennas and Propagation*, Vol. AP-15, pp. 502-515, July 1967.
- [6] B.J. Strait and K. Hirasawa, "On long wire antennas with multiples excitations and loadings", *IEEE Trans. Antennas and Propagation*, Vol. AP-18, pp. 699-700, September 1970.
- [7] A.D. Frost, "Parametric amplifier antenna", *Proc. IRE*, Vol. 48, pp. 1163-1164, June 1960.
- [8] A.D. Frost, "Parametric amplifier antenna", *IEEE Trans. Antennas and Propagation*, Vol. AP-12, pp. 234-235, March 1964.
- [9] K. Fujimoto, "Active dipole antennas with esaki diodes", *Electronic Communication in Japan*, Vol. 48, No. 4, pp. 255-265, April 1965.
- [10] J.R. Copeland, W.J. Robertson and R.G. Verstraete, "Antennafier arrays", *IEEE Trans. on Antennas and Propagation*, Vol. AP-12, pp. 227-233, March 1967.
- [11] H.H. Meinke, "Transistorized receiving antennas", Progress Report No. 6 to Air Force Avionics Laboratory, United States Air Force, Contract No. AF61 (052) - 950, 1967.
- [12] R.W.P. King and T.T. Wu, "The imperfectly conducting cylindrical transmitting antenna", *IEEE Trans. Antennas and Propagation*, Vol. AP-14, pp. 524-534, September 1966.
- [13] T.T. Wu and R.W.P. King, "The cylindrical antenna with non-reflecting resistive loading", *IEEE Trans. Antennas and Propagation*, Vol. AP-13, pp. 369-373, May 1965.

- [14] E.E. Altshuler, "The traveling-wave linear antenna", IRE Trans. Antennas and Propagation, Vol. AP-9, pp. 324-329, July 1961.
- [15] D.P. Nyquist and K.M. Chen, "The traveling-wave linear antenna with non-dissipative loading", IEEE Trans. Antennas and Propagation, Vol. AP-16, pp. 21-31, January 1968.
- [16] B.L.J. Rao, J.E. Ferris and W.E. Zimmerman, "Broad band characteristics of cylindrical antennas with exponentially tapered capacitive loading", IEEE Trans. Antennas and Propagation, Vol. AP-17, pp. 145-151, March 1969.
- [17] B.D. Popović and M.B. Dragović, "Simple broad band cylindrical antenna with quadidistributed capacitive loading", Electronics Letters, Vol. 8, pp. 148-149, March 1972.
- [18] C.J. Lin, D.P. Nyquist and K.M. Chen, "Short cylindrical antennas with enhanced radiation on high directivity", IEEE Trans. Antennas and Propagation, Vol. AP-18, pp. 576-580, July 1970.
- [19] J.A. Stratton, *Electromagnetic Theory*, New York: McGraw-Hill, Inc., 1941, pp. 424-430.
- [20] R.F. Harrington, *Field Computation by Moment Methods*, New York: The Macmillan Company, 1968, pp. 62-75.
- [21] R.W.P. King and C.W. Harrison, *Antennas And Waves: A Modern Approach*, Cambridge, Mass.: The M.I.T. Press, 1969, pp. 143-151.
- [22] R.F. Harrington, *Field Computation by Moment Methods*, New York: The Macmillan Company, 1968, pp. 1-21.
- [23] C.A. Klein and R. Mittra, "The effect of different testing functions in the moment method solution of thin-wire antenna problems", IEEE Trans. Antennas and Propagation, Vol. AP-23, pp. 258-261, March 1975.
- [24] E.C. Jordan and K.G. Balmain, *Electromagnetic Waves and Radiating Systems*, Englewood Cliffs, N.J.: Prentice-Hall, 1968, pp. 333-336.
- [25] W.L. Weeks, *Antenna Engineering*, New York: McGraw-Hill, Inc., 1968, pp. 30-31.
- [26] R.F. Harrington, *Time-Harmonic Electromagnetic Fields*, New York: McGraw-Hill, Inc., 1961, pp. 81-85.
- [27] S.A. Schelkunoff and H.T. Friis, *Antennas Theory and Practice*, New York: John Wiley & Sons, Inc., 1966, pp. 141-142.
- [28] S.A. Schelkunoff and H.T. Friis, *Antennas Theory and Practice*, New York: John Wiley & Sons, Inc., 1966, pp. 155-156.

- [29] S.A. Schelkunoff and H.T. Friis, *Antennas Theory and Practice*, New York: John Wiley & Sons, Inc., 1966, pp. 213-214.
- [30] University of Waterloo Watfiv Library Programs.
- [31] R.W.P. King, *Fundamental Electromagnetic Theory*, New York: Dover Publications, In., 1963, pp. 321-401.
- [32] L.W. Pearson, "A separation of the logarithmic singularity in the exact kernel of the cylindrical antenna integral equation", *IEEE Trans. Antennas and Propagation*, Vol. AP-23, pp. 256-258, March 1975.
- [33] B.D. Popovic, "Thin monopole antenna: finite-size belt-generator representation of coaxial-line excitation", *Proc. IEE* 120, No. 5, pp. 544-550, May 1973.
- [34] R.W.P. King and T.T. Wu, "Currents, charges and near fields of cylindrical antennas", *Radio Science, J. Res. NBS*, Vol. 69D, pp. 429-446, March 1965.